Integrated Water Flow Model
IWFM-2015
revisions 426, 448, 475

Theoretical Documentation

Central Valley Modeling Unit
Modeling Support Branch
Bay-Delta Office
September 2016

Table of Contents

List of Figures ..... **vi**

List of Tables ..... **viii**

Summary of Features for Components with Multiple Versions ..... **ix**

1. Introduction **1-1**

1.1. Overview of IWFM Theoretical Documentation 1-1

1.2. History of IWFM Development 1-2

1.3. Summary of Current Model Features in IWFM 1-4

2. Hydrological Processes Modeled in IWFM **2-1**

2.1. Groundwater Flow 2-2

2.1.1. Aquifer Layers Separated by an Aquitard 2-7

2.1.2. Aquifer Layers that are not Separated by an Aquitard 2-10

2.2. Tile Drainage and Subsurface Irrigation 2-13

2.3. Land Subsidence 2-16

2.3.1. Flow into Groundwater Storage due to Land Subsidence 2-19

2.4. Root Water Uptake from Groundwater 2.20

2.5. Initial and Boundary Conditions for the Groundwater 2-21

2.5.1. Initial Conditions 2-21

2.5.2. Specified Flux (Neumann) 2-21

2.5.3. Specified Head (Dirichlet) 2-22

2.5.4. General Head 2-23

2.5.5. Constrained General Head 2-23

2.6. Stream Flows 2-25

2.6.1. Stream Flow Routing in Component Version 4.0 2-29

2.6.1.a. Stream-Groundwater Interaction in Component Version 4.0 2-31

2.6.2. Stream Flow Routing in Component Version 4.1 2-33

2.6.2.a. Stream-Groundwater Interaction in Component Version 4.1 2-33

2.6.3. Stream Flow Routing in Component Version 5.0 2-34

2.6.3.a. Stream-Groundwater Interaction in Component Version 5.0 2-37

2.6.3.b. Initial Conditions 2-37

2.6.4. Diversions and Bypass Flows 2-38

2.7. Lakes 2-39

2.7.1. Lake-Groundwater Interaction 2-42

2.8. Land Surface and Root Zone Flow Processes 2-43

2.9. Moisture Routing in the Unsaturated Zone 2-46

2.10. Small Watersheds 2-49

3. Numerical Methods Used in Modeling of Hydrological Processes 3-1

3.1. Finite Element Representation of the Groundwater Equation 3-1

3.1.1. Shape Functions 3-11

3.1.1.a. Linear Triangular Elements 3-11

3.1.1.b. Bilinear Quadrilateral Elements 3-13

3.1.2. Computation of Integrals 3-16

3.1.2.a. Integration over Triangular Elements 3-19

3.1.2.b. Integration over Quadrilateral Elements 3-20

3.1.3. Vertical Flows when Aquifers are Separated by an Aquitard 3-23

3.1.4. Vertical Flows when Aquifers are not Separated by an Aquitard 3-26

3.1.5. Land Subsidence 3-26

3.1.6. Root Water Uptake from Groundwater..... 3-28

3.1.7. Stream-Groundwater Interaction 3-29

3.1.8. Lake-Groundwater Interaction..... 3-31

3.1.9. Tile Drains and Subsurface Irrigation..... 3-33

3.1.10. Initial Conditions 3-34

3.1.11. Boundary Conditions 3-34

3.1.11.a. Specified Flux (Neumann)..... 3-35

3.1.11.b. Specified Head (Dirichlet) 3-35

3.1.11.c. General Head 3-36

3.1.11.d. Constrained General Head 3-36

3.2. Stream Flows 3-37

3.2.1. Stream Routing Component Version 4.0 3-37

3.2.2. Stream Routing Component Version 4.1 3-38

3.2.3. Stream Routing Component Version 5.0 3-39

3.2.3.a. Initial Conditions 3-40

3.3. Lakes 3-41

3.4. Land Surface and Root Zone Flow Processes 3-45

3.5. Soil Moisture in the Unsaturated Zone..... 3-45

3.6. Small Watersheds 3-50

3.7. Solution of the System of Equations 3-52

3.7.1. Compressed Storage of Matrices 3-56

3.8. Usage of Parametric Grid 3-62

4. Demand and Supply 4-1

4.1. Land Use 4-1

4.2. Agricultural and Urban Water Demands 4-2

4.3. Supply 4-2

4.3.1. Surface Water Diversions and Deliveries 4-4

4.3.2. Groundwater Pumping and Recharge 4-6

4.3.2.a. Pumping and Recharge at Well Locations 4-7

4.3.2.b. Elemental Distribution of Pumping and Recharge 4-8

4.3.2.c. Computation of Pumping at Drying Wells 4-12

4.3.3. Re-use of Irrigation Water 4-14

4.3.4. Agricultural Water Use 4-14

4.3.5. Urban Water Use 4-15

4.4. Automated Supply Adjustment 4-16

4.4.1. Adjustment of Surface Water Diversions 4-17

4.4.2. Adjustment of Pumping 4-21

Appendix A A-1

A.1. Components of $\left\{\mathbb{F}^{\mathbf{k}}\right\}$ and $\left[\mathbb{X}^{\mathbf{k}}\right]$ for Stream Nodes A-1

A.2. Components of $\left\{\mathbb{F}^{\mathbf{k}}\right\}$ and $\left[\mathbb{X}^{\mathbf{k}}\right]$ for Lakes A-11

A.3. Components of $\left\{\mathbb{F}^{\mathbf{k}}\right\}$ and $\left[\mathbb{X}^{\mathbf{k}}\right]$ for Groundwater Nodes A-13

Appendix B - Chronology of the Development of IGSM, IGSM2, and IWFM **.....B-1**

Appendix C - References **C-1**

List of Figures

Figure 1.1 Hydrologic processes modeled in IWFM 1-5

Figure 1.2 General flowchart of IWFM 1-8

Figure 2.1 Multi-layer aquifer system 2-2

Figure 2.2 Schematic representation of two aquifer layers separated by an aquitard 2-7

Figure 2.3 Schematic representation of two aquifer layers that are not separated with an aquitard 2-10

Figure 2.4 Schematic representation of a tile drain 2-14

Figure 2.5 Flow from a subsurface irrigation pipe to the groundwater 2-15

Figure 2.6 Stream-groundwater interaction scenarios 2-26

Figure 2.7 Representation of a natural stream system by stream nodes and stream segments in IWFM 2-28

Figure 2.8 A trapezoidal channel cross-section and relevant parameters 2-37

Figure 2.9 Hydrological components that affect lake storage 2-41

Figure 2.10 Schematic representation of flow through the root zone and the unsaturated zone 2-45

Figure 3.1 Node numbering convention used in IWFM for an aquifer system with N_L layers and N=5 nodes in each layer 3-5

Figure 3.2 A representative triangular element 3-12

Figure 3.3 Transformation of a quadrilateral element from (x, y) space to (ξ, η) space 3-14

Figure 3.4 Total area that is associated with node *i* 3-24

Figure 3.5 Plots of possible lake storage functions and the modified function when lake elevation exceeds the maximum elevation 3-43

Figure 3.6 Flowchart for the unsaturated flow simulation 3-49

Figure 3.7 Hypothetical model domain 3-58

Figure 3.8 An example of parametric and finite element mesh system 3-64

Figure 4.1 Water use and supply 4-3

Figure 4.2 A stream system with 4 diversion locations 4-18

List of Tables

Table 2.1 Types of aquifer layers and their descriptions 2-3

Table 2.2 Version numbers and features of stream routing components..... 2-27

Table 3.1 Node connection scheme for the example shown in Figure 3.7 3-59

Table B.1 Chronological development of IGSM (up to version 5.0), IGSM2 and IWFM.....B-3

Summary of Features for Components with Multiple Versions

Some of the hydrologic simulation components in IWFM have multiple versions that offer different simulation capabilities. To aid the user in choosing the right component version, below is a list of these component versions and a summary of the simulation capabilities they offer.

Version	Capabilities
Root Zone Component	
4.0	• Simulation of non-ponded and ponded (rice and managed refuges) crops, urban lands, native and riparian vegetation at each element • Simulation of generic moisture (seepage from extra source of water, fog, etc.) • Ability to deliver water to an element, group of elements or a subregion to meet water demand • Ability to compute physical crop water demand dynamically based on crop, irrigation management, soil and atmospheric conditions or to pre-specify water demand to represent contractual demand
4.1	• All features listed for version 4.0 above • Simulation of riparian vegetation access to stream water to meet all or part of their evapotranspirative water demand • Simulation of root water uptake from groundwater that meets part or all of the plant evapotranspirative demand
Stream Component	
4.0	• Instantaneous routing (storage is not tracked) of stream flow • Wetted perimeter is constant
4.1	• All features listed for version 4.0 above • Simulation of varied wetted perimeter given as a flow vs. wetted perimeter rating table

5.0

- Kinematic wave routing to simulate stream flows and to track storage change in the stream channel
- Simulation of flow in rectangular, triangular and trapezoidal channels
- Flow-stage relationship is represented by the Manning's equation
- Wetted perimeter is calculated as a function of stage and channel geometry

1. Introduction

The Integrated Water Flow Model (IWFM) is a fully documented FORTRAN-based computerized mathematical model that simulates ground water flow, stream flow, and surface water – ground water interactions. IWFM was developed by staff at the California Department of Water Resources (DWR). IWFM is GNU licensed software, and all the source code, executables, documentation, and training material, are freely available on DWR's website. The model was first released to the public by DWR in 2003 as IGSM2 (Integrated Groundwater-Surface water Model version 2). IGSM2 itself was a completely revised version, in theory and code, of IGSM which was originally developed in 1990 for a group of State and local agencies in California (including DWR). This document reviews in detail the principles, theories, and assumptions that form the engine for IWFM.

1.1. Overview of IWFM Theoretical Documentation

Chapter 1 of this document reviews the history of IWFM, and briefly explains the model features.

In Chapter 2, the conservation equations that are used to model the hydrological processes simulated in IWFM are detailed. The hydrological processes that are simulated in IWFM are the groundwater heads in a multi-layer aquifer system, stream flows, lakes (open water bodies), direct runoff of precipitation, return flow from irrigation water, infiltration, evapotranspiration, vertical moisture movement in the root zone and the

unsaturated zone that lies between the root zone and the saturated groundwater system. The interaction between the aquifer, streams and lakes as well as land subsidence, tile drainage, subsurface irrigation and the runoff from small watersheds adjacent to model domain are also modeled by IWFM. Mathematical models that are used for each of the above processes are developed and discussed thoroughly in this chapter.

Chapter 3 details the numerical methods used in IWFM to solve the differential equations that model the hydrological processes listed in Chapter 2 and the interactions between them. The methods used to store large matrices in a computer-memory efficient way is also described in this chapter. Finally, techniques that are used to calculate parameter values at finite element nodes based on values measured only at a few locations are discussed.

In Chapter 4, the simulation of water demand and supply, and water allocation process are discussed. This chapter is integral to understanding one of the main objectives of the model; simulating water supply for the purpose of meeting a demand. Explanation of the land use approach in the model, and allocation of water based on land use needs are included in this chapter. The methods used to adjust water supply in order to meet the demand are also discussed.

1.2. History of IWFM Development

IWFM was first released by DWR to the public as IGSM2 in December 2002. In September 2005 the name IGSM2 was changed to IWFM to avoid confusion with another model IGSM (same acronym but a different code and theoretical basis); versions

of IGSM are still in use today. Additional details can be found in Appendix B. IGSM2 Version 1.0 was made available to the public in December 2002. IGSM2 Version 1.01 which included minor corrections was released shortly after, in January 2003. IGSM2 Version 2.0 and Version 2.01 were released in December 2003 and March 2004, respectively. Version 2.0 incorporated more robust solution techniques, new features and improved output files, whereas Version 2.01 included minor corrections. Later, IGSM2 Version 2.2 which included a new zone budgeting post-processor was released in February 2005. IGSM2 Version 2.3, which was renamed as IWFM Version 2.3, was released in September 2005 and included minor additional features and modified output files compared to IGSM2 Version 2.2. IWFM Version 2.4 that included a modified methodology for routing soil moisture in the root zone was released in May 2006. IWFM Version 3.0 mostly included structural changes in the source code that was the start of an effort to move to an object-oriented programming paradigm. Time-tracking simulations, option to print groundwater heads and subsidence values in a Tecplot-compliant format to create animations, and new features in the simulation of the root zone soil moisture were part of this version. IWFM Version 3.0 was released in February 2007. Version 3.02, which was released to the public in April 2010, included a new solver that uses the generalized preconditioned conjugate gradient method for shorter run-times, modifications to the source code to increase run-time efficiencies, and bug fixes. Version 4.0 was originally released in May 2012. The main improvement in this version was the rigorous simulation of the root zone flow processes and water demands at finite-element cell level for different agricultural crops as well as for rice and managed refuges. Additionally, this version marked the beginning of a more modular approach in IWFM

development where different simulation components were developed such that they could be used both within IWFM and as stand-alone simulation components (e.g. IWFM Demand Calculator, the IDC, which is the root zone simulation component of IWFM Version 4.0).

1.3. Summary of Current Model Features in IWFM

IWFM is a water resources management and planning model that simulates groundwater, surface water, groundwater-surface water interaction, as well as other components of the hydrologic system (Figure 1.1). Preserving the non-linear aspects of the surface and subsurface flow processes and the interactions among them is an important aspect of the current version of IWFM.

Simulation of groundwater elevations in a multi-layer aquifer system and the flows among the aquifer layers lies in the core of IWFM. Galerkin finite element method is used to solve the conservation equation for the multi-layer aquifer system. Stream flows and lake storages are also modeled in IWFM. Their interaction with the aquifer system is simulated by solving the conservation equations for groundwater, streams and lakes simultaneously.

An important aspect of IWFM that differentiates it from the other models in its class is its capability to simulate the water demand as a function of different land use and crop types, and compare it to the historical or projected amount of water supply. The agricultural water demand is computed for ponded and non-ponded crops using user-specified parameters for farm and crop management practices. Ponded crops include rice

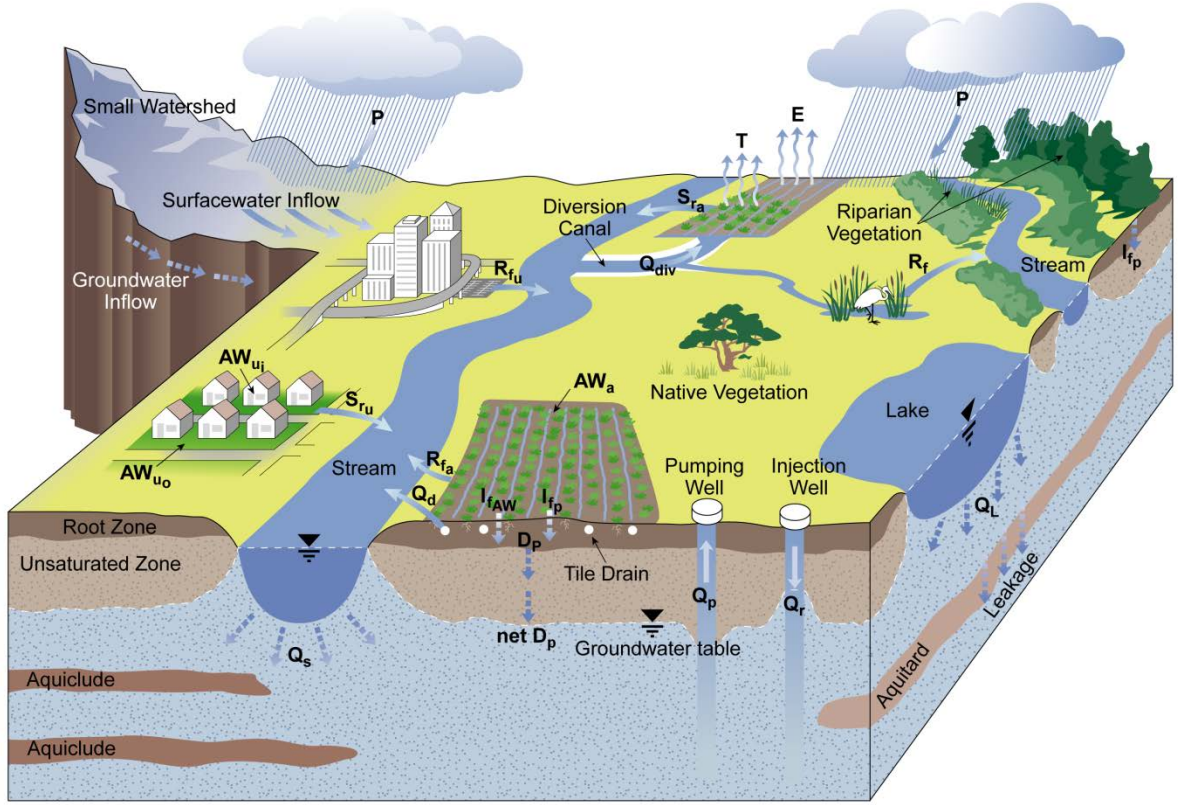

LEGEND

P.....*Precipitation*
AW_a..... *Water applied to agricultural lands*
AW_{ui}.... *Water applied to indoor urban lands*
AW_{uo}... *Water applied to outdoor urban lands*
E.....*Evaporation*
T..... *Transpiration*
I_{fp}..... *Infiltration of precipitation*
I_{fAW}..... *Infiltration of applied water*
Q_{div}..... *Surface water diversion*
S_{ra}.....*Agricultural runoff*
S_{ru}.....*Urban runoff*
R_f.....*Return flow*
R_{fa}.....*Agricultural return flow*
R_{fu}.....*Urban return flow*
D_P.....*Deep percolation of water to the unsaturated zone*
net D_p...*Recharge to the groundwater aquifer*
Q_p.....*Pumping from groundwater aquifer*
Q_r..... *Recharge to groundwater aquifer*
Q_s.....*Stream-groundwater interaction*
Q_L.....*Lake-groundwater interaction*
Q_d.....*Tile drainage flow*

Figure 1.1 Hydrologic processes modeled in IWFM

grown and decomposed using different management practices (namely rice with flooded decomposition, non-flooded decomposition or no decomposition at all). Water demands for seasonal and permanent refuges are also simulated as ponded crops since the management of these lands are very similar to those of rice fields. Non-ponded crops include all other crops that are not grown in standing water. Urban water demand is computed based on population and per-capita water usage. The user can specify stream diversion and pumping locations for the source of water supply to meet the urban and agricultural water demand. User-specified diversion and pumping amounts can be distributed over the modeled area for agricultural irrigation or municipal and industrial use. Based on the precipitation and irrigation rates, and the distribution of land use and crop types over the model domain, the infiltration, evapotranspiration and surface runoff can be computed. Vertical movement of the soil moisture through the root zone and the unsaturated zone that lies between the root zone and the saturated groundwater system can be simulated, and the recharge rates to the groundwater can be computed.

As mentioned, IWFM has the capability to compare the agricultural and urban water demands to the actual water supply (in terms of stream diversions and pumping) that is available in the modeled region from a historical or a projected point-of-view. If there is discrepancy between the water demand and the water supply (i.e. if there is a supply shortage or a supply surplus), IWFM can be used to adjust the water supplies automatically to minimize this discrepancy. The user can choose to have only diversions, only pumping amounts or both diversions and pumping adjusted to minimize the difference between the computed demand and the water supply.

IWFM allows the user to divide the entire model area into smaller sub-regions.

This division can be based on hydrologic and geologic properties (e.g. individual watersheds) or on the management practices (e.g. water districts). The division of the model into smaller regions does not affect the mass distribution over the entire regions; the sub-regions are used solely for the grouping and reporting of the simulation results. The input data required by IWFM is independent of particular sub-regions. The details about the specific data requirements for IWFM are listed in the User's Manual that accompanies this document.

This documentation discusses the theory and methodology used in IWFM Version 2015. Figure 1.2 is a general flowchart of the current version of IWFM. As new versions come online, revisions and additions will be made to this documentation.

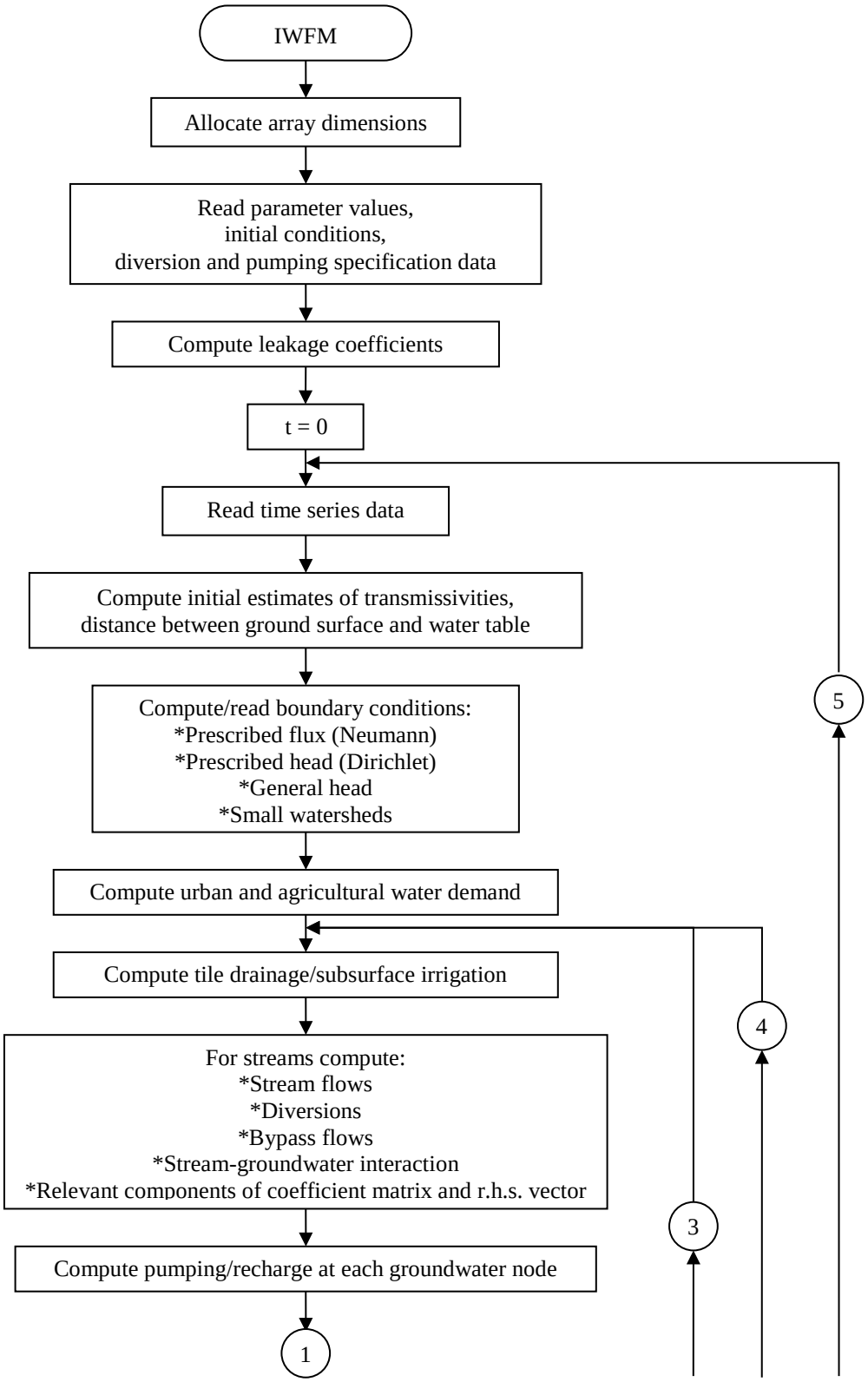

Figure 1.2 General flowchart of IWFM *(continued on next page)*

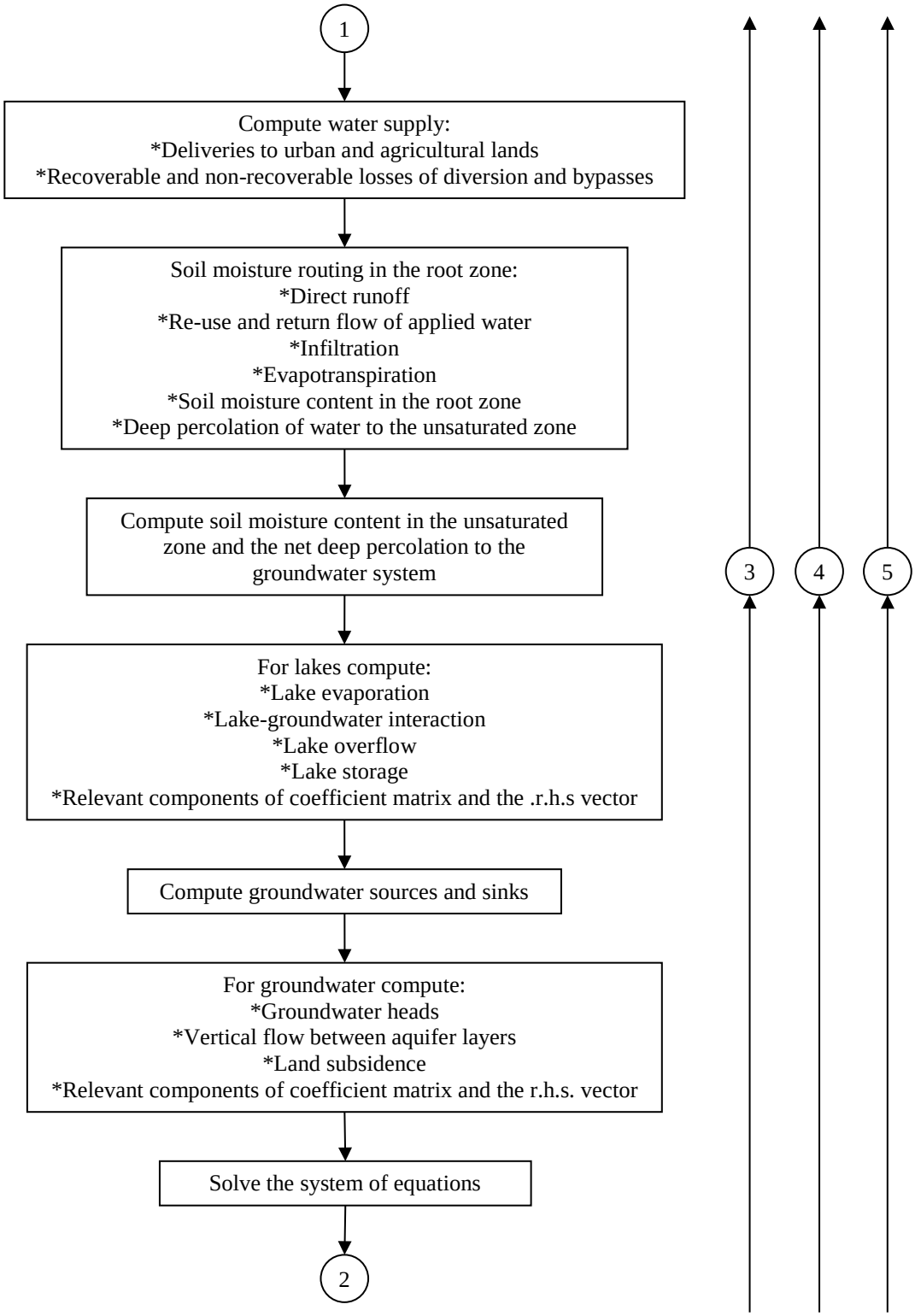

Figure 1.2 General flowchart of IWFM *(continued)*

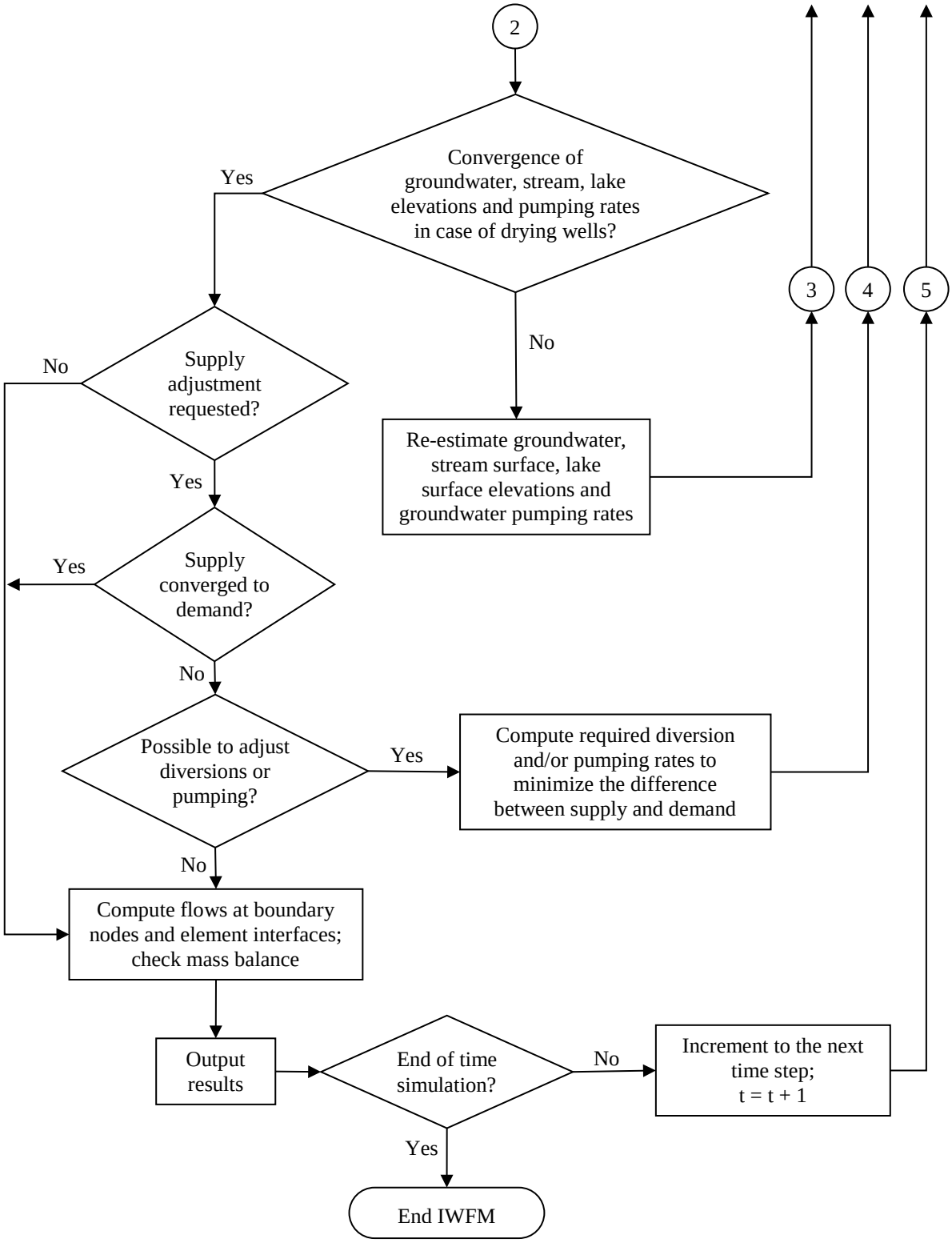

Figure 1.2 General flowchart of IWFM *(continued)*

2. Hydrological Processes Modeled in IWFM

In the core of IWFM lies the simulation of regional groundwater heads. In natural hydrological systems the regional groundwater interacts with other components of the hydrologic cycle. As precipitation falls on the ground surface, it infiltrates into the soil at a rate that is dictated by the soil type, ground cover and soil moisture. The moisture in the top soil moves downward as well as it is taken out of the soil by vegetation. The downward-moving soil moisture travels through the unsaturated zone of the soil before it replenishes the groundwater.

If the infiltration capacity of the soil is less than the precipitation rate, the portion of the precipitation that is in excess of infiltration becomes surface runoff and contributes to streams and large bodies of water such as lakes. In wet periods, streams act as water sources for the aquifer system whereas in dry periods they drain water away from the aquifer. Similarly, large bodies of water, such as lakes, affect the groundwater heads during wet and dry periods. IWFM models groundwater heads, stream flows and lake storage simultaneously as well as other components of the hydrological cycle discussed above in order to simulate the interactions between these hydrological components accurately.

In this chapter, the hydrological processes that are simulated in IWFM and the theoretical background of the simulation methods along with the accompanying simplifications and assumptions are detailed. The equations used to simulate the interactions among each of these hydrological components are also explained.

2.1. Groundwater Flow

IWFM can simulate horizontal and vertical groundwater flow in any multi-layer aquifer system that includes a combination of confined, unconfined and leaky layers. These layers may be separated by aquitards or aquicludes (Figure 2.1). Table 2.1 gives a definition for each of these aquifer types. IWFM is also capable of simulating the change

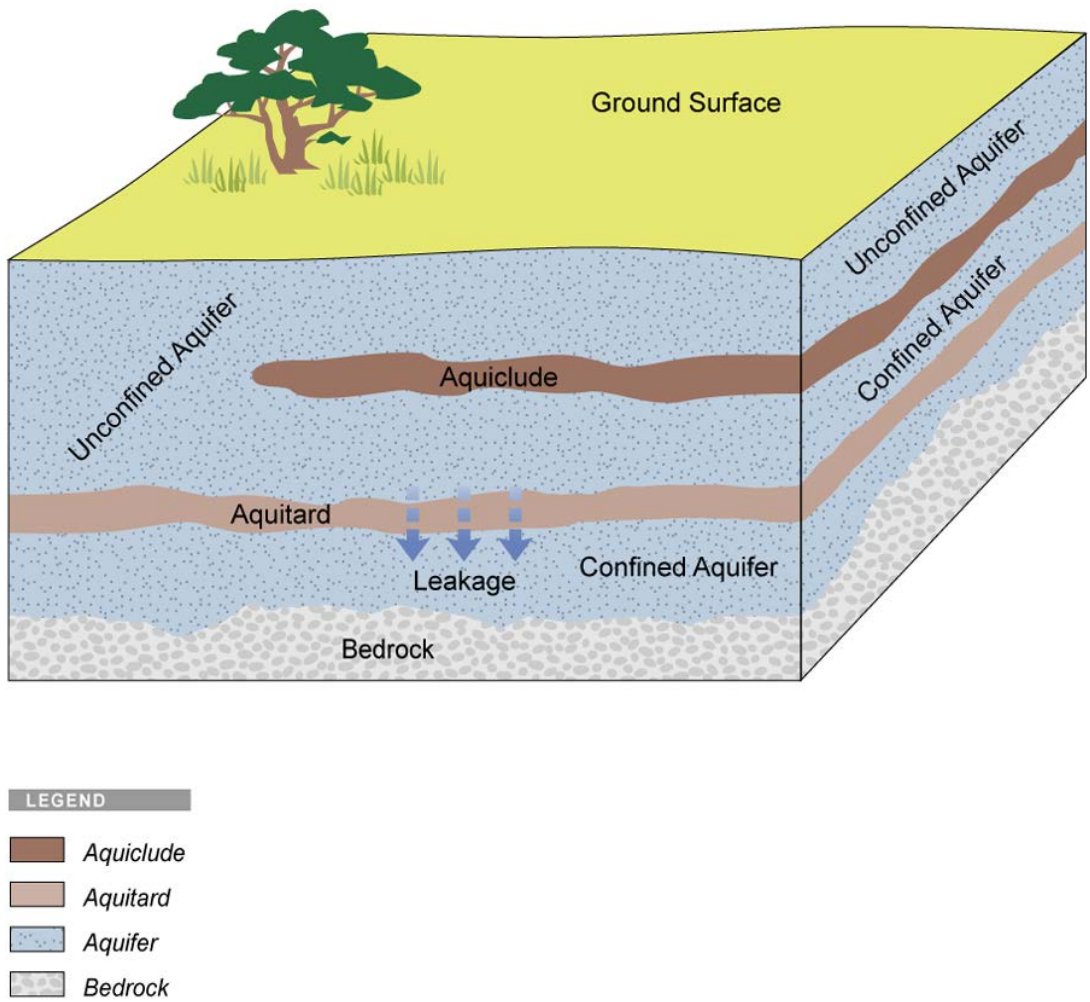

Figure 2.1 Multi-layer aquifer system

Layer Type	Layer Description
Confined aquifer	Aquifer bound above and below by impervious surfaces
Unconfined aquifer	Aquifer with a free water surface as the upper boundary
Leaky aquifer	Aquifer losing/gaining water through an aquitard that bounds the aquifer above/below
Aquiclude	Formation that may contain water, but unable to transmit significant quantities
Aquitard	Semi-pervious/leaky formation

Table 2.1 Types of aquifer layers and their descriptions

in the aquifer layer types (for instance, a confined aquifer becoming unconfined) as the groundwater head levels fluctuate. The three-dimensional nature of the flow is simulated by a quasi three-dimensional approach. In this modeling approach, the depth-integrated groundwater flow equation is solved for each aquifer layer in order to compute the two-dimensional groundwater head field. Vertical flow to and from each layer is computed through approximated leakage terms that are treated as individual head dependent sources or sinks.

The equation for the conservation of mass at a cross-section of an aquifer layer is given as

$$\frac{\partial S_s h}{\partial t} + \vec{\nabla} \cdot \vec{q} = I_u q_u + I_d q_d + q_o - q_{sd} - q_{et}$$
$$+\delta\left(x - x_s, y - y_s\right)\frac{Q_{sint}}{A_s}$$
$$+\delta\left(x - x_{lk}, y - y_{lk}\right)\frac{Q_{lkint}}{A_{lk}} \qquad (2.1)$$
$$+\delta\left(x - x_{td}, y - y_{td}\right)\frac{Q_{td}}{A_{td}}$$

where

S_s = storativity, (dimensionless). It is equal to the storage coefficient S_o, for a confined aquifer and specific yield, S_y, for an unconfined aquifer;

h = groundwater head, (L);

$\vec{q}$ = specific discharge field, (L^2/T);

q_u = rate of flow into the aquifer layer from the upper adjacent layer, (L/T);

I_u = indicator function for top aquifer layer, (dimensionless);

$$= \begin{cases} 1 & \text{if layer is not top aquifer layer} \\ 0 & \text{if layer is top aquifer layer} \end{cases};$$

q_d = rate of flow into the aquifer layer from the lower adjacent layer, (L/T);

I_d = indicator function for bottom aquifer layer, (dimensionless);

$$= \begin{cases} 1 & \text{if layer is not bottom aquifer layer} \\ 0 & \text{if layer is bottom aquifer layer} \end{cases};$$

δ = dirac delta function, (dimensionless);

x_s = x-coordinate of a stream location, (L);

y_s = y-coordinate of a stream location, (L);

Q_{sint} = stream-groundwater interaction (see the discussion on stream flows), (L^3/T);

A_s = effective area of the stream through which stream-groundwater interaction occurs, (L^2);

x_{lk} = x-coordinate of a lake location, (L);

y_{lk} = y-coordinate of a lake location, (L);

Q_{lkint} = lake-groundwater (see the discussion on lakes), (L^3/T);

A_{lk} = effective area through which lake-groundwater interaction occurs, (L^2);

x_{td} = x-coordinate of a tile drain or subsurface irrigation system, (L);

y_{td} = y-coordinate of a tile drain or subsurface irrigation system, (L);

Q_{td} = tile drain outflow from or subsurface irrigation inflow into the groundwater system, (L^3/T);

A_{td} = effective area through which tile drain outflow or subsurface irrigation inflow is occurring, (L^2);

q_o = other sources/sinks such as pumping, recharge, subsurface inflow from adjacent small watersheds, etc., (L/T);

q_{sd} = rate of flow into storage due to the compaction of interbeds, (L/T);

q_{et} = rate of flow out of storage due to root water uptake to meet plant evapotranspiration, (L/T);

$\vec{\nabla}$ = del operator, (1/L);

x = horizontal x-coordinate, (L);

y = horizontal y-coordinate, (L);

t = time, (T).

The value of S_s for a confined aquifer is different than its value for an unconfined aquifer. To model the changing aquifer conditions (e.g. a confined aquifer becoming unconfined), S_s is kept in the time-differential term in equation (2.1). Using Darcy's equation, one can express the specific discharge in terms of the groundwater head as

$$\vec{q} = -T\vec{\nabla}h \tag{2.2}$$

where

T = transmissivity, $(L^2/T) = \begin{cases} Kb & \text{for confined aquifer} \\ K\left(h - z_{ab}\right) & \text{for unconfined aquifer} \end{cases}$

K = saturated hydraulic conductivity of the aquifer material, (L/T);

b = thickness of the confined aquifer layer, (L);

h = groundwater head at the unconfined aquifer, (L);

z_{ab} = elevation of the bottom of the unconfined aquifer layer, (L).

In order to define the rate of flow into the aquifer layer from adjacent upper and lower layers, two cases have been considered: (i) adjacent aquifer layers are separated by an aquitard, and (ii) there is not an aquitard separating the adjacent aquifer layers.

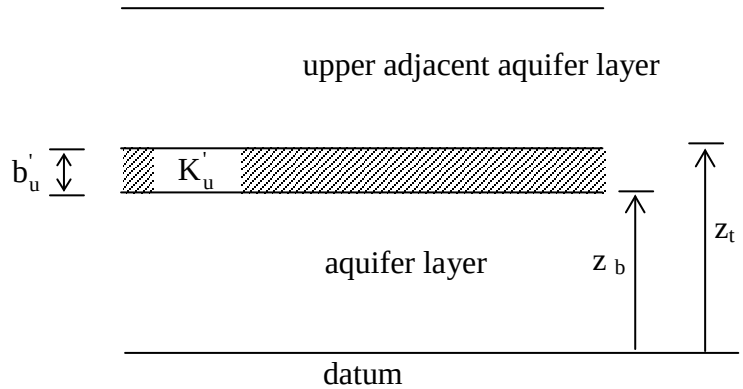

Figure 2.2 Schematic representation of two aquifer layers separated by an aquitard

2.1.1. Aquifer Layers Separated by an Aquitard

For this case, consider Figure 2.2 where a system of an aquifer layer, the adjacent upper layer and the aquitard separating these two layers is depicted. Bear and Verruijt (1987) define an aquitard as a geohydrologic layer whose permeability is at least one order of magnitude smaller than that of the adjacent aquifer layers. Assuming that the aquitard is saturated throughout its thickness, the flow in the aquitard is essentially vertical and its storage is negligible, the vertical flow can be expressed as (Bear, 1972)

$$q_u = -\frac{K_u^{'}}{b_u^{'}}\Delta h = -L_u \Delta h \qquad (2.3)$$

where

$K_u^{'}$ = vertical hydraulic conductivity of the aquitard between the aquifer layer and the upper adjacent layer, (L/T);

$b_u^{'}$ = thickness of the aquitard between the aquifer layer and the upper

adjacent layer, (L);

Δh = head difference between the top and the bottom of the aquitard, (L);

L_u = leakage coefficient between the aquifer layer and the upper adjacent layer, (1/T).

Therefore, from equation (2.3), the leakage coefficient, L_u, is expressed as

$$L_u = \frac{K_u^{'}}{b_u^{'}} \tag{2.4}$$

The head difference, Δh, between the top and the bottom of the aquitard depends on the hydraulic head in the aquifer layer and the upper adjacent aquifer layer (Figure 2.2). It can be written as

$$\Delta h = \begin{cases} h - h_u & \text{if} \quad h \geq z_b \;\; ; \;\; h_u > z_t \\ z_b - h_u & \text{if} \quad h < z_b \;\; ; \;\; h_u > z_t \\ h - z_t & \text{if} \quad h \geq z_b \;\; ; \;\; h_u = z_t \\ 0 & \text{if} \quad h < z_b \;\; ; \;\; h_u = z_t \end{cases} \tag{2.5}$$

where

h = groundwater head at the aquifer in consideration, (L);

h_u = groundwater head at the upper adjacent aquifer, (L);

z_b = bottom elevation of the aquitard, (L);

z_t = top elevation of the aquitard, (L).

Similarly, the flow rate into the aquifer layer from a lower adjacent aquifer that is separated by an aquitard can be expressed as

$$q_d = -L_d \Delta h \tag{2.6}$$

where

L_d = leakage coefficient between the aquifer layer and the lower adjacent layer, (1/T);

Δh = head difference between the top and the bottom of the aquitard that separates the aquifer and the lower adjacent aquifer, (L).

The leakage coefficient and head difference in equation (2.6) is given, respectively, as

$$L_d = \frac{K_d^{'}}{b_d^{'}} \tag{2.7}$$

$$\Delta h = \begin{cases} h - h_d & \text{if} \quad h \geq z_t \quad ; \quad h_d \geq z_b \\ z_t - h_d & \text{if} \quad h = z_t \quad ; \quad h_d \geq z_b \\ h - z_t & \text{if} \quad h \geq z_t \quad ; \quad h_d < z_b \\ 0 & \text{if} \quad h = z_t \quad ; \quad h_d < z_b \end{cases} \tag{2.8}$$

where

$K_d^{'}$ = vertical hydraulic conductivity of the aquitard between the aquifer layer and the lower adjacent layer, (L/T);

$b_d^{'}$ = thickness of the aquitard between the aquifer layer and the lower adjacent layer, (L);

h = groundwater head at the aquifer layer in consideration, (L);

h_d = groundwater head at the lower adjacent aquifer layer, (L).

Note that, in equation (2.8), z_t and z_b represent the top and bottom elevations of the semi-confining layer that underlies the aquifer layer in consideration.

2.1.2. Aquifer Layers that are not Separated by an Aquitard

For the second case where two adjacent aquifer layers have vertical hydraulic conductivities that have the same order of magnitudes with no aquitard separating them, consider Figure 2.3. Due to the continuity of the vertical flow at the interface between two layers, one can write

$$q_u = -\frac{K_u}{b_u/2}\Delta h_1 = -\frac{K}{b/2}\Delta h_2 = -L_u \Delta h \tag{2.9}$$

and

$$\Delta h = \Delta h_1 + \Delta h_2 \tag{2.10}$$

where

K_u = vertical hydraulic conductivity of the upper adjacent aquifer layer, (L/T);

b_u = thickness of the upper adjacent aquifer layer, (L);

K = vertical hydraulic conductivity of the aquifer layer in consideration, (L/T);

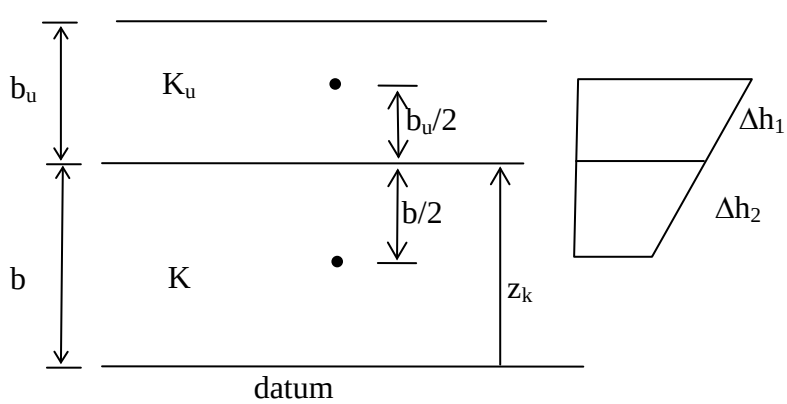

Figure 2.3 Schematic representation of two aquifer layers that are not separated with an aquitard

b	=	thickness of the aquifer layer in consideration, (L);
h	=	groundwater head at the aquifer layer in consideration, (L);
h_u	=	groundwater head at the upper adjacent aquifer layer, (L);
L_u	=	leakage coefficient between the aquifer layer and upper adjacent aquifer layer, (1/T);
Δh	=	head difference between the aquifer layer and the upper adjacent aquifer layer, (L).

Substituting equation (2.9) into (2.10) for Δh_1 and Δh_2 and solving for the leakage coefficient, L_u, one obtains the harmonic mean of the leakage coefficients of the aquifer layer in consideration and the upper adjacent aquifer layer:

$$L_u = \frac{1}{0.5\left(\frac{b_u}{K_u} + \frac{b}{K}\right)} \tag{2.11}$$

Also, the head difference between two aquifer layers can be expressed similar to equation (2.5) as

$$\Delta h = \begin{cases} h - h_u & \text{if} \quad h \geq z_k \ ; \ \ h_u > z_k \\ z_k - h_u & \text{if} \quad h < z_k \ ; \ \ h_u > z_k \\ h - z_k & \text{if} \quad h \geq z_k \ ; \ \ h_u = z_k \\ 0 & \text{if} \quad h < z_k \ ; \ \ h_u = z_k \end{cases} \tag{2.12}$$

where

z_k	=	elevation of the interface between the adjacent aquifer layers, (L).

A similar expression can be obtained for the leakage coefficient and the head difference between the aquifer layer and the lower adjacent aquifer layer when they are not separated by an aquitard as

$$L_d = \frac{1}{0.5\left(\frac{b_d}{K_d} + \frac{b}{K}\right)} \tag{2.13}$$

$$\Delta h = \begin{cases} h - h_d & \text{if} \quad h \geq z_k \;\; ; \;\; h_d \geq z_k \\ z_k - h_d & \text{if} \quad h = z_k \;\; ; \;\; h_d \geq z_k \\ h - z_k & \text{if} \quad h \geq z_k \;\; ; \;\; h_d < z_k \\ 0 & \text{if} \quad h = z_k \;\; ; \;\; h_d < z_k \end{cases} \tag{2.14}$$

After substituting equations (2.2), (2.3) and (2.6) into (2.1) and rearranging, one obtains the groundwater flow equation that is used in IWFM:

$$\begin{aligned} 0 = {} & \frac{\partial S_s h}{\partial t} - \vec{\nabla}\left(T\ \vec{\nabla} h\right) + I_u L_u \Delta h^u + I_d L_d \Delta h^d - q_o + q_{sd} + q_{et} \\ & -\delta\left(x - x_s, y - y_s\right)\frac{Q_{sint}}{A_s} \\ & -\delta\left(x - x_{lk}, y - y_{lk}\right)\frac{Q_{lkint}}{A_{lk}} \\ & -\delta\left(x - x_{td}, y - y_{td}\right)\frac{Q_{td}}{A_{td}} \end{aligned} \tag{2.15}$$

where the terms Δh^u and Δh^d are introduced in order to differentiate between the head difference between the aquifer and the upper adjacent layer, and the head difference between the aquifer and the lower adjacent layer, respectively. Based on the stratigraphic characteristics of the aquifer system, equations (2.4) and (2.7) are used for leakage coefficients when adjacent aquifer layers are separated by an aquitard. Equations (2.11) and (2.13) are used when adjacent layers are not separated by an aquitard.

Equation (2.15) is a partial differential equation that models unsteady groundwater flow in a multi-layer aquifer system that consists of confined and/or unconfined layers. These layers may be separated by semi-confining layers. Equation (2.15) is non-linear if the aquifer layer is unconfined and linear if it is confined. Equation

(2.15) also takes into account the effect of aquifer interaction with streams and lakes, and the effect of tile drainage and subsurface irrigation on the groundwater heads.

To define a well-posed problem, equation (2.15) should be coupled with initial and boundary conditions for each aquifer layer. The boundary conditions that can be defined in IWFM are (i) specified flux (Neumann), (ii) specified head (Dirichlet), and (iii) general head boundary conditions.

2.2. Tile Drainage and Subsurface Irrigation

Tile drainage is often used in farm lands in order to increase the groundwater drainage where the natural drainage of the soil is not fast enough to maintain desired agricultural conditions. Tile drains are located beneath the surface of the soil. The term tile drain is used since they are in the form of clayware pipes, which are made from clay tiles (Smedema and Rycroft, 1983). Tile drains are used for the drainage of water applied to agricultural lands for the following reasons: (i) they do not interfere with farming operations since their location is beneath the surface, and (ii) there is no loss of farming area due to the drainage system (Smedema and Rycroft, 1983; Luthin, 1973). Figure 2.4 shows a schematic representation of a tile drain.

IWFM can also simulate the effect of subsurface irrigation on the groundwater heads. Figure 2.5 illustrates subsurface irrigation, where the direction of flow is from the irrigation pipes to the groundwater. Subsurface irrigation is beneficial for deep rooted crops and trees in arid areas to avoid excessive evaporation.

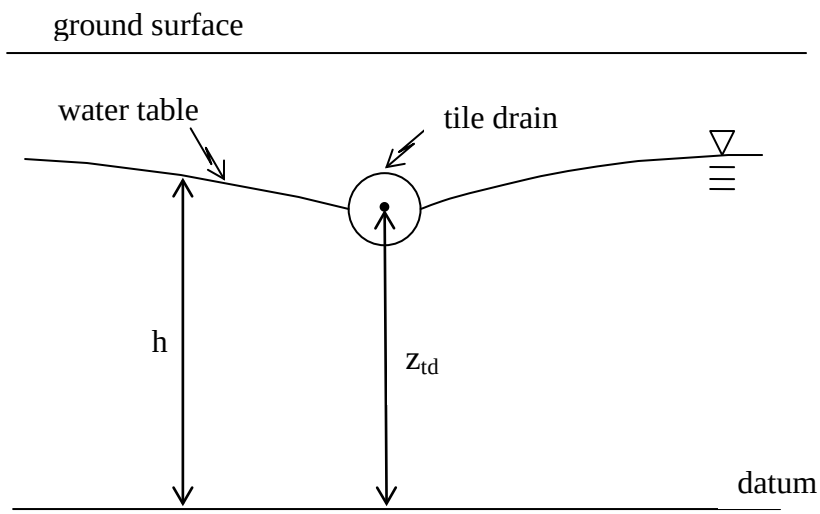

Figure 2.4 Schematic representation of a tile drain

Simulations of tile drains and subsurface irrigation are similar except that for tile drains flow direction is always from groundwater to tile drain, whereas for subsurface irrigation system the direction is always from the irrigation pipe towards the groundwater. The difference of the groundwater head and tile drain elevation (or head at the subsurface irrigation pipe) is multiplied by a conductance term to approximate the flow between groundwater and tile drain (or subsurface irrigation pipe):

$$Q_{td} = C_{td}\left(z_{td} - h\right) \tag{2.16}$$

where

Q_{td} = flow between groundwater and tile drain or subsurface irrigation pipe, (L^3/T);

C_{td} = conductance of the interface material between the tile drain/subsurface irrigation pipe and the aquifer material, (L^2/T);

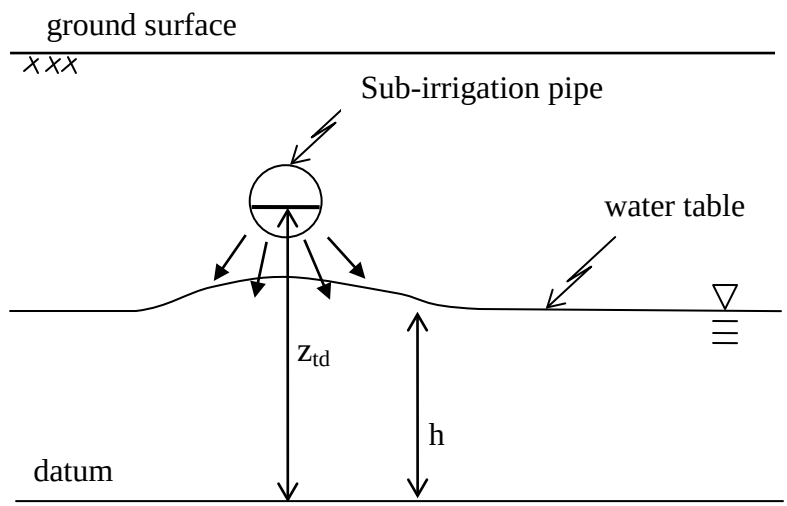

Figure 2.5 Flow from a subsurface irrigation pipe to the groundwater

z_{td} = elevation of the tile drain or the head at the subsurface irrigation pipe, (L);

h = groundwater head at the location of tile drain or subsurface irrigation pipe, (L).

The flow term, Q_{td}, is negative in modeling tile drains and positive in modeling subsurface irrigation.

The conductance term, C_{td}, can be expressed as

$$C_{td} = \frac{K_{td}}{d_{td}} A_{td} \tag{2.17}$$

where

K_{td} = hydraulic conductivity of the interface material between the tile drain/subsurface irrigation pipe and aquifer material, (L/T);

d_{td} = thickness of the interface material, (L);

A_{td} = effective area through which tile drain outflow or subsurface irrigation inflow is occurring, (L^2).

If dependable field measurements are available, they may be used to calculate the conductance, C_{td}. In many cases, however, a conductance value must be chosen somewhat arbitrarily and adjusted during model calibration.

2.3. Land Subsidence

IWFM accounts for changes in storage due to land subsidence. The change in soil structure, which causes subsidence, primarily occurs from pumping large amounts of groundwater in a given area. Modeling land subsidence is an important feature of IWFM since storage changes impact the available water supply.

The change in storage can be temporary or permanent, depending upon the amount of stress placed on the soils. A temporary change in storage means that the soils were not permanently displaced and the elasticity of the soil is preserved. Given the compaction is elastic, the soil may still expand. Extraction of large amounts of water from the aquifer may increase the effective stress of the soils beyond a threshold value, causing permanent displacement of soils and a permanent decrease in the storage capacity of the aquifer.

IWFM calculates the groundwater head changes due to subsidence in relation to the vertical compaction of interbeds. Interbeds are lenses that have poor permeability within a relatively permeable aquifer. The following three items are used as criteria when defining an interbed (Leake and Prudic, 1988):

- The hydraulic conductivity of the interbed is significantly lower than the hydraulic conductivity of the aquifer material.
- The lateral extent of the interbed must be small enough so that it is not considered a confining bed that separates adjacent aquifers.
- The interbed thickness must be small in comparison to its lateral extent.

Land subsidence is a function of the change in the effective stress, elastic and inelastic specific storages of the interbed, and the initial interbed thickness, given that the geostatic and the hydrostatic pressures over the interbed are constant. The elastic change in the interbed thickness can be written as (Riley, 1969; Helm, 1975)

$$\Delta b_{se} = \frac{\Delta p'}{\gamma_w} S_{se} b_o \tag{2.18}$$

where

Δb_{se} = elastic change in interbed thickness, positive for compaction and negative for expansion, (L);

$\Delta p'$ = change in effective stress, positive for increase and negative for decrease, (F/L^2);

γ_w = unit weight of water, (F/L^3);

S_{se} = elastic specific storage, (1/L);

b_o = the initial thickness of the interbed, (L).

For an interbed located in an aquifer where geostatic pressure is constant, the change in effective stress as a function of the change in head can be expressed as (Poland and Davis, 1969)

$$\Delta p' = -\gamma_w \Delta h \tag{2.19}$$

where

Δh = change in head; positive for increase and negative for decrease in head, (L).

Substituting (2.19) into (2.18), one can express the change in interbed thickness in terms of change in the head as

$$\Delta b_{se} = -\Delta h S_{se} b_o \tag{2.20}$$

Similarly, inelastic change in the interbed thickness can be approximately related to the change in head at an aquifer where geostatic pressure is constant as (Leake and Prudic, 1988)

$$\Delta b_{si} = -\Delta h S_{si} b_o \tag{2.21}$$

where

Δb_{si} = inelastic change in interbed thickness, positive for compaction and negative for expansion, (L);

S_{si} = inelastic specific storage, (1/L).

The total compaction, i.e. elastic and inelastic compaction, can be computed by adding the elastic and inelastic compactions computed by equations (2.20) and (2.21).

Equations (2.20) and (2.21) require that the geostatic pressure in the aquifer is constant. Geostatic pressure is constant in confined aquifers but it changes in an unconfined aquifer as the water table fluctuates. In IWFM it is assumed that the change in geostatic pressure is negligible in unconfined aquifers so that equations (2.20) and (2.21) can be used for modeling the land subsidence in unconfined as well as confined

aquifers. Normally, the compaction is less for an unconfined aquifer compared to the compaction in a confined aquifer. By using the assumption that equations (2.20) and (2.21) are applicable to unconfined aquifers, the actual compaction in unconfined aquifers is slightly overestimated in IWFM.

2.3.1. Flow into Groundwater Storage due to Land Subsidence

The groundwater flow equation used in IWFM is given in equation (2.15). The first term on the right hand side of equation (2.15) represents the flow rate into groundwater storage due to fluctuating head values. To incorporate the flow into storage due to interbed compaction, an additional term, q_{sd}, has been included in equation (2.15). This additional term can be expressed as (Leake and Prudic, 1988)

$$q_{sd} = S_s^{'} \frac{\partial h}{\partial t} \tag{2.22}$$

where

q_{sd} = rate of flow into or out of storage due to compaction or expansion of interbeds, (L/T);

$S_s^{'}$ = skeletal storativity of interbeds, (dimensionless).

The skeletal storativity value in (2.22) varies between the elastic and inelastic specific storage values multiplied by the interbed thickness, b_o, depending on the relation of the head to the pre-consolidation head. If the head is above the pre-consolidation head, $S_s^{'}$ takes the value of elastic specific storage multiplied by the interbed thickness and if the head falls below the pre-consolidation head, it takes the value of inelastic

specific storage multiplied by the interbed thickness:

$$S_s^{'} = \begin{cases} S_{se} b_o & \text{if } h > h_c \\ \\ S_{si} b_o & \text{if } h \le h_c \end{cases} \tag{2.23}$$

where

h_c = pre-consolidation head.

The pre-consolidation head value is also adjusted during the simulation period. It is assigned the most recent lowest head value if the head falls below the pre-compaction head. Equations (2.15) and (2.22) reveal that when the rate of change of groundwater head is positive (i.e. increasing groundwater head) flow out of the storage will occur due to expansion of the interbeds. If the rate of change of head is negative (i.e. decreasing groundwater head) flow into the groundwater storage will occur due to the compaction of the interbeds. If the head falls below the pre-consolidation head, h_c, the compaction is irreversible. If the head stays above the pre-consolidation then the interbeds will expand again upon recharge of the aquifer.

2.4. Root Water Uptake from Groundwater

Shallow groundwater can contribute to the plant evapotranspiration and meet part or all of the evapotranspirative demand. In IWFM, the part of the capillary rise above the saturated groundwater table and the saturated groundwater itself that intersect with the root zone is considered to be the maximum potential contribution of groundwater to evapotranspiration. The height of the capillary rise is specified by the user. It is further assumed that the soil moisture is at total porosity at groundwater table and decreases

linearly to zero at a height equal to the capillary rise above the groundwater table. The actual amount of root water uptake from groundwater is calculated as part of the land surface and root zone flow processes that are simulated by the *IWFM Demand Calculator* (IDC) within IWFM. These processes as well as the root water uptake from groundwater are explained in detail in a separate document for IDC (DWR, 2015).

2.5. Initial and Boundary Conditions for the Groundwater

The solution of the groundwater flow equation (2.15) requires specification of boundary and initial conditions, which constrain the problem and make solutions unique. Initial and boundary conditions are not only necessary in solving the groundwater equation, but the accuracy is important as well. If inconsistent or incomplete boundary conditions are specified, the problem is ill defined (Wang and Anderson, 1982).

2.5.1. Initial Conditions

The solution of equation (2.15) requires the knowledge of groundwater head values at the beginning of the simulation period. Therefore, $h(x, y, t = 0)$ needs to be specified for all aquifer layers by the user.

2.5.2. Specified Flux (Neumann)

A Neumann boundary condition is applied when the flow is known across surfaces bounding the domain. Given a specified flux boundary, the flux normal to the

boundary is prescribed for all the points of the boundary as a function of location and time:

$$q_\Gamma = -T\frac{\partial h}{\partial n} = f\left(x, y, t\right) \tag{2.24}$$

where

q_Γ	=	specified flux at the boundary, (L^2/T);
T	=	transmissivity, (L^2/T);
h	=	groundwater head at the boundary, (L);
n	=	distance that is measured perpendicular and outward to the boundary, (L);
f(x,y,t)	=	known function for all points on the part of the boundary where flux is specified, (L^2/T).

This type of boundary condition typically occurs in an aquifer adjacent to bedrock, where there is no flux. Aquifers adjacent to another source of water with fixed flux into or out of the aquifer system also involve this type of boundary condition.

2.5.3. Specified Head (Dirichlet)

A Dirichlet boundary condition is set when the hydraulic head is known for surfaces bounding the flow domain. This type of boundary condition assumes a constant head value for the designated points of the boundary. For instance, a specified head boundary may occur when the flow domain is adjacent to an open body of water. At every point on this type of boundary, the piezometric head is the same as the head in the

aquifer at the point adjacent to it. In groundwater flow, this occurs at the interface between a saturated porous medium and a river, lake or sea (Bear, 1972).

2.5.4. General Head

The general head boundary condition is applied when the head value is known at a distance from the boundary nodes. The known head value is usually at a body of water located at a given distance from the boundary nodes. It can also come from a subsurface source, such as the groundwater head at a nearby groundwater basin. The general head boundary inflow at a finite element node can be expressed as

$$Q_{GHB} = \frac{K_{\Gamma} A_{\Gamma}}{d_{\Gamma}} \left(h_{GHB} - h_{\Gamma} \right) \tag{2.25}$$

where

Q_{GHB} = general head boundary flow, (L^3/T);

K_{Γ} = hydraulic conductivity of the aquifer at the boundary, (L/T);

A_{Γ} = cross-sectional area at the boundary that flow passes through, (L^2);

d_{Γ} = distance between the boundary and the location of the known head, (L);

h_{Γ} = head value at the boundary, (L);

h_{GHB} = head at the nearby surface water body or aquifer, (L).

2.5.5. Constrained General Head

The constrained general head boundary condition is introduced in IWFM to

simulate, for instance, the stream-aquifer or lake-aquifer interaction when the groundwater simulation component is linked to models other than IWFM or stream/lake elevations are computed outside IWFM and used as input as general head boundary conditions. In a regular general head boundary condition, groundwater head value at the boundary, h_Γ, is a continuous function of space (see equation (2.25)). In a constrained general head boundary condition, there exists a limiting head value:

$$Q_{CGHB} = \begin{cases} \dfrac{K_\Gamma A_\Gamma}{d_\Gamma}\left(h_{GHB} - h_\Gamma\right) & \text{if} \quad h_\Gamma \geq h_{C\Gamma} \\ \\ \dfrac{K_\Gamma A_\Gamma}{d_\Gamma}\left(h_{GHB} - h_{C\Gamma}\right) & \text{if} \quad h_\Gamma < h_{C\Gamma} \end{cases} \tag{2.26}$$

where

Q_{CGHB} = constrained general head boundary flow, (L^3/T);

$h_{C\Gamma}$ = limiting head value at the boundary, (L).

As an example, $h_{C\Gamma}$ can be set to the stream bed elevation in a situation where stream surface elevations are computed outside of IWFM by an external stream model and are used to represent h_{GHB} in equation (2.26). In such a case, if the groundwater head, h_Γ, falls below the stream bed elevation, $h_{C\Gamma}$, equation (2.26) ensures that stream-aquifer interactions are computed properly.

Additionally, Q_{CGHB} in equation (2.26) can be limited with a maximum flow value:

$$Q_{CGHB} \leq Q_{CGHB_{max}} \tag{2.27}$$

For instance, this might be the case when stream-aquifer interaction is simulated

using stream elevations computed outside of IWFM by another model. These stream elevations might correspond to stream flows which might be less than Q_{CGHB} computed using equation (2.26). Therefore, equation (2.27) guarantees that stream-aquifer interactions are limited by the maximum available stream flows, $Q_{CGHB_{max}}$, when streams are losing.

2.6. Stream Flows

Streams are an important component of the hydrological cycle. During the periods when groundwater heads are low, they contribute water to the groundwater and during periods when the groundwater heads are high, they drain water away (Figure 2.6). In regions where agricultural and urban development is high, they are also used as a source of water supply. A portion of the water that is diverted from the streams and used to meet agricultural and urban water demands seeps into the groundwater at locations far from streams. This further complicates the stream-groundwater system.

IWFM offers three separate versions of stream routing components within the stream package that simulate the stream flows as a function of inflows from the upstream tributaries and reaches, surface runoff, agricultural and urban return flow, diversions and bypasses, flow from upstream lakes and the exchange of water between the stream and the groundwater. These versions differ in how the stream wetted perimeter is calculated and if the storage in the stream is tracked or not. Table 2.2 lists the features and properties of each of the stream routing component.

The stream system is divided into segments that are termed *stream reaches*. Each

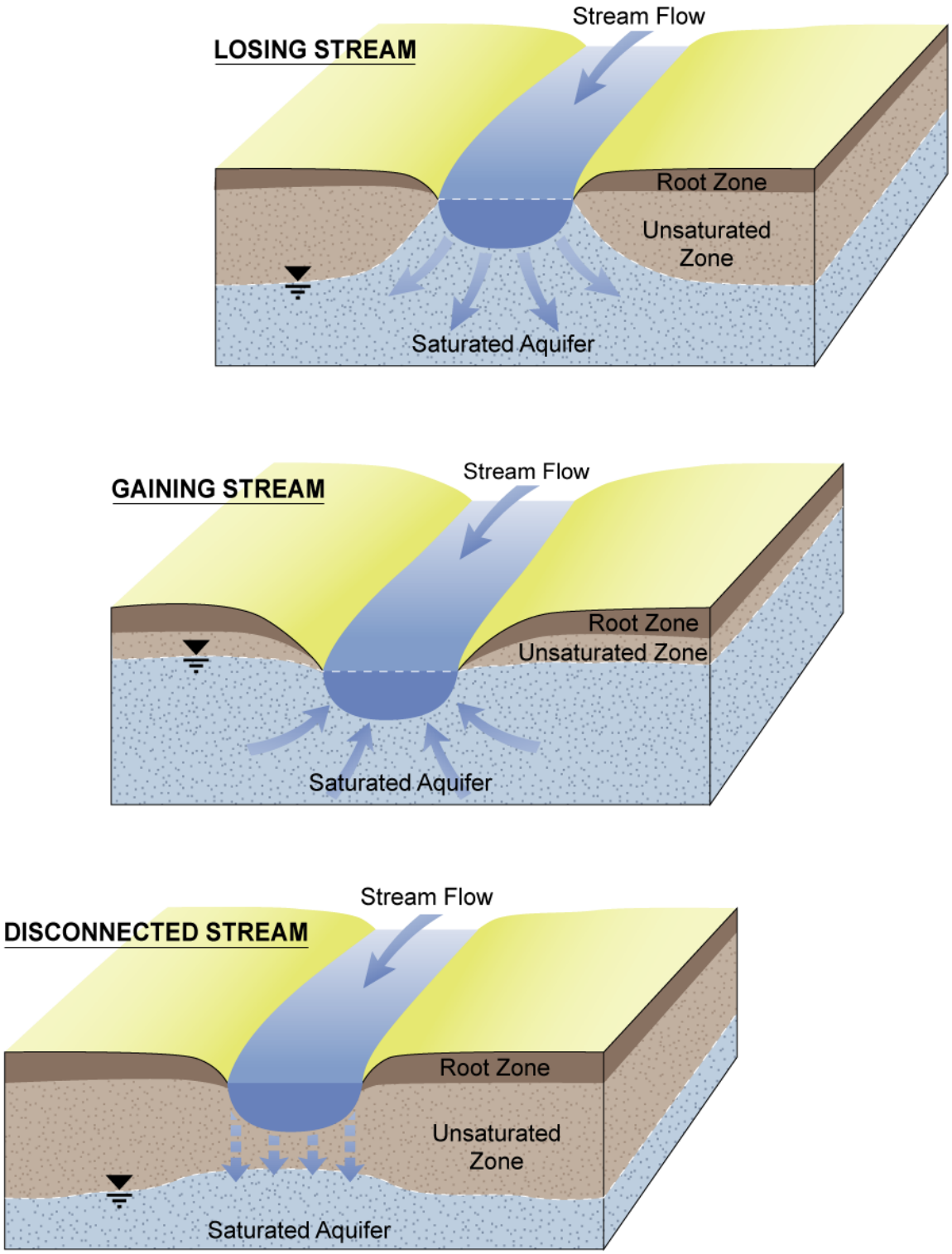

Figure 2.6 Stream-groundwater interaction scenarios

reach consists of multiple stream nodes. Each stream node represents a section of the stream reach which is termed as *stream segment*. Stream flows are simulated at each stream node. An example of the representation of a natural stream system by stream nodes and stream segments is depicted in Figure 2.7. In Figure 2.7.c, stream segments that are represented by stream nodes are shown between two consecutive dash lines. It should be noted that at a confluence there are as many nodes as the number of stream reaches meeting at the confluence. Even though stream nodes at a confluence are located

Version	Features
4.0	• Instantaneous routing (storage is not tracked) of stream flows • Flow- stage relationship is specified using a rating table • Wetted perimeter at each stream node is constant and does not change with respect to stream stage
4.1	• Instantaneous routing of stream flow (same as version 4.0) • Flow -stage relationship is specified as a rating table (same as version 4.0) • Simulation of wetted perimeter as a function of stage; wetted perimeter-stage relationship is specified using a rating table • Ability to simulate flow over flood plains through proper specification of wetted perimeter-stage rating table
5.0	• Kinematic wave routing to simulate stream flows and to track storage change in the stream channel • Simulation of flow in rectangular, triangular and trapezoidal channels • Flow-stage relationship is represented by the Manning's equation • Wetted perimeter is calculated as a function of stage and channel geometry

Table 2.2 Version numbers and features of the stream routing components

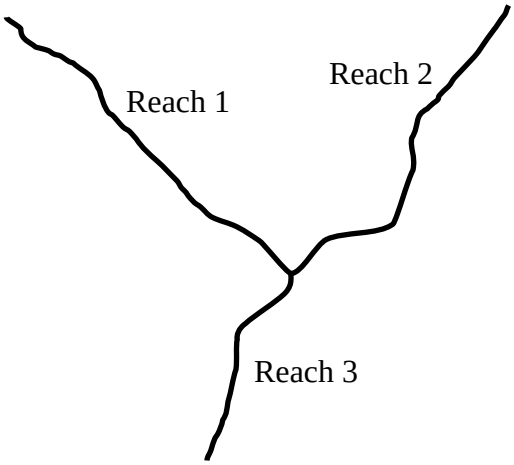

(a) Example of a natural stream system

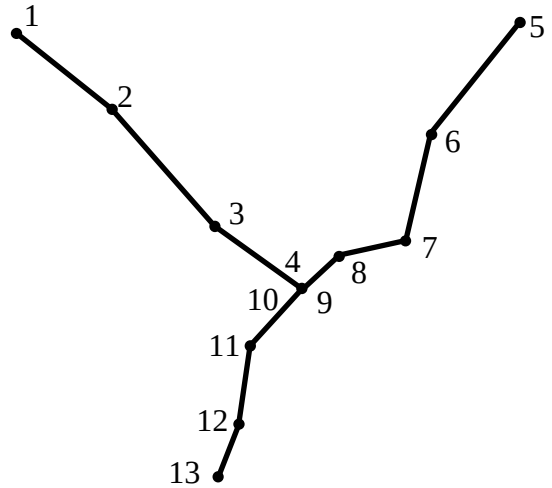

(b) Representation of the stream system with stream nodes

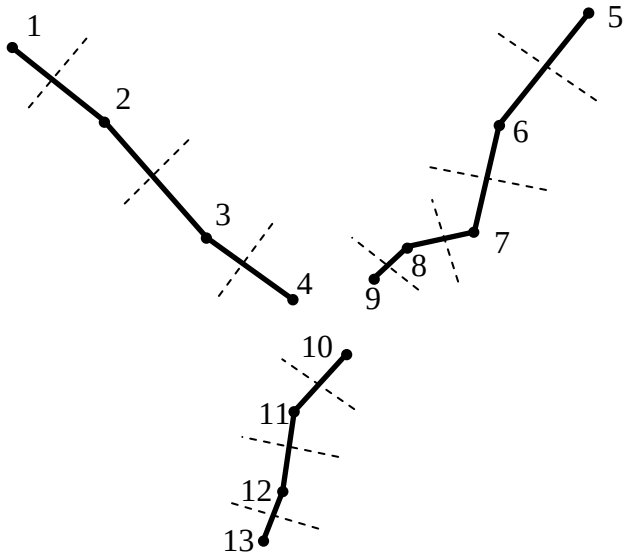

(c) Stream segments associated with each node

Figure 2.7 Representation of a natural stream system by stream nodes and stream segments in IWFM

at the same coordinates, the stream segments that they represent are different (Figure 2.7.c).

Simulation of stream flows is different in each of the stream routing component. The methods used in each of these components to route stream flows are explained in the next sections.

2.6.1. Stream Flow Routing in Component Version 4.0

In this version of stream routing component, it is assumed that stream flow travels through the stream network instantaneously and, therefore, change in storage within the stream channel is not tracked. This assumption is valid when the characteristic travel time of a wave through the entire modeled stream network is less than the time step used in the simulation of the hydrologic system. For instance, the zero-storage assumption can be used if a wave travels from the upstream end to downstream end of the modeled stream network within a week while a monthly simulation time step is used.

The continuity equation where storage at stream node *i* is assumed to be zero is expressed as

$$0 = Q_{in} - Q_{out} \tag{2.28}$$

and

$$Q_{in} = \sum_j Q_{s_j} + R_f + S_r + Q_{ws} + Q_{brs} + Q_{td} + Q_{lko} + Q_h \tag{2.29}$$

$$Q_{out} = Q_{rip} + Q_{bdiv} + Q_{sint} + Q_{s_i} \tag{2.30}$$

$$Q_{bdiv} = Q_b + Q_{div} \tag{2.31}$$

where

Q_{s_j} = flow from upstream node *j*, (L^3/T);

R_f = surface water return flow from agricultural irrigation and urban water use, (L^3/T);

S_r = direct runoff due to rainfall excess and subsurface flow that seeps onto the ground surface, (L^3/T);

Q_{ws} = inflow from the tributaries to the stream node (see small stream boundary conditions), (L^3/T);

Q_{brs} = inflow from bypasses, (L^3/T);

Q_{td} = inflow from tile drains, (L^3/T);

Q_{lko} = inflow due to lake overflow (see the discussion on lakes for the computation of this term), (L^3/T);

Q_h = inflows other than those listed above, (L^3/T);

Q_{rip} = outflow due to riparian vegetation evapotranspiration, (L^3/T);

Q_b = outflow that is diverted as bypass flow, (L^3/T);

Q_{div} = flow that is diverted for agricultural and urban water use, (L^3/T);

Q_{sint} = rate of water exchange between the stream and the groundwater, (L^3/T);

Q_{s_i} = net flow at stream node *i* that contributes to the flow at the downstream node, (L^3/T).

The number of stream nodes that are considered in the summation term on the right hand side of equation (2.29) depends on the location of the stream node *i* (Figure

2.7). If node *i* is in the middle of a stream reach, there will be only one upstream node from which flow will be contributing to the flow at node *i*. On the other hand, if node *i* is located at a confluence, then there will be as many upstream nodes as the number of upstream reaches meeting at the confluence. As an example, consider node 3 of reach 1 in Figure 2.7.c. Writing equation (2.29) for node 3, only node 2 will appear as upstream node. On the other hand, writing equation (2.29) for node 10, nodes 4 and 9 will appear as the upstream nodes.

Substituting equation (2.30) into equation (2.28) and rearranging, one obtains

$$Q_{s_i} - Q_{in} + Q_{rip} + Q_{bdiv} + Q_{s\,int} = 0 \tag{2.32}$$

In IWFM, stream flows are related to stream surface elevations through a rating curve:

$$Q_{s_i} = Q_{s_i}\left(h_{s_i}\right) \tag{2.33}$$

where

h_{s_i} = elevation of the stream surface at stream node *i* with respect to a common datum, (L).

2.6.1.a. Stream-Groundwater Interaction in Component Version 4.0

The stream-groundwater interaction is included in IWFM to capture its effect on stream flows and groundwater heads. The exchange of water between the stream and the groundwater along a stream segment is modeled in this version of the stream routing component approximately as (McDonald and Harbaugh, 1988)

$$Q_{sint} = C_{s_i}\left[\max\left(h_{s_i}, h_{b_i}\right) - \max\left(h, h_{b_i}\right)\right] \tag{2.34}$$

where

Q_{sint} = stream-groundwater interaction, (L^3/T);

C_{s_i} = conductance of the streambed material at stream node *i*, (L^2/T);

h_{s_i} = stream surface elevation, (L);

h = groundwater head at stream node *i*, (L);

h_{b_i} = elevation of the stream bottom at node *i*, (L);

The conductance of the stream bed material that appear in (2.34) can be expressed as

$$C_{s_i} = \frac{K_{s_i}}{d_{s_i}} L_i W_i = \frac{K_{s_i}}{d_{s_i}} A_{s_i} \tag{2.35}$$

where

K_{s_i} = hydraulic conductivity of the stream bed material, (L/T);

d_{s_i} = thickness of the stream bed material, (L);

L_i = length of the stream segment represented by stream node *i*, (L);

W_i = wetted perimeter, (L);

A_{s_i} = effective area of the stream segment represented by node *i* through which stream-groundwater interaction occurs, (L^2).

In version 4.0 of the stream routing component it is assumed that the stream channels are rectangular and wide enough with respect to stream flow depth so that the wetted perimeter, W_i, can be taken as a constant at each stream node. It should also be

noted that Q_{sint} and A_{s_i} that appear in equations (2.34) and (2.35) are the same terms that appear in the groundwater conservation equation (2.15). Stream flow equation (2.32) is coupled with groundwater conservation equation (2.15) through the stream-groundwater interaction term, Q_{sint}. In order to compute groundwater heads, stream flows and stream-groundwater interaction properly, it is necessary to solve equations (2.15) and (2.32), simultaneously. The solution methodology used in IWFM will be discussed in detail later in this document.

2.6.2. Stream Flow Routing in Component Version 4.1

Assumptions and stream flow routing in component version 4.1 are exactly the same as in component version 4.0 (see section 0) except for the calculation of stream-aquifer interaction. Equation (2.32) is used to simulate the stream flow along with equation (2.33) that is given as a rating table which defines the relationship between the stream flow and stream surface elevation.

2.6.2.a. Stream-Groundwater Interaction in Component Version 4.1

In component version 4.1, stream-aquifer interaction and the stream bed conductance are still expressed using equations (2.34) and (2.35), respectively. Wetted perimeter, W_i, on the other hand is related to the stream surface elevation or the groundwater head at the stream node, whichever is greater, through a rating table:

$$W_i = W_i\left[\max\left(h_{s_i}, h\right)\right] \tag{2.36}$$

This approach, along with the stream flow-stream surface elevation rating table, allows the representation of stream flow through channels with a wide variety of cross-section geometries. For instance, stream flows as well as the stream-aquifer interactions through flood plains along a stream channel can easily be represented using rating tables expressed in equations (2.33) and (2.36).

2.6.3. Stream Flow Routing in Component Version 5.0

Component versions 4.0 and 4.1 do not track the change in storage at a stream channel. As mentioned earlier, this approach can be used when the simulation time step (e.g. a month) is larger than the characteristic travel time (e.g. a week) of a wave through the modeled stream network. However, it is sometimes necessary to use a shorter time step to simulate other flow processes more accurately. An example is the simulation of land surface and root zone flow processes where the characteristic time scales range from a few hours to a day. Using short time step such as a day to simulate these flow processes more accurately may invalidate the zero-storage approach for the simulation of stream flows. To remedy this problem, component version 5.0 keeps track of the change in storage within the stream channel and the stream flow is routed through the stream network using the kinematic wave approach.

The governing conservation equation for stream flow can be expressed as follows (Chaundry, 1993):

$$\frac{\partial Q_s}{\partial x} + \frac{\partial A}{\partial t} = \frac{Q_{in} - Q_{out}}{L} \tag{2.37}$$

where

Q_s = stream flow, (L^3/T);

A = flow cross-sectional area, (L^2);

L = length of the stream channel, (L);

x = direction along the stream channel, (L);

t = time, (T).

To solve equation (2.37), a relationship between the stream flow, Q_s, and the flow cross-sectional area, A, must be defined. For this purpose, stream routing component version 5.0 uses Manning's equation (Chaundry, 1993):

$$Q_s = \frac{\gamma}{n} A R^{2/3} \sqrt{S_f} \tag{2.38}$$

where

n = Manning's roughness coefficient, ($T/L^{1/3}$);

R = hydraulic radius, (L);

S_f = slope of the energy line, (L/L);

γ = conversion factor (e.g. γ = 1.0 if SI units are used, γ = 1.49 if foot-pound-second units are used).

Component version 5.0 uses the kinematic wave approach in which the slope of the energy line, S_f, is represented with the slope of the stream bed, S_o. Using the kinematic wave approach, equation (2.38) can be expressed as

$$Q_s = \frac{\gamma}{n} A R^{2/3} \sqrt{S_o} \tag{2.39}$$

Kinematic waves travel along the stream channel without any diffusion as long as the wave celerity, $c = \frac{dQ_s}{dA}$, stays constant. Additionally, they travel only in the downstream direction so backwater effects due to confluences or hydraulic structures cannot be simulated.

Stream routing component version 5.0 allows flow routing in rectangular, trapezoidal and triangular channels. The stream channel can have different cross-section and physical parameters (i.e. channel slope and Manning's roughness) at different stream nodes. Figure 2.8 shows the cross-section of a trapezoidal channel with the relevant parameters to calculate the flow area, wetted perimeter and hydraulic radius. According to Figure 2.8, when s = 0 the channel has a rectangular cross-section. If B = 0, then the channel has a triangular cross-section. Based on Figure 2.8 flow area, wetted perimeter and hydraulic radius can be represented generically for all rectangular, trapezoidal and triangular cross sections as follows:

$$A = y_s\left(B + sy_s\right) \tag{2.40}$$

$$W = B + 2y_s\sqrt{1+s^2} \tag{2.41}$$

$$R = \frac{A}{W} = \frac{y_s\left(B + sy_s\right)}{B + 2y_s\sqrt{1+s^2}} \tag{2.42}$$

$$y_s = h_s - h_b \tag{2.43}$$

where

y_s = stream flow depth, (L);

h_b = stream bed elevation, (L).

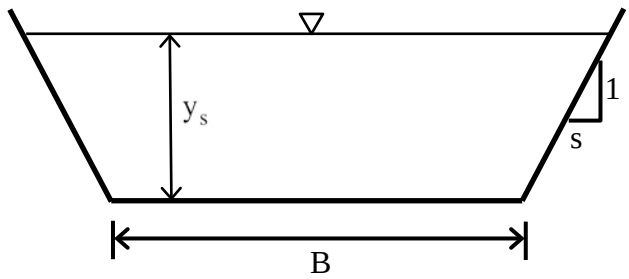

Figure 2.8 A trapezoidal channel cross-section and relevant parameters

Using equations (2.39) - (2.43) along with the conservation equation (2.37), stream routing component version 5.0 routes stream flow through the simulated stream network .

2.6.3.a. Stream-Groundwater Interaction in Component Version 5.0

Stream-groundwater flow exchange in component version 5.0 is calculated using equations (2.34) and (2.35) along with equation (2.41) to represent the wetted perimeter, W. Similar to component version 4.0, flood plains along stream channels cannot be represented in component version 5.0.

2.6.3.b. Initial Conditions

Unlike versions 4.0 and 4.1 where change in storage in the stream channel is not tracked, version 5.0 requires the specification of initial stream flow or stream flow depth to calculate the initial storage within the stream network. Therefore, $h_s(t=0)$ needs to be specified along the stream by the user.

2.6.4. Diversions and Bypass Flows

In general, diversion rates and bypass flows that occur at a stream node are pre-specified values. In certain occasions bypass flows can also be specified through a rating curve that renders them as a function of the stream flow. If there is enough flow at the stream node so that the total of the diversion and bypass flows can be taken out of the stream, the pre-specified values remain unchanged. If the stream flow is not enough for the required diversion and bypass flows, it is necessary to compute how much of the specified flows can actually be taken out of the stream. To achieve this, it is assumed that diversions occur before the bypass flows. After the diversion flows are taken out of the stream flow, bypass flows are allowed to be taken out of the stream. As such, defining the required diversion and bypass flow rates as Q_{divreq} and Q_{breq}, respectively, one can compute the actual diversion and bypass flow rates that take place at stream node *i* as

$$Q_{div} = \begin{cases} Q_{divreq} & \text{if } Q_{in} \geq Q_{divreq} \\ Q_{in} & \text{if } Q_{in} < Q_{divreq} \end{cases} \tag{2.44}$$

$$Q_b = \begin{cases} Q_{breq} & \text{if } Q^*_{s_i} \geq Q_{breq} \\ Q^*_{s_i} & \text{if } Q^*_{s_i} < Q_{breq} \end{cases} \tag{2.45}$$

where

$$Q^*_{s_i} = Q_{in} - Q_{div} \tag{2.46}$$

and Q_{in} is given by equation (2.29). Equations (2.44)-(2.46) reveal that diversions and bypasses are assumed to take place before the stream-groundwater interaction which is detailed in the following section.

2.7. Lakes

Lakes and similar large water bodies are as important in the hydrological cycle as the groundwater and streams. Lakes interact with groundwater and streams, and can affect the groundwater heads and stream flows drastically. For this reason, the capability of modeling lake storage and its interaction with groundwater and streams has been included in IWFM. Figure 2.9 shows some of the hydrological components modeled in IWFM that affect the lake storage.

The conservation equation for lake storage can be expressed as

$$\frac{\partial S_{lk}}{\partial t} - \sum_{i=1}^{N_{lk}} \left(P_{lk_i} A_{lk_i} - EV_{lk_i} A_{lk_i} - Q_{lkint_i} \right) - Q_{divlk} - Q_{bplk} - Q_{rflk} - Q_{rtlk} - Q_{inlk} + Q_{lko} = 0 \tag{2.47}$$

where

S_{lk}	=	lake storage, (L^3);
i	=	lake node that represents an area of lake, (dimensionless);
N_{lk}	=	total number of lake nodes that represent the entire lake area, (dimensionless);
P_{lk_i}	=	precipitation onto the lake area represented by node *i*, (L/T);

EV_{lk_i} = evaporation from the lake area represented by node *i*, (L/T);

Q_{lkint_i} = lake-groundwater interaction, (L^3/T);

A_{lk_i} = lake area represented by node *i*, (L^2);

Q_{divlk} = inflow from stream diversions, (L^3/T);

Q_{bplk} = inflow from bypass flows, (L^3/T);

Q_{rflk} = rainfall runoff into the lake, (L^3/T);

Q_{rtlk} = inflow into the lake due to the return flow of agricultural and urban applied water, (L^3/T);

Q_{inlk} = inflow from upstream lakes, (L^3/T);

Q_{lko} = outflow from lake in case lake surface elevation exceeds a pre-specified maximum elevation, (L^3/T);

t = time, (T).

As can be seen in equation (2.47), diversion and bypass flows can be set as inflow to the lake. Additionally, rainfall runoff and return flow of applied water can be directed into the lakes. At a lake node *i*, evaporation rate is pre-specified as a function of time. Furthermore, lake storage is related to the lake surface elevation through a rating table:

$$S_{lk} = S_{lk}\left(h_{lk}\right) \quad ; \quad h_{lk} \le h_{lk_{max}} \tag{2.48}$$

where

h_{lk} = elevation of lake surface, (L);

$h_{lk_{max}}$ = maximum elevation of lake surface, (L).

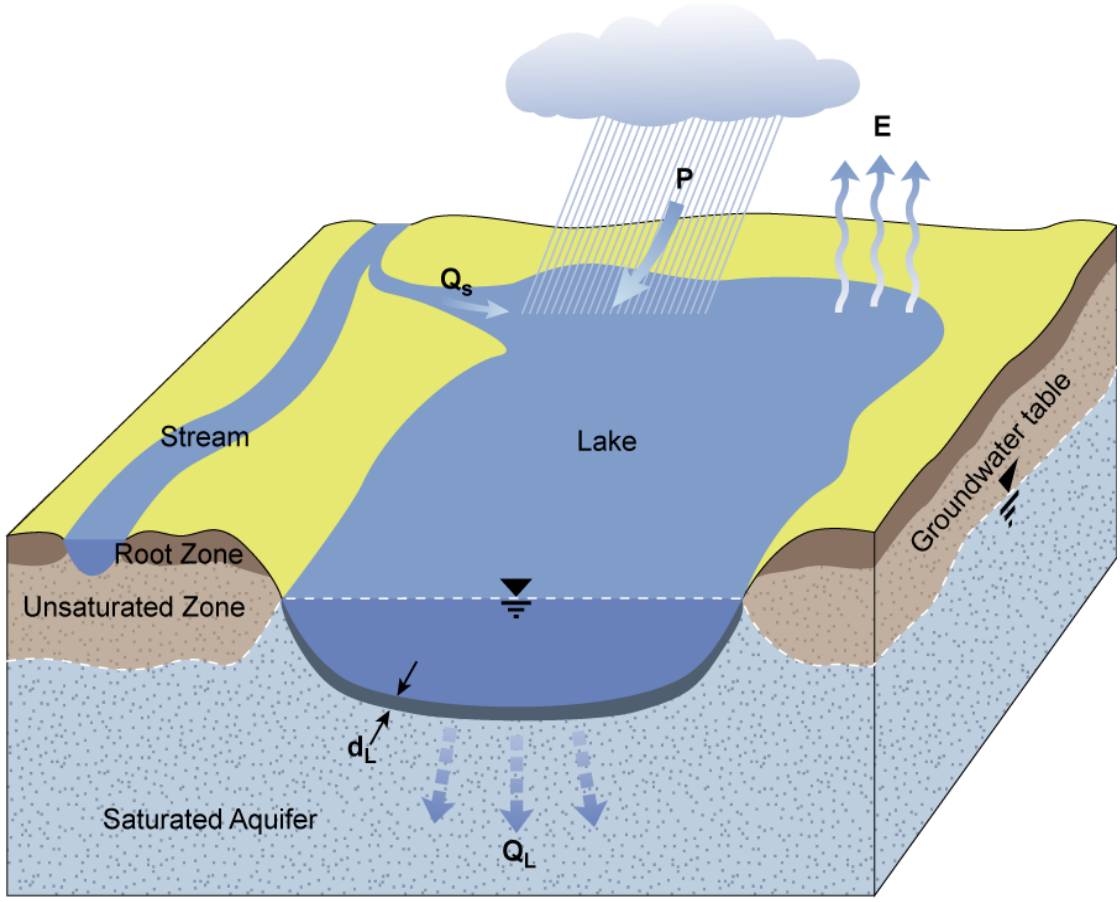

LEGEND

P..... *Precipitation*

E..... *Evaporation*

d_L.....*Thickness of the lake bed*

Q_s... *Streamflow into lake*

Q_L... *Lake-groundwater interaction*

Figure 2.9 Hydrological components that affect lake storage

If the lake surface elevation exceeds the maximum elevation, the excess water becomes lake outflow, Q_{lko}. This outflow can be directed into a stream node or into a downstream lake.

2.7.1. Lake-Groundwater Interaction

Similar to stream-groundwater interaction, lake-groundwater interaction can be expressed as

$$Q_{lkint_i} = C_{lk_i}\left[\max\left(h_{lk}, h_{blk_i}\right) - \max\left(h, h_{blk_i}\right)\right] \tag{2.49}$$

where

Q_{lkint_i} = lake-groundwater interaction, (L^3/T);

C_{lk_i} = conductance of the lake bed material at lake node *i*, (L^2/T);

h_{lk} = lake surface elevation, (L);

h = groundwater head at lake node *i*, (L);

h_{blk_i} = elevation of the lake bottom at node *i*, (L);

The conductance of the lake bed material that appear in (2.49) can be expressed as

$$C_{lk_i} = \frac{K_{lk_i}}{d_{lk_i}} A_{lk_i} \tag{2.50}$$

where

K_{lk_i} = hydraulic conductivity of the lake bed material, (L/T);

d_{lk_i} = thickness of the lake bed material, (L).

It should be noted that Q_{lkint_i} and A_{lk_i} that appear in equations (2.49) and (2.50) are the same terms that appear in the groundwater conservation equation (2.15). Lake storage equation (2.47) is coupled with groundwater conservation equation (2.15) through the lake-groundwater interaction term, Q_{lkint_i}. In order to compute groundwater heads, lake storage and lake-groundwater interaction properly, it is necessary to solve equations (2.15) and (2.47), simultaneously. The solution methodology used in IWFM will be discussed in detail later in this document.

2.8. Land Surface and Root Zone Flow Processes

Precipitation is the natural source for the replenishment of groundwater, stream flows and lake storage. The amount of precipitation that falls directly on the streams and lakes contributes to stream flow and lake storage immediately. Precipitation that falls on the ground surface infiltrates into the soil at a rate dictated by the type of ground cover, physical characteristics of the soil and the soil moisture content. The portion of the precipitation that is in excess of the infiltration rate generates a surface flow and runs towards nearby streams, lakes or other bodies of water in the direction dictated by the contours of the ground surface. In situations where groundwater table rises high enough and intersects with the ground surface, the groundwater seeps onto the surface contributing to the surface flow generated by the precipitation in excess of infiltration (Dunne, 1978). In IWFM, the surface flow generated through these means is termed as *direct runoff*. Direct runoff can also infiltrate into the soil further down the slope or evaporate before it even reaches a nearby body of water. However, modeling this

complex nature of direct runoff requires highly detailed information on physical characteristics of the soil, ground cover, topography, evaporation patterns, etc. This information is generally not available at the scale that IWFM is designed for. Therefore, the infiltration and evaporation of direct runoff on its course to a nearby body of water are neglected in IWFM. Instead, once the direct runoff is computed it is immediately carried to a pre-specified location such as a stream or a lake.

Irrigation of agricultural lands and urban outdoor water use also follow similar infiltration and runoff patterns of precipitation. In IWFM the surface flows generated by the agricultural irrigation and urban water use is termed as *return flow*. Return flow generated by agricultural irrigation runs in the direction dictated by the contours of the ground surface, whereas return flow generated by the urban water use generally follow man-made structures. In both cases, IWFM treats return flows similar to the direct runoff and these flows are immediately carried to a pre-specified location.

Even though groundwater table can rise and intersect with the ground surface saturating the entire soil profile, an unsaturated zone generally exists between the ground surface and the groundwater table. An unsaturated zone is defined as the soil profile where pore space saturation is less than 100%. The water from precipitation and irrigation water that infiltrate into the soil have to flow through this unsaturated zone before reaching the groundwater as recharge. The top layer of this unsaturated zone designated by the depth of the plant roots through which moisture is drawn out of the soil is called the *root zone*. As moisture in the root zone flows downward due to the gravitational force, it is also drawn out of the soil through plant roots for transpiration and the process of evaporation. The combined processes of plant root uptake for transpiration

purposes and evaporation is termed as *evapotranspiration*. Figure 2.10 illustrates an example of a system of root zone and unsaturated zone, and the hydrological processes in these zones as it is modeled in IWFM. To connect the groundwater system with the surface flow processes, simulation of storage and flow through the root zone and unsaturated zone is necessary. In general, moisture in the root and unsaturated zones can move in horizontal direction as well as the vertical direction. In IWFM, it is assumed that the horizontal movement of the moisture in the root and unsaturated zones is negligible compared to the vertical movement, therefore only the flow of the moisture in the vertical direction is addressed. To increase the accuracy of the simulated vertical flow, IWFM

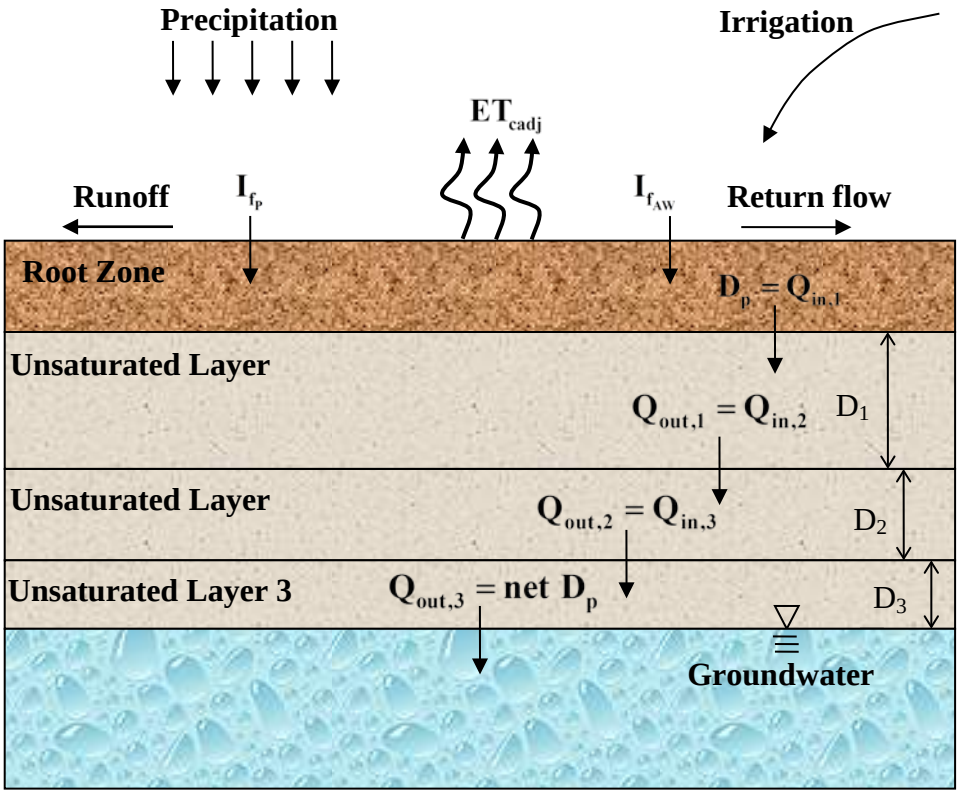

Figure 2.10 Schematic representation of flow through the root zone and

has the functionality to separate the unsaturated zone into multiple layers (Figure 2.10). The moisture that leaves the root zone and enters the unsaturated zone is termed as *deep percolation*. The moisture travels downward through the unsaturated zone and eventually recharges the groundwater. The groundwater recharge is named as *net deep percolation* (Figure 2.10). As the groundwater rises through net deep percolation, the unsaturated zone between the root zone and the water table becomes smaller and the groundwater can start contributing to the plant evapotranspiration. This process of the plants drawing some or all of their evapotranspirative needs from the groundwater is referred as the *root water uptake from groundwater* and is already described in section 2.4. Root water uptake from groundwater is generally controlled and minimal in agricultural areas to promote vertical drainage in the root zone, and hence, leaching of the soils. On the other hand, root water uptake from groundwater can be substantial in areas with native vegetation where groundwater elevations are not controlled.

The methods that are used to simulate land surface and root zone processes in IWFM are discussed in detail in a separate document (see DWR, 2015) and will not be discussed any further here. DWR (2015) details the IWFM Demand Calculator (IDC) which is also used as the root zone and land surface flow simulation component in IWFM.

2.9. Moisture Routing in the Unsaturated Zone

Moisture routing in the unsaturated zone is performed over a pre-specified number of unsaturated layers. The simulation of moisture through multiple layers

approximates the vertical movement of water in the physical system more precisely because of the finer spatial discretization created. The lag between the time when moisture enters the unsaturated zone above and the time it leaves the unsaturated zone below can be simulated more accurately.

The methodology for routing moisture through unsaturated layers is similar to that used in the root zone as described by DWR (2015). The conservation equation for an unsaturated layer m is

$$\frac{\partial\left(D_n\theta_{u,n}\right)}{\partial t} = Q_{in,n} - Q_{out,n} \tag{2.51}$$

where

n	=	unsaturated layer number counting from top down, (dimensionless);
D_n	=	thickness of layer n, (L);
$\theta_{u,n}$	=	soil moisture in n^{th} unsaturated layer, (L/L);
$Q_{in,n}$	=	inflow into unsaturated layer n from layer n−1, (L/T);
$Q_{out,n}$	=	outflow from unsaturated layer n to layer n+1, (L/T);
t	=	time, (T).

Assuming that the vertical head gradient is unity, using van Genuchten-Mualem equation (Mualem, 1976; van Genuchten, 1980) and assuming residual moisture content is negligible, the flow out of layer n, $Q_{out,n}$, can be expressed as

$$Q_{out,n} = K_{u,n} \tag{2.52}$$

and

$$K_{u,n} = K_{s,n}\left(\frac{\theta_{u,n}}{\eta_{T,n}}\right)^{1/2}\left\{1-\left[1-\left(\frac{\theta_{u,n}}{\eta_{T,n}}\right)^{1/m}\right]^{m}\right\}^{2} \tag{2.53}$$

$$m = \frac{\lambda_n}{\lambda_n + 1} \tag{2.54}$$

where

$K_{u,n}$ = unsaturated hydraulic conductivity of layer n, (L/T);

$K_{s,n}$ = saturated hydraulic conductivity of layer n, (L/T);

$\eta_{T,n}$ = total porosity of unsaturated layer n, (L/L);

λ_n = pore size distribution index of unsaturated layer n, (dimensionless).

As an alternative to the van Genuchten-Mualem equation, IWFM can use Campbell's approach (Campbell, 1974) to represent the unsaturated hydraulic conductivity:

$$K_{u,n} = K_{s,n}\left(\frac{\theta_{u,n}}{\eta_{T,n}}\right)^{3+\frac{2}{\lambda_n}} \tag{2.55}$$

where the assumption of negligible residual moisture content is applied.

Equation (2.51), coupled with (2.52), is solved for each unsaturated layer from top down in a sequential order. At each layer, the inflow term $Q_{in,n}$ is known from the routing of moisture at the layer above, i.e. $Q_{in,n} = Q_{out,n-1}$. For the first unsaturated layer (i.e. n = 1), $Q_{in,n}$ is equal to the deep percolation computed by the root zone component of IWFM (DWR, 2015). The outflow at the last unsaturated layer is the net deep percolation into the groundwater system.

The number of layers and their thicknesses are predefined input parameters. Based on the elevation of the groundwater table, three scenarios can occur for an unsaturated layer during the simulation period: (i) the total thickness of the layer is unsaturated; (ii) the groundwater table intersects the unsaturated layer so that the partial thickness of the layer is saturated and (iii) the layer is occupied completely by groundwater, and is no longer unsaturated. If the elevation of the groundwater table is lower than the bottom of the last unsaturated layer, then IWFM re-computes the thickness of the last layer and extends it down to the groundwater table. If a layer becomes fully saturated during the simulation period due to the rising groundwater table, the moisture routing in that unsaturated layer is ceased until the layer is at least partially unsaturated again. If a layer is partially occupied by saturated groundwater, then the thickness of the layer, $D_{u,n}$, that appears in equation (2.51) is computed as the unsaturated thickness of that layer. Therefore, even though the thicknesses of each unsaturated layer are pre-specified, they are in fact dynamic, and computed internally in IWFM through the simulation period.

2.10. Small Watersheds

Small watersheds adjacent to a model area can contribute to surface and subsurface flows occurring in the model area. To account for the flow contributions of small watersheds, surface and subsurface flows at these watersheds are simulated with an approximate method. It is assumed that flow between the small watersheds and the

modeled region is one-way; the direction of subsurface and surface flows is always from small watersheds into the modeled region.

The surface flow that occurs in a small watershed is assumed to be due solely to the direct runoff of precipitation:

$$S_{wr} = \frac{1}{\Delta t} \frac{\left(P_w \Delta t - 0.2 S_w\right)^2}{P_w \Delta t + 0.8 S_w} A_w \tag{2.56}$$

where

S_{wr} = direct runoff from the small watershed, (L^3/T);

P_w = precipitation rate at the small watershed, (L/T);

S_w = retention parameter at small watershed modified with respect to the soil moisture in the unsaturated zone (see previous sections for the computation of this term), (L);

Δt = time period over which the precipitation rate has occurred, (T);

A_w = surface area of the small watershed, (L^2).

As described earlier, once the direct runoff is computed the infiltration that occurs at the small watershed can be computed as

$$I_{wf_p} = \left(P_w - S_{wr}\right) A_w \tag{2.57}$$

where

I_{wf_p} = infiltration of precipitation at the small watershed, (L^3/T).

The vertical movement of moisture in the unsaturated zone at the small watershed is computed using the methods described in preceding sections and in DWR (2015). The computed deep percolation, as an outcome of the soil moisture accounting, represents the

inflow to the groundwater storage at a small watershed. The conservation equation for the groundwater storage at the small watershed is expressed as

$$\frac{\partial S_{wg}}{\partial t} = D_{wp} - Q_{wg} - Q_{wgs} \tag{2.58}$$

where

S_{wg} = groundwater storage within the small watershed boundary, (L^3);

D_{wp} = net deep percolation, i.e. recharge, to the groundwater storage within the small watershed domain (computed using the methods described in the preceding section), (L^3/T);

Q_{wg} = subsurface outflow from the small watershed that contributes to the groundwater storage at the modeled area, (L^3/T);

Q_{wgs} = contribution of groundwater storage to the surface flow at the small watershed, (L^3/T);

t = time, (T).

The subsurface flow from the small watershed, Q_{wg}, contributes to the groundwater storage at the modeled area at pre-specified locations. It is approximated as

$$Q_{wg} = C_{wg} S_{wg} \tag{2.59}$$

where

C_{wg} = subsurface flow recession coefficient, (1/T).

Contribution of the groundwater storage to the surface flow at the small watershed, Q_{wgs}, is computed as a non-zero value only if the groundwater storage, S_{wg}, exceeds a predefined threshold value:

$$Q_{wgs} = C_{ws}\left(S_{wg} - S_{wgt}\right) \tag{2.60}$$

where

C_{ws} = surface runoff recession coefficient, (1/T);

S_{wgt} = threshold value for groundwater storage within the small watershed above which groundwater at the small watershed contributes to surface flow, (L^3).

Finally, the total surface flow from the small watershed that contributes to the surface flows at predefined locations in the modeled area is computed as

$$Q_{ws} = Q_{wgs} + S_{wr} \tag{2.61}$$

where

Q_{ws} = total surface flow from the small watershed that contributes to the surface flows in the modeled area, (L^3/T).

3. Numerical Methods Used in Modeling of Hydrological Processes

The conservation equations for the hydrological processes modeled in IWFM are detailed in previous chapter. In order to model the hydrological processes and the interactions among them, it is necessary to solve these equations simultaneously. However, since most of these equations are non-linear and the interaction terms are complex, it is impossible to obtain an analytical solution except for very simple, hypothetical cases. For this reason, IWFM utilizes numerical techniques to obtain approximate solutions to the equations listed in the previous chapter. This chapter is devoted to the explanation of the numerical methods used in IWFM.

3.1. Finite Element Representation of the Groundwater Equation

The conservation equation for the groundwater system is given in the previous chapter as

$$\begin{aligned} 0 = \frac{\partial S_s h}{\partial t} - \vec{\nabla}\left(T\ \vec{\nabla} h\right) + I_u L_u \Delta h^u + I_d L_d \Delta h^d - q_o + q_{sd} + q_{et} \\ -\delta\left(x - x_s, y - y_s\right)\frac{Q_{sint}}{A_s} \\ -\delta\left(x - x_{lk}, y - y_{lk}\right)\frac{Q_{lkint}}{A_{lk}} \\ -\delta\left(x - x_{td}, y - y_{td}\right)\frac{Q_{td}}{A_{td}} \end{aligned} \tag{3.1}$$

Equation (3.1) is a partial differential equation that models the unsteady groundwater head field in a multi-layer aquifer system that consists of confined and/or unconfined layers. In order to solve this equation, IWFM utilizes the Galerkin finite

element method to discretize the spatial domain and obtain a set of ordinary differential equations in which the unknowns are the groundwater heads at a finite number of nodal points within the model domain. The spatially and temporally continuous groundwater head field in an aquifer layer m, can be approximated by the head values at discrete nodal points as (Huyakorn and Pinder, 1983):

$$\hat{h}(x,y,t) = \sum_{j=N\cdot(m-1)+1}^{N\cdot m} \omega_j(x,y)\, h_j(t) \tag{3.2}$$

where

$\hat{h}(x,y,t)$ = approximation of h(x, y, t), (L);

$\omega_j(x,y)$ = shape functions, (dimensionless);

$h_j(t)$ = nodal hydraulic head values, (L);

m = aquifer layer number, (dimensionless);

N = total number of nodal points in an aquifer layer, (dimensionless).

Equation (3.2) is valid for all layers of an aquifer system that consists of N_L layers. Substitution of (3.2) into (3.1) will generally result in a nonzero residual ε:

$$\begin{aligned}\varepsilon = {} & \frac{\partial S_s \hat{h}}{\partial t} - \vec{\nabla}\left(T\ \vec{\nabla}\ \hat{h}\right) + I_u L_u \Delta\hat{h}^u + I_d L_d \Delta\hat{h}^d - q_o + q_{sd} + q_{et} \\ & -\delta\left(x - x_s, y - y_s\right)\frac{Q_{sint}}{A_s} \\ & -\delta\left(x - x_{lk}, y - y_{lk}\right)\frac{Q_{lkint}}{A_{lk}} \\ & -\delta\left(x - x_{td}, y - y_{td}\right)\frac{Q_{td}}{A_{td}}\end{aligned} \tag{3.3}$$

According to the Galerkin approach, the inner products of equation (3.3) and the shape functions ω_i are required to be equal to zero. That is, equation (3.3) is multiplied by

the shape functions $\omega_i \left(i = N \cdot (m-1)+1, \cdots, N \cdot m\right)$ for each aquifer layer. The resulting $N \times N_L$ equations are integrated over the entire domain and the result of each of these integrals is required to be equal to zero (Huyakorn and Pinder, 1983):

$$
\begin{aligned}
0 = \iint_{\Omega} \Bigg(& \frac{\partial S_s \hat{h}}{\partial t} - \vec{\nabla}\left(T\ \vec{\nabla}\ \hat{h}\right) + I_u L_u \Delta\hat{h}^u + I_d L_d \Delta\hat{h}^d - q_o + q_{sd} + q_{et} \\
& -\delta\left(x - x_s, y - y_s\right)\frac{Q_{sint}}{A_s} \\
& -\delta\left(x - x_{lk}, y - y_{lk}\right)\frac{Q_{lkint}}{A_{lk}} \\
& -\delta\left(x - x_{td}, y - y_{td}\right)\frac{Q_{td}}{A_{td}}\Bigg)\omega_i d\Omega \qquad \begin{array}{c} i = N \cdot (m-1)+1, \cdots, N \cdot m \\ m = 1, \cdots, N_L \end{array}
\end{aligned}
\tag{3.4}
$$

where

Ω = spatial domain of the problem.

It should be noted that the shape functions depend only on the geometric characteristics of the finite elements, therefore they are the same for each layer, i.e. $\omega_i = \omega_{i+N} = \cdots = \omega_{i+N\cdot(N_L-1)}$ where $i = 1, \cdots, N$.

Equation (3.4) is valid for all layers of a multi-layer aquifer system with N_L layers. In fact it is necessary to define equation (3.4) for all layers of the aquifer system in order to obtain a closed system of equations. Figure 3.1 depicts the node numbering convention used in IWFM for a hypothetical aquifer system with N_L layers and each layer discretized into 2 elements with N=5 nodes. This node numbering convention is used interchangeably in the rest of this document to express L_u, L_d, h_u and h_d (refer to previous chapter for a definition of the terms) for a node as L_{j-N}, L_{j+N}, h_{j-N} and h_{j+N}, respectively.

Substituting equation (3.2) into (3.4) and applying Green's theorem to eliminate the second order derivatives result in the following equation:

$$
\begin{aligned}
0 = & \iint_{\Omega} \sum_{j=N\cdot(m-1)+1}^{N\cdot m} \frac{\partial S_{s_j} h_j}{\partial t} \omega_i \omega_j d\Omega \\
& - \iint_{\Gamma} \sum_{j=N\cdot(m-1)+1}^{N\cdot m} T\omega_i \vec{\nabla}\left(h_j \omega_j\right) \cdot \vec{n}\ d\Gamma + \iint_{\Omega} \sum_{j=N\cdot(m-1)+1}^{N\cdot m} T\vec{\nabla}\left(h_j \omega_j\right) \cdot \vec{\nabla}\omega_i d\Omega \\
& + H\left(m-2\right) \iint_{\Omega} \sum_{j=N\cdot(m-1)+1}^{N\cdot m} L_{j-N} \Delta h_j^u \omega_i \omega_j d\Omega \\
& + \left[1 - H\left(m - N_L\right)\right] \iint_{\Omega} \sum_{j=N\cdot(m-1)+1}^{N\cdot m} L_{j+N} \Delta h_j^d \omega_i \omega_j d\Omega \\
& - \iint_{\Omega} q_o \omega_i d\Omega + \iint_{\Omega} q_{sd} \omega_i d\Omega + \iint_{\Omega} q_{et} \omega_i d\Omega \\
& - \iint_{\Omega} \delta\left(x - x_s, y - y_s\right) \frac{Q_{sint}}{A_s}\ \omega_i d\Omega \\
& - \iint_{\Omega} \delta\left(x - x_{lk}, y - y_{lk}\right) \frac{Q_{lkint}}{A_{lk}}\ \omega_i d\Omega \\
& - \iint_{\Omega} \delta\left(x - x_{td}, y - y_{td}\right) \frac{Q_{td}}{A_{td}}\ \omega_i d\Omega \qquad \begin{array}{c} i = N\cdot(m-1)+1, \cdots, N\cdot m \\ m = 1, \cdots, N_L \end{array}
\end{aligned}
\tag{3.5}
$$

where

Γ	=	boundary of the spatial domain, (L);
$\vec{n}$	=	outward unit vector perpendicular to the boundary, (dimensionless);
N_L	=	total number of aquifer layers, (dimensionless);

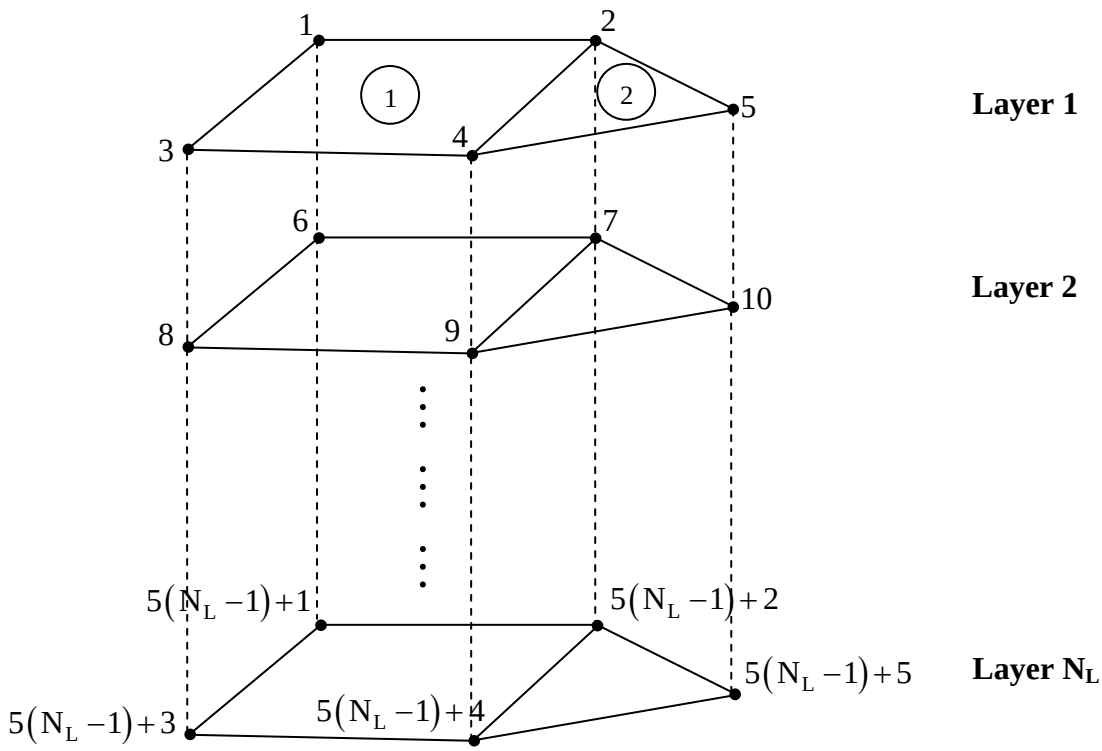

Figure 3.1 Node numbering convention used in IWFM for an aquifer system with N_L layers and N=5 nodes in each layer

$H(\bullet)$ = Heaviside (step) function to express the indicator functions I_u and I_d in terms of the layer number m, explicitly, (dimensionless);

The vertical head differences, Δh_j^u and Δh_j^d, at a finite element node are also introduced in (3.5). These terms are computed by using the head values in the vertical direction at a finite element node; i.e. h_{j-N}, h_j and h_{j+N}.

IWFM utilizes a mass lumping method to simplify equation (3.5). According to this method, it is assumed that the head over an element can be approximated by a head value at any one of the nodes; i. e. $\hat{h} = h_j$. The choice of the node for this purpose is

based solely on the index j. It has been suggested, particularly in non-linear equations, that mass lumping typically generates a smoother numerical solution than that arising from the strict Galerkin, or *consistent*, formulation (Allen, et al., 1988). Applying the mass lumping technique to the storage and leakage terms of (3.5) (i.e. first, fourth and fifth integral terms), and performing the differentiations in the third integral term results in

$$
\begin{aligned}
0 = & \iint_{\Omega} \frac{\partial S_{s_i} h_i}{\partial t} \omega_i d\Omega \\
& - \iint_{\Gamma} q_{\Gamma} \omega_i d\Gamma + \sum_{j=N\cdot(m-1)+1}^{N\cdot m} \iint_{\Omega} Th_j \left(\frac{\partial \omega_i}{\partial x} \frac{\partial \omega_j}{\partial x} + \frac{\partial \omega_i}{\partial y} \frac{\partial \omega_j}{\partial y} \right) d\Omega \\
& + H(m-2) \iint_{\Omega} L_{i-N} \Delta h_i^u \omega_i d\Omega \\
& + \left[1 - H(m - N_L) \right] \iint_{\Omega} L_{i+N} \Delta h_i^d \omega_i d\Omega \\
& - \iint_{\Omega} q_o \omega_i d\Omega + \iint_{\Omega} q_{sd} \omega_i d\Omega + \iint_{\Omega} q_{et} \omega_i d\Omega \\
& - \iint_{\Omega} \delta(x - x_s, y - y_s) \frac{Q_{sint}}{A_s} \omega_i d\Omega \\
& - \iint_{\Omega} \delta(x - x_{lk}, y - y_{lk}) \frac{Q_{lkint}}{A_{lk}} \omega_i d\Omega \\
& - \iint_{\Omega} \delta(x - x_{td}, y - y_{td}) \frac{Q_{td}}{A_{td}} \omega_i d\Omega \qquad \begin{array}{c} i = N \cdot (m-1) + 1, \cdots, N \cdot m \\ m = 1, \cdots, N_L \end{array} \qquad (3.6)
\end{aligned}
$$

where $q_\Gamma = \sum_{j=N\cdot(m-1)+1}^{N\cdot m} T\vec{\nabla}\left(h_j\omega_j\right)\cdot\vec{n}$ is the inflow that is perpendicular to the boundary of aquifer layer m. Equation (3.6) is valid for all layers of a multi-layer aquifer system. Therefore, it represents a set of $N\times N_L$ ordinary differential equations for an aquifer system that is comprised of N_L layers with the unknown groundwater head values at $N\times N_L$ nodal points.

To solve equation (3.6), the time coordinate is also discretized using the fully implicit discretization method. Utilization of this method results in the following equation:

$$
\begin{aligned}
0 = & \iint_{\Omega} \frac{S_{s_i}^{t+1}\left(h_i^{t+1} - TOP_i\right) + S_{s_i}^{t}\left(TOP_i - h_i^{t}\right)}{\Delta t}\omega_i d\Omega \\
& - \iint_{\Gamma} q_{\Gamma}^{t+1}\omega_i d\Gamma + \sum_{j=N\cdot(m-1)+1}^{N\cdot m} \iint_{\Omega} T^{t+1} h_j^{t+1}\left(\frac{\partial\omega_i}{\partial x}\frac{\partial\omega_j}{\partial x} + \frac{\partial\omega_i}{\partial y}\frac{\partial\omega_j}{\partial y}\right) d\Omega \\
& + H(m-2)\iint_{\Omega} L_{i-N}\left(\Delta h_i^{u}\right)^{t+1}\omega_i d\Omega \\
& + \left[1 - H(m - N_L)\right]\iint_{\Omega} L_{i+N}\left(\Delta h_i^{d}\right)^{t+1}\omega_i d\Omega \\
& - \iint_{\Omega} q_o^{t+1}\omega_i d\Omega + \iint_{\Omega} q_{sd}^{t+1}\omega_i d\Omega + \iint_{\Omega} q_{et}^{t+1}\omega_i d\Omega \\
& - \iint_{\Omega} \delta\left(x - x_s, y - y_s\right)\frac{Q_{sint}^{t+1}}{A_s}\omega_i d\Omega \\
& - \iint_{\Omega} \delta\left(x - x_{lk}, y - y_{lk}\right)\frac{Q_{lkint}^{t+1}}{A_{lk}}\omega_i d\Omega \\
& - \iint_{\Omega} \delta\left(x - x_{td}, y - y_{td}\right)\frac{Q_{td}^{t+1}}{A_{td}}\omega_i d\Omega \qquad \begin{array}{c} i = N\cdot(m-1)+1,\cdots,N\cdot m \\ m = 1,\cdots,N_L \end{array} \qquad (3.7)
\end{aligned}
$$

where

TOP_i = top elevation of the aquifer at node *i*, (L);

Δt = length of time step, (T);

t = index for time step, (dimensionless).

The time discretization of the first integral term in (3.7) reflects the effort to simulate changing aquifer conditions. As an example, consider the case where the

aquifer converts from confined to unconfined during a simulation period Δt. At time step t, $S_{s_i}^{t}$ is equal to the storage coefficient, S_{o_i}, of the confined aquifer. At time step t+1, $S_{s_i}^{t+1}$ is equal to the specific yield, S_{y_i}, of the unconfined aquifer. In this case, the rate of release of water from storage during the time step has two components (McDonald and Harbaugh, 1988):

$$\frac{S_{o_i}\left(TOP_i - h_i^t\right)}{\Delta t} \tag{3.8}$$

and

$$\frac{S_{y_i}\left(h_i^{t+1} - TOP_i\right)}{\Delta t} \tag{3.9}$$

Equation (3.8) is the rate of release of water from the confined storage and equation (3.9) is the rate of release of water from the unconfined storage.

To compute the integrals in (3.7), it is necessary to define the global shape functions, ω_i, explicitly. In finite element method, the shape functions are defined separately for each element so that an *element shape function*, ω_i^e, is non-zero only over the particular element it is defined for, and is zero for the rest of the spatial domain. When the element shape functions are combined, they will produce the global shape functions within the model domain. Since element shape functions are non-zero only over the particular element, the integrals in (3.7) defined over the entire domain, Ω, will reduce to integrals over the part of the domain occupied by individual elements, Ω^e. With this approach, the task is reduced to the computation of the contribution of each element to the global set of equations given in (3.7). Based on the above discussion, (3.7)

can be expressed as

$$
\begin{aligned}
0 = \sum_{e=N_e\cdot(m-1)+1}^{N_e\cdot m} \Bigg\{ & \iint_{\Omega^e} \frac{S_{s_i}^{t+1}\left(h_i^{t+1}-TOP_i\right)+S_{s_i}^{t}\left(TOP_i-h_i^{t}\right)}{\Delta t}\omega_i^e d\Omega^e \\
& -\iint_{\Gamma^e} q_{\Gamma^e}^{t+1}\omega_i^e d\Gamma^e + \sum_{j=N\cdot(m-1)+1}^{N\cdot m} \iint_{\Omega^e} \left(T^e\right)^{t+1} h_j^{t+1}\left(\frac{\partial\omega_i^e}{\partial x}\frac{\partial\omega_j^e}{\partial x}+\frac{\partial\omega_i^e}{\partial y}\frac{\partial\omega_j^e}{\partial y}\right)d\Omega^e \\
& +H(m-2)\iint_{\Omega^e} L_{i-N}\left(\Delta h_i^u\right)^{t+1}\omega_i^e d\Omega^e \\
& +\left[1-H(m-N_L)\right]\iint_{\Omega^e} L_{i+N}\left(\Delta h_i^d\right)^{t+1}\omega_i^e d\Omega^e \\
& -\iint_{\Omega^e} q_{o_i}^{t+1}\omega_i^e d\Omega^e + \iint_{\Omega^e} q_{sd}^{t+1}\omega_i^e d\Omega^e + \iint_{\Omega^e} q_{et}^{t+1}\omega_i^e d\Omega^e \\
& -\iint_{\Omega^e} \delta\left(x-x_s, y-y_s\right)\frac{Q_{sint}^{t+1}}{A_s}\omega_i^e d\Omega^e \\
& -\iint_{\Omega^e} \delta\left(x-x_{lk}, y-y_{lk}\right)\frac{Q_{lkint}^{t+1}}{A_{lk}}\omega_i^e d\Omega^e \\
& -\iint_{\Omega^e} \delta\left(x-x_{td}, y-y_{td}\right)\frac{Q_{td}^{t+1}}{A_{td}}\omega_i^e d\Omega^e \Bigg\} \qquad \begin{matrix} i = N\cdot(m-1)+1,\cdots,N\cdot m \\ m=1,\cdots,N_L \end{matrix}
\end{aligned}
\tag{3.10}
$$

where

ω_i^e = element shape function defined at node *i* of element *e*, (dimensionless);

Ω^e = portion of the model domain occupied by element *e*, (L^2);

Γ^e = face of element *e* that lies on the model boundary, (L);

e = index for element number, (dimensionless);

N_e = number of elements in an aquifer layer, (dimensionless).

A particular equation from the equation set (3.10) represents the approximate form of the groundwater conservation equation at a node *i*. The element shape functions will be non-zero only for those elements that connect at node *i*. Therefore, only the integrals of (3.10) that are defined over these elements will have non-zero values.

In IWFM, the finite element method is implemented with linear triangular and/or bilinear quadrilateral elements. In this approach, three nodes define a triangular element, whereas a quadrilateral element consists of four nodes. For both types of elements, the nodes are the points within the problem domain where heads are calculated. In the following section, the expressions of the element shape functions for linear triangular and bilinear quadrilateral elements are derived.

3.1.1. Shape Functions

3.1.1.a. Linear Triangular Elements

For a linear triangular element with nodes i, j, k in the counterclockwise direction (Figure 3.2), the head over the element *e* can be approximated by a linear interpolation function (Huyakorn and Pinder, 1983):

$$\hat{h}^e(x, y) = a_1 + a_2 x + a_3 y \tag{3.11}$$

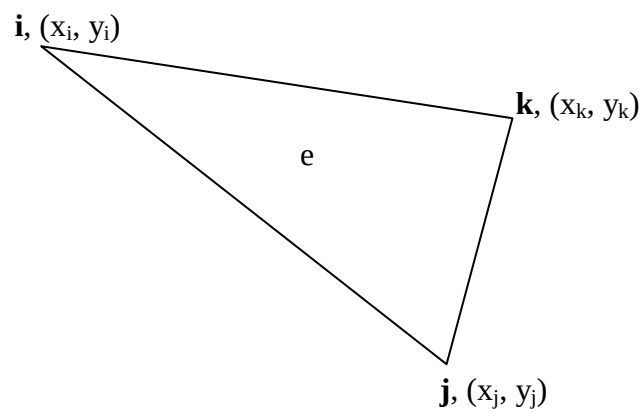

Figure 3.2 A representative triangular element

Substituting the coordinates and the head values at each node into (3.11) will generate 3 equations with 3 unknowns, namely a_1, a_2 and a_3. Solving the system of equations and rearranging terms results in an estimate of the head that is valid over the linear triangular element *e*:

$$\hat{h}^e(x,y) = \omega_i^e(x,y)h_i + \omega_j^e(x,y)h_j + \omega_k^e(x,y)h_k \tag{3.12}$$

where

$$\omega_i^e(x,y) = \frac{1}{2A^e}\left[\left(x_j y_k - x_k y_j\right) + \left(y_j - y_k\right)x + \left(x_k - x_j\right)y\right] \tag{3.13}$$

$$\omega_j^e(x,y) = \frac{1}{2A^e}\left[\left(x_k y_i - x_i y_k\right) + \left(y_k - y_i\right)x + \left(x_i - x_k\right)y\right] \tag{3.14}$$

$$\omega_k^e(x,y) = \frac{1}{2A^e}\left[\left(x_i y_j - x_j y_i\right) + \left(y_i - y_j\right)x + \left(x_j - x_i\right)y\right] \tag{3.15}$$

$$A^e = \frac{1}{2}\left[\left(x_i y_j - x_j y_i\right) + \left(x_k y_i - x_i y_k\right) + \left(x_j y_k - x_k y_j\right)\right]$$

$$= \frac{1}{2}\left[\left(x_i - x_k\right)\left(y_j - y_k\right) + \left(x_j - x_k\right)\left(y_k - y_i\right)\right] \tag{3.16}$$

In (3.12), $\omega_i^e, \omega_j^e, \omega_k^e$ are the element shape functions and A^e is the area of the triangular element.

3.1.1.b. Bilinear Quadrilateral Elements

To define the shape functions for bilinear quadrilateral elements, the element coordinates are transformed from (x, y) space into (ξ, η) space (see Figure 3.3) so as to use efficient numerical techniques in carrying out the integrals given in equation (3.10). Using the Lagrange polynomials, x and y can be expressed in terms of ξ and η in the following form (Huyakorn and Pinder, 1983):

$$x = \sum_{m=1}^{4} \omega_m^e(\xi, \eta)\ x_m \tag{3.17}$$

$$y = \sum_{m=1}^{4} \omega_m^e(\xi, \eta)\ y_m \tag{3.18}$$

where $\omega_m^e(\xi, \eta)$ are the element shape functions in (ξ, η) space.

The shape functions $\omega_m^e(\xi, \eta)$ can be expressed in terms of first-degree Lagrange polynomials as

$$\omega_m^e\left(\xi, \eta\right) = \prod_{\substack{i=1 \\ \xi_i \neq \xi^m}}^{2} \left(\frac{\xi - \xi_i}{\xi^m - \xi_i}\right) \prod_{\substack{k=1 \\ \eta_k \neq \eta^m}}^{2} \left(\frac{\eta - \eta_k}{\eta^m - \eta_k}\right), \qquad m = 1, \cdots, 4 \tag{3.19}$$

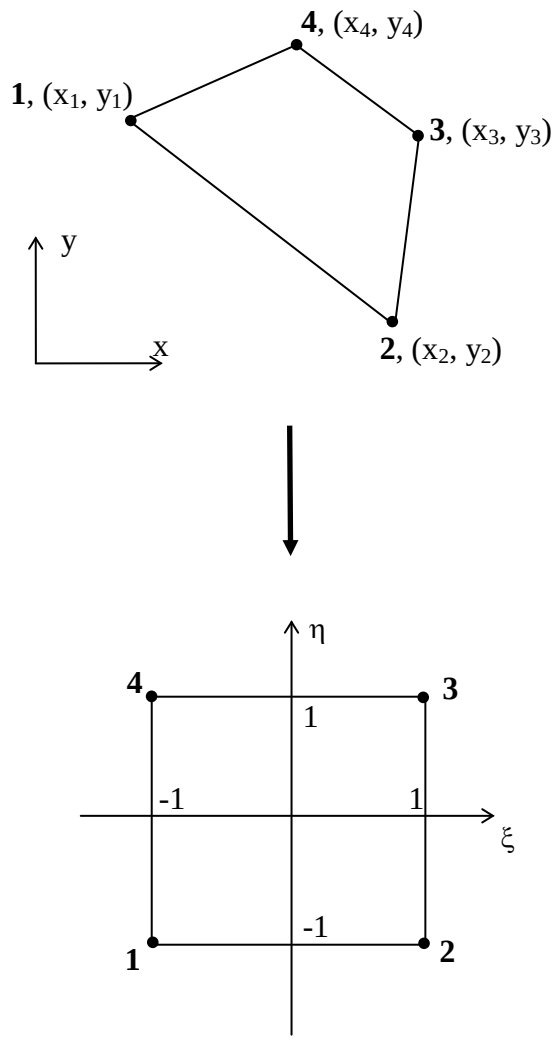

Figure 3.3 Transformation of a quadrilateral element from (x, y) space to (ξ, η) space

where ξ^m and η^m are the coordinate values of node m in (ξ, η) space, whereas $\xi_1 = \eta_1 = -1$ and $\xi_2 = \eta_2 = 1$. The formulation in (3.19) results in the following shape functions:

$$\omega_1^e(\xi,\eta) = \frac{1}{4}(\xi - 1)(\eta - 1) \tag{3.20}$$

$$\omega_2^e(\xi,\eta) = \frac{1}{4}(1 + \xi)(1 - \eta) \tag{3.21}$$

$$\omega_3^e(\xi,\eta) = \frac{1}{4}(\xi + 1)(\eta + 1) \tag{3.22}$$

$$\omega_4^e(\xi,\eta) = \frac{1}{4}(1 - \xi)(1 + \eta) \tag{3.23}$$

Furthermore, an integral defined over the element area in (x, y) space can be expressed in (ξ, η) space as

$$\int_{y_a}^{y_b}\int_{x_a}^{x_b} f(x,y)\ dx\ dy = \int_{-1}^{1}\int_{-1}^{1} f(\xi,\eta)\ |J|\ d\xi\ d\eta \tag{3.24}$$

where $|J|$ is the determinant of the Jacobian of the transformation from (x, y) space into (ξ, η) space:

$$|J| = \begin{vmatrix} \dfrac{\partial x}{\partial \xi} & \dfrac{\partial y}{\partial \xi} \\ \\ \dfrac{\partial x}{\partial \eta} & \dfrac{\partial y}{\partial \eta} \end{vmatrix} = \frac{\partial x}{\partial \xi}\ \frac{\partial y}{\partial \eta} - \frac{\partial y}{\partial \xi}\frac{\partial x}{\partial \eta} \tag{3.25}$$

The partial derivatives that appear in (3.25) can be calculated by substituting (3.20)-(3.23) into (3.17) and (3.18), and by performing the appropriate partial differentiation. After algebraic manipulations, (3.25) can be written as

$$|J| = \frac{1}{8}\left(a + b\xi + c\eta\right) \tag{3.26}$$

where

$$a = \left(x_1 - x_3\right)\left(y_2 - y_4\right) - \left(x_2 - x_4\right)\left(y_1 - y_3\right) \tag{3.27}$$

$$b = \left[-\left(x_1 - x_2\right)\left(y_3 - y_4\right) + \left(x_3 - x_4\right)\left(y_1 - y_2\right)\right] \tag{3.28}$$

$$c = \left[-\left(x_1 - x_4\right)\left(y_2 - y_3\right) + \left(x_2 - x_3\right)\left(y_1 - y_4\right)\right] \tag{3.29}$$

3.1.2. Computation of Integrals

Of all the terms included in the integrands that appear in (3.10), only ω_i^e, $\left(T^e\right)^{t+1}$ and the dirac delta functions (namely, $\delta\left(x - x_s, y - y_s\right)$, $\delta\left(x - x_{lk}, y - y_{lk}\right)$ and $\delta\left(x - x_{td}, y - y_{td}\right)$) are spatial functions. The rest of the terms of the integrands are either constant over an element or only functions of time (refer to the following sections which demonstrate that land subsidence, stream-groundwater interaction, lake-groundwater interaction and tile drain/subsurface irrigation flows over an element as functions of time only). It should be noted that the boundary flow, $\sum_{e=N_e\cdot(m-1)+1}^{N_e\cdot m} \iint_{\Gamma^e} q_{\Gamma^e}^{t+1} \omega_i^e d\Gamma^e$, is a part of the boundary conditions and its value should already be available. A common practice in finite element method is to assume that the transmissivity, $\left(T^e\right)^{t+1}$, is constant over an individual element but differs from one element to another. In IWFM, $\left(T^e\right)^{t+1}$ is

computed as the average transmissivity over an element. Approximating $\left(T^e\right)^{t+1}$ using the element shape functions and averaging it over an element *e*, one obtains

$$\left(T^e\right)^{t+1} = \frac{1}{A^e}\iint_{\Omega^e}\left(\sum_{j=1}^{n_e} T_j^{t+1}\omega_j^e\right)d\Omega^e \tag{3.30}$$

where

n_e = number of nodes that constitute element *e*; 3 for a triangular element and 4 for a quadrilateral element, (dimensionless);

A^e = area of element *e*, (L^2);

T_j^{t+1} = transmissivity at the jth node that constitute element *e*, (L^2/T).

Once the elemental transmissivity, $\left(T^e\right)^{t+1}$, is defined, IWFM utilizes a simplification procedure on the conductance term (third integral of equation (3.10)) in order to decrease the required computer storage. At node *i*, the conductance term is expressed as

$$\sum_{j=N\cdot(m-1)+1}^{N\cdot m}\iint_{\Omega^e}\left(T^e\right)^{t+1} h_j^{t+1}\left(\frac{\partial\omega_i^e}{\partial x}\frac{\partial\omega_j^e}{\partial x}+\frac{\partial\omega_i^e}{\partial y}\frac{\partial\omega_j^e}{\partial y}\right)d\Omega^e$$

$$=\left(T^e\right)^{t+1}\iint_{\Omega^e}\left(\sum_{\substack{j=N\cdot(m-1)+1\\ j\neq i}}^{N\cdot m}\left(\bar{\nabla}\omega_i^e\bar{\nabla}\omega_j^e h_j^{t+1}\right)+\bar{\nabla}\omega_i^e\bar{\nabla}\omega_i^e h_j^{t+1}\right)d\Omega^e \tag{3.31}$$

In equation (3.31), the ith term of the summation is simply separated from the summation notation. It can be shown that the shape functions for both linear triangular and bilinear quadrilateral elements sum up to unity:

$$\sum_{j=N\cdot(m-1)+1}^{N\cdot m} \omega_j^e = 1 \tag{3.32}$$

From (3.32)

$$\sum_{j=N\cdot(m-1)+1}^{N\cdot m} \vec{\nabla}\omega_j^e = \vec{\nabla}\omega_i^e + \sum_{\substack{j=N\cdot(m-1)+1 \\ j\neq i}}^{N\cdot m} \vec{\nabla}\omega_j^e = 0 \tag{3.33}$$

or

$$\vec{\nabla}\omega_i^e = -\sum_{\substack{j=N\cdot(m-1)+1 \\ j\neq i}}^{N\cdot m} \vec{\nabla}\omega_j^e \tag{3.34}$$

Substituting (3.34) into (3.31) results in

$$\sum_{j=N\cdot(m-1)+1}^{N\cdot m} \iint_{\Omega^e} \left(T^e\right)^{t+1} h_j^{t+1} \left(\frac{\partial\omega_i^e}{\partial x}\frac{\partial\omega_j^e}{\partial x} + \frac{\partial\omega_i^e}{\partial y}\frac{\partial\omega_i^e}{\partial y} \right) d\Omega^e$$

$$= \left(T^e\right)^{t+1} \iint_{\Omega^e} \left(\sum_{\substack{j=N\cdot(m-1)+1 \\ j\neq i}}^{N\cdot m} \left(\vec{\nabla}\omega_i^e \vec{\nabla}\omega_j^e h_j^{t+1}\right) - \sum_{\substack{j=N\cdot(m-1)+1 \\ j\neq i}}^{N\cdot m} \left(\vec{\nabla}\omega_i^e \vec{\nabla}\omega_j^e h_i^{t+1}\right) \right) d\Omega^e$$

$$= -\left(T^e\right)^{t+1} \iint_{\Omega^e} \left(\sum_{\substack{j=N\cdot(m-1)+1 \\ j\neq i}}^{N\cdot m} \vec{\nabla}\omega_i^e \vec{\nabla}\omega_j^e \left(h_i^{t+1} - h_j^{t+1}\right) \right) d\Omega^e \tag{3.35}$$

After substituting (3.30) and (3.35) into (3.10), the only spatial functions defined over an element are the element shape functions. The rest of the terms included in the integrands can be moved out of the integrals. After this procedure only the following integrals remain to be computed for each element in (3.10):

$$\iint_{\Omega^e} \omega_i^e d\Omega^e \tag{3.36}$$

$$\iint_{\Omega^e} \delta\left(x - x_o, y - y_o\right) \omega_i^e d\Omega^e \tag{3.37}$$

$$\iint_{\Omega^e} \left(\frac{\partial \omega_i^e}{\partial x} \frac{\partial \omega_j^e}{\partial x} + \frac{\partial \omega_i^e}{\partial y} \frac{\partial \omega_j^e}{\partial y} \right) d\Omega^e \tag{3.38}$$

In (3.37) x_o and y_o represent either the coordinates of a stream location, (x_s, y_s), the coordinates of a lake location, (x_{lk}, y_{lk}), or the coordinates of a tile drain/subsurface irrigation system, (x_{td}, y_{td}), depending on the integral being computed in (3.10).

3.1.2.a. Integration over Triangular Elements

After substituting any of the equations (3.13)-(3.15) into (3.36), it can be shown that (Huyakorn and Pinder, 1983)

$$\iint_{\Omega^e} \omega_i^e d\Omega^e = \frac{A^e}{3} \tag{3.39}$$

where A^e is the area of the triangular element and it is given in equation (3.16).

In IWFM, it is assumed that the integral in (3.37) yields the area of stream, lake or tile drain/subsurface irrigation system that lies over the part element *e* that is associated with node *i*:

$$\iint_{\Omega^e} \delta\left(x - x_o, y - y_o\right) \omega_i^e d\Omega^e \cong A_{o,i}^e \tag{3.40}$$

where $A_{o,i}^e$ is the elemental area of the stream, lake or tile drain/subsurface irrigation system depending on the integral being computed in (3.10).

By differentiating the equations (3.13)-(3.15) with respect to x and y, and substituting them into (3.38) one obtains (Huyakorn and Pinder, 1983)

$$\iint_{\Omega^e} \left(\frac{\partial \omega_i^e}{\partial x} \frac{\partial \omega_j^e}{\partial x} + \frac{\partial \omega_i^e}{\partial y} \frac{\partial \omega_j^e}{\partial y} \right) d\Omega^e$$

$$= \frac{1}{4A^e} \left[\left(y_j - y_k \right) \left(y_k - y_i \right) + \left(x_j - x_k \right) \left(x_k - x_i \right) \right] \tag{3.41}$$

3.1.2.b. Integration over Quadrilateral Elements

IWFM utilizes the coordinate transformation from (x, y) space into (ξ, η) space and uses 2-point Gaussian quadrature technique in order to calculate the integrals in (3.36) and (3.38) numerically for quadrilateral elements (Gerald and Wheatley, 1994). Using the equality given in (3.24)

$$\iint_{\Omega^e} \omega_i^e \left(x, y \right) d\Omega^e = \int_{-1}^{1} \int_{-1}^{1} \omega_i^e (\xi, \eta) \left| J \right| d\xi d\eta \tag{3.42}$$

where $\omega_i \left(\xi, \eta \right)$ is given in (3.19).

Application of the 2-point Gaussian quadrature on the integral in (3.42) results in

$$\int_{-1}^{1}\int_{-1}^{1} \omega_i^e(\xi,\eta)|J|\,d\xi\,d\eta$$

$$= \int_{-1}^{1}\int_{-1}^{1} G(\xi,\eta)\,d\xi\,d\eta$$

$$\cong \left[G\left(\frac{1}{\sqrt{3}},\frac{1}{\sqrt{3}}\right) + G\left(\frac{1}{\sqrt{3}},-\frac{1}{\sqrt{3}}\right) + G\left(-\frac{1}{\sqrt{3}},\frac{1}{\sqrt{3}}\right) + G\left(-\frac{1}{\sqrt{3}},-\frac{1}{\sqrt{3}}\right)\right] \qquad (3.43)$$

where $G(\xi,\eta) = \omega_i^e(\xi,\eta)|J|$ and $|J|$ is given in (3.26).

Similar to the assumption made for triangular elements, it is assumed that the integral given in (3.37) is equal to the area of stream, lake or tile drain/subsurface irrigation system over the part of quadrilateral element *e* that is associated with node *i*:

$$\iint_{\Omega^e} \delta(x-x_o, y-y_o)\,\omega_i^e d\Omega^e \cong A_{o,i}^e \qquad (3.44)$$

To compute the integral in (3.38) for a quadrilateral element, it is necessary to define the partial derivatives in terms of ξ and η. Using the chain rule, one obtains

$$\frac{\partial \omega_i^e}{\partial \xi} = \frac{\partial \omega_i^e}{\partial x}\frac{\partial x}{\partial \xi} + \frac{\partial \omega_i^e}{\partial y}\frac{\partial y}{\partial \xi}$$

$$\frac{\partial \omega_i^e}{\partial \eta} = \frac{\partial \omega_i^e}{\partial x}\frac{\partial x}{\partial \eta} + \frac{\partial \omega_i^e}{\partial y}\frac{\partial y}{\partial \eta}$$

which can be expressed in matrix form as

$$\begin{Bmatrix} \dfrac{\partial \omega_i^e}{\partial \xi} \\ \\ \dfrac{\partial \omega_i^e}{\partial \eta} \end{Bmatrix} = J \begin{Bmatrix} \dfrac{\partial \omega_i^e}{\partial x} \\ \\ \dfrac{\partial \omega_i^e}{\partial y} \end{Bmatrix} \qquad (3.45)$$

where $J = \begin{bmatrix} \dfrac{\partial x}{\partial \xi} & \dfrac{\partial y}{\partial \xi} \\ \\ \dfrac{\partial x}{\partial \eta} & \dfrac{\partial y}{\partial \eta} \end{bmatrix}$ is the Jacobian of the transformation whose determinant is given in (3.25). Equation (3.45) can be solved for $\dfrac{\partial \omega_i^e}{\partial x}$ and $\dfrac{\partial \omega_i^e}{\partial y}$ using matrix algebra:

$$\begin{Bmatrix} \dfrac{\partial \omega_i^e}{\partial x} \\ \\ \dfrac{\partial \omega_i^e}{\partial y} \end{Bmatrix} = J^{-1} \begin{Bmatrix} \dfrac{\partial \omega_i^e}{\partial \xi} \\ \\ \dfrac{\partial \omega_i^e}{\partial \eta} \end{Bmatrix} \tag{3.46}$$

In (3.46), $|J|$ stands for the determinant of the Jacobian, which is given in (3.25). Based on these results, the integral in (3.38) can be transformed into the (ξ, η) space as

$$\iint_{\Omega^e} \left(\frac{\partial \omega_i^e}{\partial x} \frac{\partial \omega_j^e}{\partial x} + \frac{\partial \omega_i^e}{\partial y} \frac{\partial \omega_j^e}{\partial y} \right) d\Omega^e$$

$$= \int_{-1}^{1} \int_{-1}^{1} G(\xi, \eta)\, d\xi\, d\eta$$

$$\cong \left[G\left(\frac{1}{\sqrt{3}}, \frac{1}{\sqrt{3}} \right) + G\left(\frac{1}{\sqrt{3}}, -\frac{1}{\sqrt{3}} \right) + G\left(-\frac{1}{\sqrt{3}}, \frac{1}{\sqrt{3}} \right) + G\left(-\frac{1}{\sqrt{3}}, -\frac{1}{\sqrt{3}} \right) \right] \tag{3.47}$$

where

$$G(\xi,\eta)=\frac{1}{|J|}\left\{\left(\frac{\partial y}{\partial \eta}\frac{\partial \omega_i^e}{\partial \xi}-\frac{\partial y}{\partial \xi}\frac{\partial \omega_i^e}{\partial \eta}\right)\left(\frac{\partial y}{\partial \eta}\frac{\partial \omega_j^e}{\partial \xi}-\frac{\partial y}{\partial \xi}\frac{\partial \omega_j^e}{\partial \eta}\right)\right.$$

$$\left.+\left(-\frac{\partial x}{\partial \eta}\frac{\partial \omega_i^e}{\partial \xi}+\frac{\partial x}{\partial \xi}\frac{\partial \omega_i^e}{\partial \eta}\right)\left(-\frac{\partial x}{\partial \eta}\frac{\partial \omega_j^e}{\partial \xi}+\frac{\partial x}{\partial \xi}\frac{\partial \omega_j^e}{\partial \eta}\right)\right\} \tag{3.48}$$

The integral $\iint_{\Omega^e} \omega_i^e d\Omega^e$ in (3.36) can be interpreted as the part of the area of element *e* that is associated with node *i*. Summation of all such areas of elements that connect at node *i* defines the total area that is associated with node *i* (Figure 3.4). Therefore, one can express the area associated with a node *i* as

$$A_i = \sum_{e=N_e\cdot(m-1)+1}^{N_e\cdot m} A_i^e \tag{3.49}$$

where

$A_i^e = \iint_{\Omega^e} \omega_i^e d\Omega^e$ = part of the area of element *e* that is associated with node *i*, (L^2);

A_i = total area associated with a node *i*, (L^2).

To be able to solve equation (3.10) numerically, it is also necessary to discretize the vertical flows, subsidence, stream-groundwater interaction, lake-groundwater interaction and tile drains/subsurface irrigation terms as well as boundary and initial conditions. In the following sections, the temporal and spatial discretization of these terms will be discussed.

3.1.3. Vertical Flows when Aquifers are Separated by an Aquitard

The head difference between the aquifer layer in consideration (i.e. layer m) and

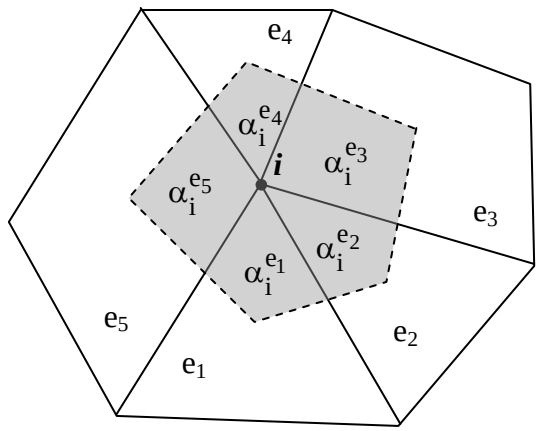

Figure 3.4 Total area that is associated with node *i*

the upper adjacent layer (i.e. layer m-1) is expressed in the finite element notation as

$$\left(\Delta h_i^u\right)^{t+1} = \begin{cases} h_i^{t+1} - h_{i-N}^{t+1} & \text{if} \quad h_i^t \geq z_{b_i} \quad ; \quad h_{i-N}^t > z_{t_i} \\ z_{b_i} - h_{i-N}^{t+1} & \text{if} \quad h_i^t < z_{b_i} \quad ; \quad h_{i-N}^t > z_{t_i} \\ h_i^{t+1} - z_{t_i} & \text{if} \quad h_i^t \geq z_{b_i} \quad ; \quad h_{i-N}^t = z_{t_i} \\ 0 & \text{if} \quad h_i^t < z_{b_i} \quad ; \quad h_{i-N}^t = z_{t_i} \end{cases} \tag{3.50}$$

where

h_i	=	head at node *i*, (L);
h_{i-N}	=	head at upper adjacent node, (L);
z_{b_i}	=	bottom elevation of the aquitard at node *i*, (L);
z_{t_i}	=	top elevation of the aquitard at node *i*, (L);
t	=	index for previous time step, (dimensionless);
t+1	=	index for present time step, (dimensionless).

It should be noted that the decision on how to compute $\left(\Delta h_i^u\right)^{t+1}$ in (3.50) is based

on the known head values at time step *t*. During the development of IWFM, it has been observed that using the unknown head values at time step *t+1* to perform the above computations creates convergence problems. On the other hand, the formulation given in equation (3.50) results in robust solutions.

Similarly, the head difference between the aquifer in consideration (i.e. layer m) and the lower adjacent layer (i.e. layer m+1) can be expressed in the finite element notation as

$$\left(\Delta h_i^d\right)^{t+1} = \begin{cases} h_i^{t+1} - h_{i+N}^{t+1} & \text{if} \quad h_i^t \geq z_{t_i} \;\; ; \;\; h_{i+N}^t \geq z_{b_i} \\ z_{t_i} - h_{i+N}^{t+1} & \text{if} \quad h_i^t = z_{t_i} \;\; ; \;\; h_{i+N}^t \geq z_{b_i} \\ h_i^{t+1} - z_{t_i} & \text{if} \quad h_i^t \geq z_{t_i} \;\; ; \;\; h_{i+N}^t < z_{b_i} \\ 0 & \text{if} \quad h_i^t = z_{t_i} \;\; ; \;\; h_{i+N}^t < z_{b_i} \end{cases} \tag{3.51}$$

Substituting (3.50) and (3.51) into equation (3.10), one can express the vertical flow terms as

$$\sum_{e=N_e\cdot(m-1)+1}^{N_e\cdot m} H(m-2) \iint_{\Omega^e} L_{i-N} \left(\Delta h_i^u\right)^{t+1} \omega_i^e d\Omega^e$$

$$= H(m-2) L_{i-N} \left(\Delta h_i^u\right)^{t+1} A_i \tag{3.52}$$

$$\sum_{e=N_e\cdot(m-1)+1}^{N_e\cdot m} \left[1 - H(m-N_L)\right] \iint_{\Omega^e} L_{i+N} \left(\Delta h_i^d\right)^{t+1} \omega_i^e d\Omega^e$$

$$= \left[1 - H(m-N_L)\right] L_{i+N} \left(\Delta h_i^d\right)^{t+1} A_i \tag{3.53}$$

3.1.4. Vertical Flows when Aquifers are not Separated by an Aquitard

As in the previous section, the head difference between the aquifer layer in consideration and the upper adjacent layer can be expressed in finite element notation as

$$\left(\Delta h_i^u\right)^{t+1} = \begin{cases} h_i^{t+1} - h_{i-N}^{t+1} & \text{if} \quad h_i^t \geq z_{k_i} \quad ; \quad h_{i-N}^t > z_{k_i} \\ z_{k_i} - h_{i-N}^{t+1} & \text{if} \quad h_i^t < z_{k_i} \quad ; \quad h_{i-N}^t > z_{k_i} \\ h_i^{t+1} - z_{k_i} & \text{if} \quad h_i^t \geq z_{k_i} \quad ; \quad h_{i-N}^t = z_{k_i} \\ 0 & \text{if} \quad h_i^t < z_{k_i} \quad ; \quad h_{i-N}^t = z_{k_i} \end{cases} \tag{3.54}$$

where

z_{k_i} = elevation of the interface between the aquifer in consideration and the upper adjacent aquifer layer at node *i*, (L).

Similarly, one can express the discretized head difference between the aquifer and the lower adjacent aquifer layer as

$$\left(\Delta h_i^d\right)^{t+1} = \begin{cases} h_i^{t+1} - h_{i+N}^{t+1} & \text{if} \quad h_i^t \geq z_{k_i} \quad ; \quad h_{i+N}^t \geq z_{k_i} \\ z_{k_i} - h_{i+N}^{t+1} & \text{if} \quad h_i^t = z_{k_i} \quad ; \quad h_{i+N}^t \geq z_{k_i} \\ h_i^{t+1} - z_{k_i} & \text{if} \quad h_i^t \geq z_{k_i} \quad ; \quad h_{i+N}^t < z_{k_i} \\ 0 & \text{if} \quad h_i^t = z_{k_i} \quad ; \quad h_{i+N}^t < z_{k_i} \end{cases} \tag{3.55}$$

3.1.5. Land Subsidence

The expression for the rate of flow out of storage due to land subsidence, q_{sd}, is already given in previous chapter. Utilizing this expression and the approximate head field from equation (3.2), q_{sd} at an aquifer layer m can approximately be expressed as

$$q_{sd} \cong \sum_{j=N\cdot(m-1)+1}^{N\cdot m} S'_{s_j} \frac{\partial h_j}{\partial t} \omega_j \qquad m = 1, \cdots, N_L \tag{3.56}$$

Equation (3.56) is the spatially discretized version of the rate of flow out of storage due to land subsidence. To discretize (3.56) in time, IWFM uses the methodology described by Leake and Prudic (1988):

$$q_{sd}^{t+1} = \sum_{j=N\cdot(m-1)+1}^{N\cdot m} \left\{ \left(S'_{s_j}\right)^t \frac{\left(h_j^{t+1} - h_{c_j}^t\right)}{\Delta t} + S_{se_j} b_{o_j}^t \frac{\left(h_{c_j}^t - h_j^t\right)}{\Delta t} \right\} \omega_j \tag{3.57}$$

where

$$\left(S'_{s_j}\right)^t = \begin{cases} S_{se_j} b_{o_j}^t & \text{if} \quad h_j^{t+1} > h_{c_j}^t \\ S_{si_j} b_{o_j}^t & \text{if} \quad h_j^{t+1} \le h_{c_j}^t \end{cases} \tag{3.58}$$

S_{se_j} = elastic specific storage at node *j*, (1/L);

S_{si_j} = inelastic specific storage at node *j*, (1/L);

b_{o_j} = the thickness of the interbed at node *j*, (L);

h_{c_j} = pre-consolidation head at node *j*, (L).

Multiplying (3.57) by element shape functions, ω_i^e, integrating over individual elements and utilizing the mass lumping technique previously, one obtains

$$\sum_{e=N_e\cdot(m-1)+1}^{N_e\cdot m} \iint_{\Omega^e} q_{sd}^{t+1} \omega_i^e d\Omega^e \cong \left\{ \left(S'_{s_i}\right)^t \frac{\left(h_i^{t+1} - h_{c_i}^t\right)}{\Delta t} + S_{se_i} b_{o_i}^t \frac{\left(h_{c_i}^t - h_i^t\right)}{\Delta t} \right\} A_i \tag{3.59}$$

Once the groundwater flow equation is solved for a time step, the total compaction at a node can be computed by inserting the change in head, $\Delta h_i^{t+1} = h_i^{t+1} - h_i^t$,

into expressions for the elastic and inelastic change in the interbed thickness given in previous chapter, and summing the elastic and inelastic compactions:

$$\Delta b_{o_i}^{t+1} = \Delta b_{se_i}^{t+1} + \Delta b_{si_i}^{t+1} \tag{3.60}$$

$$\Delta b_{se_i}^{t+1} = -\Delta h_i^{t+1} S_{se_i} b_{o_i}^{t} \tag{3.61}$$

$$\Delta b_{si_i}^{t+1} = -\Delta h_i^{t+1} S_{si_i} b_{o_i}^{t} \tag{3.62}$$

Finally, the thickness of the interbed at a node can be computed by

$$b_{o_i}^{t+1} = b_{o_i}^{t} - \Delta b_{o_i}^{t+1} \tag{3.63}$$

In (3.63), the change in the interbed thickness, $\Delta b_{o_i}^{t+1}$, is subtracted from the previous thickness of the interbed, $b_{o_i}^{t}$, since a positive value represents compaction.

If an inelastic compaction occurs, it is also necessary to modify the pre-compaction head. In this case, the pre-compaction head is assigned the new head at the groundwater node:

$$h_{c_i}^{t+1} = \begin{cases} h_{c_i}^{t} & \text{if} \quad h_i^{t+1} \geq h_{c_i}^{t} \\ h_i^{t+1} & \text{if} \quad h_i^{t+1} < h_{c_i}^{t} \end{cases} \tag{3.64}$$

3.1.6. Root Water Uptake from Groundwater

The computation of root water uptake from groundwater, q_{et}^{t+1}, is discussed in detail in a separate document for IDC (DWR, 2015). As described in the previous chapter, it is a function of the elevation of the groundwater table and the extent of capillary rise above the groundwater table (among other atmospheric, plant and soil

properties) with respect to the rooting depth. In order to avoid excessive additional non-linearities and excessive iterations to resolve these non-linearities, IWFM uses the known groundwater heads from previous time step to compute the root water uptake from groundwater:

$$q_{et}^{t+1} = q_{et}^{t+1}\left(h_i^t\right) \tag{3.65}$$

Once q_{et}^{t+1} is computed by the land surface and root zone component of IWFM, it is substituted into equation (3.10). Then using equation (3.49), the discretized root water uptake from groundwater can be expressed as

$$\sum_{e=1}^{N_e} \iint_{\Omega^e} q_{et}^{t+1} \omega_i^e d\Omega^e = q_{et}^{t+1} A_i \tag{3.66}$$

3.1.7. Stream-Groundwater Interaction

The expression for stream-groundwater interaction, Q_{sint}, that occurs at a section of the stream represented by a stream node is given in previous chapter. In IWFM, it is required that a stream node coincides with a groundwater node. Utilizing the expression for Q_{sint} as given in previous chapter, one can write

$$\delta\left(x - x_s, y - y_s\right)\frac{Q_{sint}^{t+1}}{A_s} \cong \sum_{i=N\cdot(m-1)+1}^{N\cdot m} \delta\left(x - x_s, y - y_s\right)\frac{C_{s_i}\left[\max\left(h_{s_i}^{t+1}, h_{b_i}\right) - \max\left(h_i^{t+1}, h_{b_i}\right)\right]}{A_{s_i}}\omega_i \tag{3.67}$$

where

C_{s_i} = stream bed conductance at groundwater node *i*, (L^2/T);

h_{s_i} = stream surface elevation at groundwater node *i*, (L);

h_{b_i} = elevation of the stream bottom at groundwater node *i*, (L);

A_{s_i} = effective area of the stream segment at groundwater node *i*, (L^2).

Computation of stream bed conductance, C_{s_i}, in equation (3.67) varies depending on the version of the stream component being used:

$$C_{s_i} = \begin{cases} \dfrac{K_{s_i}}{d_{s_i}} L_i W_i & \text{version 4.0} \\ \dfrac{K_{s_i}}{d_{s_i}} L_i W_i \left(h_{s_i}^{t+1}\right) & \text{versions 4.1 and 5.0} \end{cases} \tag{3.68}$$

In stream component version 4.0, the wetted perimeter, W_i, is a constant value specified by the user. In stream component version 4.1, it is represented as a function of the stream head, $h_{s_i}^{t+1}$, using a rating table whereas in version 5.0 it is calculated based on the channel geometry specified by the user and $h_{s_i}^{t+1}$.

Equation (3.67) is valid only at the groundwater nodes where a stream node exists. Mathematically, this is represented by multiplying by the dirac delta function, $\delta\left(x - x_s, y - y_s\right)$, as shown in equation (3.67). Furthermore, (3.67) is defined for all aquifer layers only for the completeness of the mathematical derivation. In reality, stream nodes coincide with only the groundwater nodes at the top most layer (i.e. m=1) and (3.67) vanishes for other aquifer layers (i.e. $m = 2, \cdots, N_L$).

After multiplying (3.67) by the element shape functions, ω_i^e and integrating over individual elements, one obtains

$$\sum_{e=N_e\cdot(m-1)+1}^{N_e\cdot m}\iint_{\Omega^e}\delta\left(x-x_s,y-y_s\right)\frac{Q_{sint}^{t+1}}{A_s}\omega_i^e d\Omega^e$$

$$=\frac{C_{s_i}\left[\max\left(h_{s_i}^{t+1},h_{b_i}\right)-\max\left(h_i^{t+1},h_{b_i}\right)\right]}{A_{s_i}}\sum_{e=N_e\cdot(m-1)+1}^{N_e\cdot m}\iint_{\Omega^e}\delta\left(x-x_s,y-y_s\right)\omega_i^e d\Omega^e$$

$$=C_{s_i}\left[\max\left(h_{s_i}^{t+1},h_{b_i}\right)-\max\left(h_i^{t+1},h_{b_i}\right)\right] \tag{3.69}$$

Based on the expressions given in (3.40) and (3.44), the following equivalence is used in (3.69):

$$A_{s_i}=\sum_{e=N_e\cdot(m-1)+1}^{N_e\cdot m}\iint_{\Omega^e}\delta\left(x-x_s,y-y_s\right)\omega_i^e d\Omega^e \tag{3.70}$$

3.1.8. Lake-Groundwater Interaction

The expression for lake-groundwater interaction, Q_{lkint}, that occurs through an effective area of the lake represented by a lake node is given in previous chapter. In IWFM, it is required that a lake node coincides with a groundwater node. Utilizing the expression for Q_{lkint} as given in previous chapter, one can write

$$\delta\left(x-x_{lk},y-y_{lk}\right)\frac{Q_{lkint}^{t+1}}{A_{lk}}$$

$$\cong\sum_{j=N\cdot(m-1)+1}^{N\cdot m}\delta\left(x-x_{lk},y-y_{lk}\right)\frac{C_{lk_j}\left[\max\left(h_{lk}^{t+1},h_{blk_j}\right)-\max\left(h_j^{t+1},h_{blk_j}\right)\right]}{A_{lk_j}}\omega_j \tag{3.71}$$

where

C_{lk_j} = lake bed conductance at groundwater node *j*, (L^2/T);

h_{lk} = lake surface elevation, (L);

h_{blk_j} = elevation of the lake bottom at groundwater node *j*, (L);

A_{lk_j} = effective area of the lake at groundwater node *j*, (L^2).

After multiplying (3.71) by the element shape functions, ω_i^e and integrating over individual elements, one obtains

$$\sum_{e=N_e\cdot(m-1)+1}^{N_e\cdot m} \iint_{\Omega^e} \delta\left(x-x_{lk}, y-y_{lk}\right) \frac{Q_{lkint}^{t+1}}{A_{lk}} \omega_i^e d\Omega^e$$

$$= \frac{C_{lk_i}\left[\max\left(h_{lk}^{t+1}, h_{blk_i}\right) - \max\left(h_i^{t+1}, h_{blk_i}\right)\right]}{A_{lk_i}} \sum_{e=N_e\cdot(m-1)+1}^{N_e\cdot m} \iint_{\Omega^e} \delta\left(x-x_{lk}, y-y_{lk}\right) \omega_i^e d\Omega^e$$

$$= C_{lk_i}\left[\max\left(h_{lk}^{t+1}, h_{blk_i}\right) - \max\left(h_i^{t+1}, h_{blk_i}\right)\right] \tag{3.72}$$

Due to the expressions given in (3.40) and (3.44), the following equivalence is used in (3.72):

$$A_{lk_i} = \sum_{e=N_e\cdot(m-1)+1}^{N_e\cdot m} \iint_{\Omega^e} \delta\left(x-x_{lk}, y-y_{lk}\right) \omega_i^e d\Omega^e \tag{3.73}$$

In equations (3.71)-(3.72), the lake surface elevation, h_{lk}^{t+1}, appears without the subscript for the corresponding groundwater node. This is due to the fact that the changes in the lake surface elevation over an individual lake are assumed to be negligible in IWFM. For this reason, the same lake surface elevation prevails for all lake nodes that represent an individual lake.

3.1.9. Tile Drains and Subsurface Irrigation

Similar to stream-groundwater interaction and lake-groundwater interaction, the term for the tile drains/subsurface irrigation can also be discretized as follows:

$$\delta\left(x - x_{td}, y - y_{td}\right)\frac{Q_{td}^{t+1}}{A_{td}} \cong \sum_{j=N\cdot(m-1)+1}^{N\cdot m} \delta\left(x - x_{td}, y - y_{td}\right)\frac{C_{td_j}\left(z_{td_j} - h_j^{t+1}\right)}{A_{td_j}}\omega_j \tag{3.74}$$

where

C_{td_j} = conductance of the interface material between the tile drain/subsurface irrigation system at groundwater node *j*, (L^2/T);

z_{td_j} = elevation of the tile drain or the head at the subsurface irrigation system, (L);

A_{td_j} = effective area through which tile drain outflow or subsurface irrigation inflow at groundwater node *j* is occurring, (L^2).

After multiplying (3.74) by the element shape functions, ω_i^e and integrating over individual elements, one obtains

$$\sum_{e=N_e\cdot(m-1)+1}^{N_e\cdot m} \iint_{\Omega^e} \delta\left(x-x_{td}, y-y_{td}\right) \frac{Q_{td}^{t+1}}{A_{td}} \omega_i^e d\Omega^e$$

$$= \frac{C_{td_i}\left(z_{td_i} - h_i^{t+1}\right)}{A_{td_i}} \sum_{e=N_e\cdot(m-1)+1}^{N_e\cdot m} \iint_{\Omega^e} \delta\left(x-x_{td}, y-y_{td}\right) \omega_i^e d\Omega^e \tag{3.75}$$

$$= C_{td_i}\left(z_{td_i} - h_i^{t+1}\right)$$

and

$$A_{td_i} = \sum_{e=N_e\cdot(m-1)+1}^{N_e\cdot m} \iint_{\Omega^e} \delta\left(x-x_{td}, y-y_{td}\right) \omega_i^e d\Omega^e \tag{3.76}$$

3.1.10. Initial Conditions

The solution of equation (3.10) requires the knowledge of groundwater head values at the previous time step, t. Therefore, for the first time step, the head values at $t = 0$ need to be defined by the user (i.e. initial head values $h_i^{t=0}$).

3.1.11. Boundary Conditions

Boundary conditions are also required to solve (3.10). Boundary conditions, as well as initial conditions, constrain the problem and make solutions unique. Boundary conditions are not only necessary in solving the groundwater equation, but the accuracy is important as well. If inconsistent or incomplete boundary conditions are specified, the problem is ill defined (Wang and Anderson, 1982).

IWFM has the functionality to incorporate the following boundary conditions into the groundwater equation: (i) specified flux (Neumann), (ii) specified head (Dirichlet), (iii) general head and (iv) constrained general head. These boundary conditions can be constant over time or time-variant. In the following sections, the implementation of these boundary conditions into the numerical solution procedure will be discussed.

3.1.11.a. Specified Flux (Neumann)

In a finite element representation the specified flux value is multiplied by element shape functions and integrated over the element face for which the flux is specified:

$$\iint_{\Gamma^e} q_{\Gamma^e}^{t+1} \omega_i^e d\Gamma^e = -\iint_{\Gamma^e} f\left[x, y, (t+1)\cdot\Delta t\right] \omega_i^e d\Gamma^e \tag{3.77}$$

In IWFM, $-\iint_{\Gamma^e} f\left[x, y, (t+1)\cdot\Delta t\right] \omega_i^e d\Gamma^e$ is the boundary flow specified by the user and evaluated at time $(t+1)\cdot\Delta t$. Equation (3.77) replaces the second integral term of equation (3.10).

3.1.11.b. Specified Head (Dirichlet)

In the case that the head is specified at a finite element node *r*, the rth equation in the system of equations given in (3.10) becomes redundant. There is no longer a necessity to solve this equation since the head h_r^{t+1} at node *r* is known. Therefore, this equation is dropped from the system of equations.

3.1.11.c. General Head

The general head boundary inflow at a finite element node *r* can be expressed as

$$Q_{GHB_r}^{t+1} = \frac{K_r A_r}{d_r}\left(h_{GHB}^{t+1} - h_r^{t+1}\right) \tag{3.78}$$

where

Q_{GHB_r} = general head boundary flow at node *r*, (L^3/T);

K_r = hydraulic conductivity of the aquifer at node *r*, (L/T);

A_r = cross-sectional area at node *r* that flow passes through, (L^2);

d_r = distance between the boundary node *r* and the location of the known head, (L);

h_r = head value at the boundary node *r*, (L);

h_{GHB} = head at the nearby surface water body or aquifer, (L);

t = index for time step, (dimensionless).

When general head type boundary condition is defined at node *r*, equation (3.78) is subtracted from the rth equation of the equation system (3.10).

3.1.11.d. Constrained General Head

Similar to the inflow from a general head boundary condition, the inflow from a constrained general head boundary condition at a finite element node *r* can be expressed as

$$Q_{CGHB_r}^{t+1} = \begin{cases} \dfrac{K_r A_r}{d_r}\left(h_{GHB}^{t+1} - h_r^{t+1}\right) & \text{if} \quad h_r^{t+1} \geq h_{Cr} \\ \\ \dfrac{K_r A_r}{d_r}\left(h_{GHB}^{t+1} - h_{Cr}\right) & \text{if} \quad h_r^{t+1} < h_{Cr} \end{cases} \tag{3.79}$$

and

$$Q^{t+1}_{CGHB_r} \le Q^{t+1}_{CGHB_{r_{max}}} \tag{3.80}$$

where

h_{Cr} = limiting head value at node *r*, (L);

$Q_{CGHB_{r_{max}}}$ = maximum general head boundary flow, (L^3/T).

The only differences between a general head boundary condition and a constrained general head boundary condition are that i) if the groundwater head at node *r* falls below the limiting head value, h_{Cr}, the limiting head value is used in calculating the head gradient instead of the groundwater head itself, and ii) boundary flow in the constrained general head boundary condition can be limited with a maximum flow rate.

3.2. Stream Flows

3.2.1. Stream Routing Component Version 4.0

Stream flow equations given in previous chapter for stream routing component version 4.0 are already in algebraic form. Therefore, they are ready to be coupled with the discretized groundwater equation described in the preceding sections. The main stream flow equation can be re-written for the present time step as

$$Q_{s_i}\left(h^{t+1}_{s_i}\right) - Q^{t+1}_{in_i} + Q^{t+1}_{bdiv_i} + C_{s_i}\left[\max\left(h^{t+1}_{s_i}, h_{b_i}\right) - \max\left(h^{t+1}_{i}, h_{b_i}\right)\right] = 0 \tag{3.81}$$

The explicit expression for the stream-groundwater interaction, $Q^{t+1}_{sint_i}$, has been substituted into (3.81). The expressions for $Q^{t+1}_{in_i}$ and $Q^{t+1}_{bdiv_i}$ are given in previous chapter. Equation (3.81) is coupled and solved simultaneously with equation (3.10) for

stream surface elevation, $h_{s_i}^{t+1}$, and groundwater head at the stream node, h_i^{t+1}.

3.2.2. Stream Routing Component Version 4.1

In component version 4.1, stream bed conductance, C_{s_i}, is a function of stream surface elevation, h_{s_i}, since the wetted perimeter, W_{s_i}, is a function of h_{s_i}. Therefore, the stream flow equation re-written for the present time step in component version 4.1 is similar to equation (3.81) except for the different representation of C_{s_i}:

$$Q_{s_i}\left(h_{s_i}^{t+1}\right) - Q_{in_i}^{t+1} + Q_{bdiv_i}^{t+1}$$

$$+C_{s_i}\left[\max\left(h_{s_i}^{t+1}, h_i^{t+1}\right)\right] \times \left[\max\left(h_{s_i}^{t+1}, h_{b_i}\right) - \max\left(h_i^{t+1}, h_{b_i}\right)\right] = 0 \qquad (3.82)$$

Similar to equation (3.81), equation (3.82) is coupled and solved simultaneously with equation (3.10) for stream surface elevation, $h_{s_i}^{t+1}$, and groundwater head at the stream node, h_i^{t+1}.

3.2.3. Stream Routing Component Version 5.0

Stream flow conservation equation used in component version 5.0 is presented in the previous chapter. It is a partial differential equation and must be discretized both in space and time. IWFM uses the fully implicit finite difference scheme (Chaundry, 1993) with backward differencing for this purpose:

$$\frac{\left(A_i^{t+1}+A_{i-1}^{t+1}\right)-\left(A_i^{t}+A_{i-1}^{t}\right)}{2\Delta t}+\frac{Q_{s_i}^{t+1}-Q_{s_{i-1}}^{t+1}}{\Delta x_i}$$

$$-\frac{1}{2}\left(\frac{Q_{in_i}^{t+1}-Q_{out_i}^{t+1}}{L_i}+\frac{Q_{in_{i-1}}^{t+1}-Q_{out_{i-1}}^{t+1}}{L_{i-1}}\right)=0 \quad ; \quad i=2,\cdots,N_s \qquad (3.83)$$

$$h_{s_i}^{t+1}-F\left(Q_{s_i}^{t+1}\right)=0 \quad ; \quad i=1 \qquad (3.84)$$

where

i	=	stream node number, (dimensionless);
N_s	=	number of stream nodes in each stream reach, (dimensionless);
Δx_i	=	stream channel length between stream node *i* and *i–1*, (L);
L_i	=	length of stream segment associated with stream node *i* (see previous chapter for a detailed definition of stream segment); (L).

In equations (3.83) and (3.84), both A_i^{t+1} and $Q_{s_i}^{t+1}$ are functions of the stream surface elevation, $h_{s_i}^{t+1}$, as defined in the previous chapter.

Equation (3.83) is written for each stream node, except for the most upstream node, in each stream reach. For the most upstream node, stream flows defined as boundary conditions are used to calculate the stream head as shown in equation (3.84). Equations (3.83) and (3.84) are coupled and solved simultaneously with (3.10) for the stream heads, $h_{s_i}^{t+1}$.

The relationship depicted in equation (3.84) is given by the Manning's equation as discussed in the previous chapter. In a stream reach, if the most upstream node is also the most upstream node for the entire stream network that is modeled, then $Q_{s_1}^{t+1}$ is

specified by the user as the stream flow boundary condition. On the other hand, if the stream reach has one or more upstream reaches flowing into it, then $Q_{s_1}^{t+1}$ is the sum of the outflow from these reaches as calculated by the stream routing component version 5.0.

Equation (3.83) is unconditionally stable for all ranges of the spatiotemporal grid spacing (Holden and Stephenson, 1995). However, depending on the value of the Courant number, $c\frac{\Delta t}{\Delta x_i}$, numerical diffusion can be observed (Chaundry, 1983; Holden and Stephenson, 1995). Even though kinematic waves are not supposed to have diffusion, it is assumed in stream component version 5.0 that in real-world applications that is targeted by IWFM, there will always be some level of diffusion, and that the numerical diffusion can be modified through the calibration of the stream channel parameters to match the simulated stream flows with their observed counterparts.

3.2.3.a. Initial Conditions

The solution of equation (3.83) requires the knowledge of stream surface elevations at the previous time step, t. Therefore, for the first time step, these elevations at $t = 0$ need to be defined by the user (i.e. initial values $h_{s_i}^{t=0}$).

3.3. Lakes

The conservation equation for lake storage given in previous chapter is discretized as

$$\frac{S_{lk}\left(h_{lk}^{t+1}\right)-S_{lk}\left(h_{lk}^{t}\right)}{\Delta t}-Q_{divlk}^{t+1}-Q_{bplk}^{t+1}-Q_{rflk}^{t+1}-Q_{rtlk}^{t+1}-Q_{inlk}^{t+1}+Q_{lko}^{t+1}$$

$$-\sum_{i=1}^{N_{lk}}\left\{P_{lk_i}^{t+1}A_{lk_i}-EV_{lk_i}^{t+1}A_{lk_i}\right.$$

$$\left.-C_{lk_i}\left[\max\left(h_{lk}^{t+1},h_{blk_i}\right)-\max\left(h_{i}^{t+1},h_{blk_i}\right)\right]\right\}=0 \qquad (3.85)$$

In (3.85), the explicit expression for the lake-groundwater interaction, $Q_{lkint_i}^{t+1}$, has been used.

The total evaporation from the lake area represented by a lake node, $EV_{lk_i}^{t+1}A_{lk_i}$, is limited by the amount of water available at that lake node. This is represented in IWFM by the following formulation:

$$EV_{lk_i}^{t+1}A_{lk_i}\le\frac{A_{lk_i}}{\Delta t}\max\left(h_{lk}^{t+1}-b_{lk_i},0\right)+P_{lk_i}^{t+1}A_{lk_i}+\frac{A_{lk_i}}{A_{lk}}\left(Q_{brlk}^{t+1}+Q_{inlk}^{t+1}\right) \qquad (3.86)$$

Equation (3.86) suggests that the effect of precipitation and inflows to the water storage at a lake node is considered before the computation of evaporation. Also, the last term of equation (3.86) suggests that the inflows into the lake from diversions, bypasses and upstream lakes are distributed among the lake nodes evenly.

Equation (3.85) is valid when the lake surface elevation is less than the pre-specified maximum lake surface elevation, $h_{lk_{max}}$, or when the outflow from lake, Q_{lko}^{t+1}, is zero. If the lake surface elevation exceeds the maximum lake surface elevation, simply assigning h_{lk}^{t+1} to $h_{lk_{max}}$ does not satisfy equation (3.85) and violates the requirement for

the conservation of mass. In order to compute the lake outflow and still conserve mass by keeping lake elevation at its maximum, IWFM utilizes an alternative method.

Assuming that the groundwater head value is known, a function, F_{lk}, can be defined as equal to (3.85) less Q_{lko}^{t+1}:

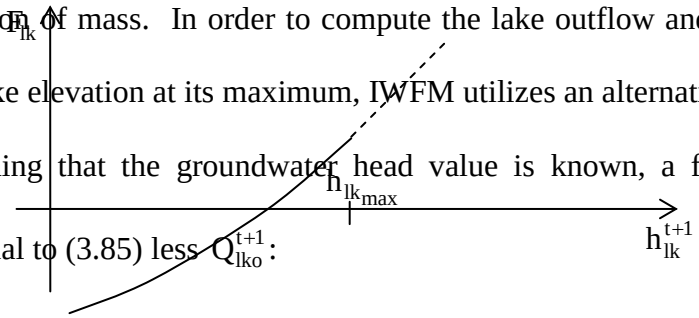

(a) Lake elevation does not exceed the maximum lake surface elevation

$$F_{lk}\left(h_{lk}^{t+1}\right)=\frac{S_{lk}\left(h_{lk}^{t+1}\right)-S_{lk}\left(h_{lk}^{t}\right)}{\Delta t}-Q_{divlk}^{t+1}-Q_{bplk}^{t+1}-Q_{rflk}^{t+1}-Q_{rtlk}^{t+1}-Q_{inlk}^{t+1}$$

$$-\sum_{i=1}^{F_{lk}}\left\{P_{lk_i}^{t+1}A_{lk_i}-EV_{lk_i}^{t+1}A_{lk_i}\right. \tag{3.87}$$

$$\left.-C_{lk_i}\left[\max\left(h_{lk}^{t+1},h_{blk_i}\right)-\max\left(Q_{lko}^{t+1},h_{blk_i}\right)h_{lk}^{t+1}\right]\right\}$$

Equating (3.87) to zero and solving is equivalent to finding its root with respect to h_{lk}^{t+1}.

(b) Lake elevation exceeds the maximum lake surface elevation

Figures 3.5.a and 3.5.b show two possible cases when (3.87) is plotted as a function of h_{lk}^{t+1}. The dashed parts of the curves represent F_{lk} when $h_{lk_{max}}$ is assumed to be large enough so that it does not have an effect on F_{lk}. However, in reality, F_{lk} is not defined beyond $h_{lk_{max}}$. When the root of (3.87) is below $h_{lk_{max}}$ (Figure 3.5.a), lake outflow,

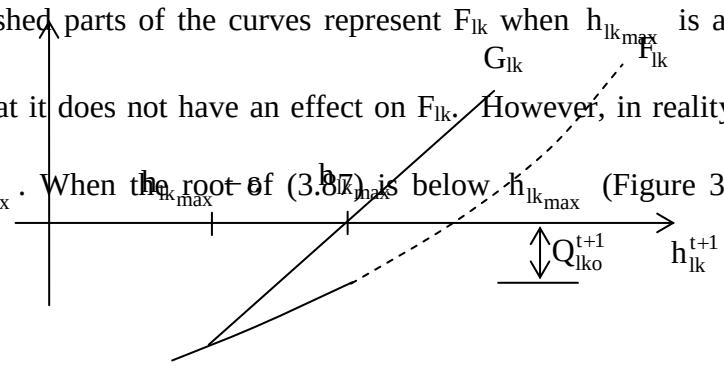

(c) Modified function, G_{lk}, when lake elevation exceeds the maximum elevation

Figure 3.5 Plots of possible lake storage functions and the modified function when lake elevation exceeds the maximum elevation

Q_{lko}^{t+1}, is zero and the computed root also satisfies (3.85). On the other hand, when the root of F_{lk} is above $h_{lk_{max}}$ (Figure 3.5.b), then Q_{lko}^{t+1} is non-zero. IWFM uses an iterative solution technique (namely, Newton-Raphson method which is explained later in this chapter) to find the root of (3.87). This method requires that the gradient of the function whose root is being sought for is non-zero and finite. In the case depicted in Figure 3.5.b, however, the gradient of F_{lk} at $h_{lk_{max}}$ is infinite. In this case, IWFM modifies the function F_{lk} in the vicinity of $h_{lk_{max}}$ so that the gradient of the modified function will be non-zero and finite, and its root is guaranteed to be equal to $h_{lk_{max}}$ (see Figure 3.5.c):

$$F_{lk}^{*} = \begin{cases} F_{lk} & \text{if} \quad h_{lk}^{t+1} \le h_{lk_{max}} - \varepsilon \\ \\ G_{lk} & \text{if} \quad h_{lk}^{t+1} > h_{lk_{max}} - \varepsilon \end{cases} \tag{3.88}$$

where

$$G_{lk} = F_{lk}\left(h_{lk_{max}}\right) \times \left[1 + \frac{h_{lk_{max}} - \varepsilon - h_{lk}^{t+1}}{\varepsilon}\right]; \tag{3.89}$$

F_{lk}^{*} = modified version of F_{lk}.

ε is chosen so that its value is small enough compared to the convergence criteria used for the iterative solution method. In this case, lake outflow, Q_{lko}^{t+1}, can be expressed as (Figure 3.5.c)

$$Q_{lko}^{t+1} = -F_{lk}\left(h_{lk_{max}}\right) \tag{3.90}$$

This approach allows for imposing the maximum lake elevation without disturbing the conservation of mass and the efficient use of numerical techniques for the

solution of non-linear equations. Equation (3.85) is coupled and solved simultaneously with (3.10) for lake elevation, h_{lk}^{t+1}, and groundwater head at lake node, h_i^{t+1}.

3.4. Land Surface and Root Zone Flow Processes

Mathematical models used in IWFM for the simulation of land surface and root zone flow processes are described in detail in another document (DWR, 2015) and they will not be covered in this documentation.

3.5. Soil Moisture in the Unsaturated Zone

The conservation equation that models the vertical movement of soil moisture in the unsaturated zone is discretized in IWFM as follows:

$$D_n^t \frac{\theta_{u,n}^{t+1} - \theta_{u,n}^t}{\Delta t} = Q_{in,n}^{t+1} - K_{u,n}^{t+1} \tag{3.91}$$

where

D_n	=	thickness of layer n, (L);
$\theta_{u,n}$	=	soil moisture in the nth unsaturated layer, (L/L);
Δt	=	length of time step, (T);
$Q_{in,n}$	=	inflow into unsaturated layer m from layer n-1, (L/T);
$K_{u,n}$	=	unsaturated hydraulic conductivity of layer n, (L/T);
t	=	time step, (dimensionless);
n	=	unsaturated layer number, (dimensionless).

The unsaturated hydraulic conductivity in equation (3.91), $K_{u,n}^{t+1}$, can be represented either by Mualem-van Genuchten (vGM) approach or Campbell's method:

$$K_{u,n}^{t+1} = \begin{cases} K_{s,n}\left(\dfrac{\theta_{u,n}^{t+1}}{\eta_{T,n}}\right)^{1/2}\left\{1-\left[1-\left(\dfrac{\theta_{u,n}^{t+1}}{\eta_{T,n}}\right)^{1/m}\right]^{m}\right\}^{2} & ;\ \text{vGM} \\ K_{s,n}\left(\dfrac{\theta_{u,n}^{t+1}}{\eta_{T,n}}\right)^{3+\frac{2}{\lambda_n}} & ;\ \text{Campbell} \end{cases} \tag{3.92}$$

and

$$m = \frac{\lambda_n}{\lambda_n + 1} \tag{3.93}$$

where

$\eta_{T,n}$ = total porosity of the unstaturated layer n, (L/L);

λ_n = pore size distribution index of unsaturated layer n, (dimensionless).

Due to the non-linearity of equation (3.91), it is solved for $\theta_{u,n}^{t+1}$, iteratively. IWFM uses a combination of bisection and Newton's methods to solve for the soil moisture in the unsaturated layer n (Gerald and Wheatley, 1994). The iterative solution methodology starts and continues with Newton iterations:

$$\left(\theta_{u,n}^{t+1}\right)^{k+1} = \left(\theta_{u,n}^{t+1}\right)^{k} - \frac{F\left[\left(\theta_{u,n}^{t+1}\right)^{k}\right]}{F'\left[\left(\theta_{u,n}^{t+1}\right)^{k}\right]} \tag{3.94}$$

where

$$F\left[\left(\theta_{u,n}^{t+1}\right)^{k}\right]=\begin{cases} Q_{in,n}^{t+1}-D_{n}^{t}\left(\dfrac{\left(\theta_{u,n}^{t+1}\right)^{k}-\theta_{u,n}^{t}}{\Delta t}\right) \\ \quad -K_{s,n}\left(\dfrac{\theta_{u,n}^{t+1}}{\eta_{T,n}}\right)^{1/2}\left\{1-\left[1-\left(\dfrac{\theta_{u,n}^{t+1}}{\eta_{T,n}}\right)^{1/m}\right]^{m}\right\}^{2} & ;\ \text{vGM} \\ \\ Q_{in,n}^{t+1}-D_{n}^{t}\left(\dfrac{\left(\theta_{u,n}^{t+1}\right)^{k}-\theta_{u,n}^{t}}{\Delta t}\right) \\ \quad -K_{s,n}\left(\dfrac{\theta_{u,n}^{t+1}}{\eta_{T,n}}\right)^{3+\frac{2}{\lambda_{n}}} & ;\ \text{Campbell} \end{cases} \tag{3.95}$$

$$F'\left[\left(\theta_{u,n}^{t+1}\right)^{k}\right]=\begin{cases} -\dfrac{D_{n}^{t}}{\Delta t}-\dfrac{K_{s,n}G_{1}^{2}}{2\eta_{T,n}\sqrt{\dfrac{\left(\theta_{u,n}^{t+1}\right)^{k}}{\eta_{T,n}}}} \\ \quad +2mK_{s,n}G_{1}G_{2}^{m-1}\left(dG_{2}\right)\sqrt{\dfrac{\left(\theta_{u,n}^{t+1}\right)^{k}}{\eta_{T,n}}} & ;\ \text{vGM} \\ \\ -\dfrac{D_{n}^{t}}{\Delta t} \\ \quad -K_{s,n}\left(\dfrac{3+\frac{2}{\lambda_{n}}}{\eta_{T,n}}\right)\left(\dfrac{\left(\theta_{u,n}^{t+1}\right)^{k}}{\eta_{T,n}}\right)^{3+\frac{2-\lambda_{n}}{\lambda_{n}}} & ;\ \text{Campbell} \end{cases} \tag{3.96}$$

$$G_1 = 1 - G_2^m \tag{3.97}$$

$$G_2 = 1 - \left(\frac{\left(\theta_{u,n}^{t+1}\right)^k}{\eta_{T,n}} \right)^{1/m} \tag{3.98}$$

$$dG_2 = -\frac{1}{m\eta_{T,n}} \left(\frac{\left(\theta_{u,n}^{t+1}\right)^k}{\eta_{T,n}} \right)^{\frac{1-m}{m}} \tag{3.99}$$

In equations (3.94)-(3.99), k is the iteration number and vGM represents the van Genuchten-Mualem approach.

Newton's method is used until the estimate for the soil moisture goes above total porosity less 10% of the user-defined convergence tolerance for the iterative solver. At this point, bisection method is used as the iterative method. The reason for this switch between the two methods is that the gradient of the van Genuchten-Mualem equation near saturation becomes very large and this leads to convergence issues with Newton's method. Bisection method has slower convergence but is more robust; therefore it is preferred when soil moisture is close to saturation.

Equation (3.94) is solved iteratively until a user-specified convergence level is achieved; i.e. until $\left| \left(\theta_{u,m}^{t+1}\right)^{k+1} - \left(\theta_{u,m}^{t+1}\right)^{k} \right|$ is less than a pre-defined value.

The flowchart for the routing of moisture in a multi-layer unsaturated zone is illustrated in Figure 3.6. As shown in this figure, the water that percolates through the

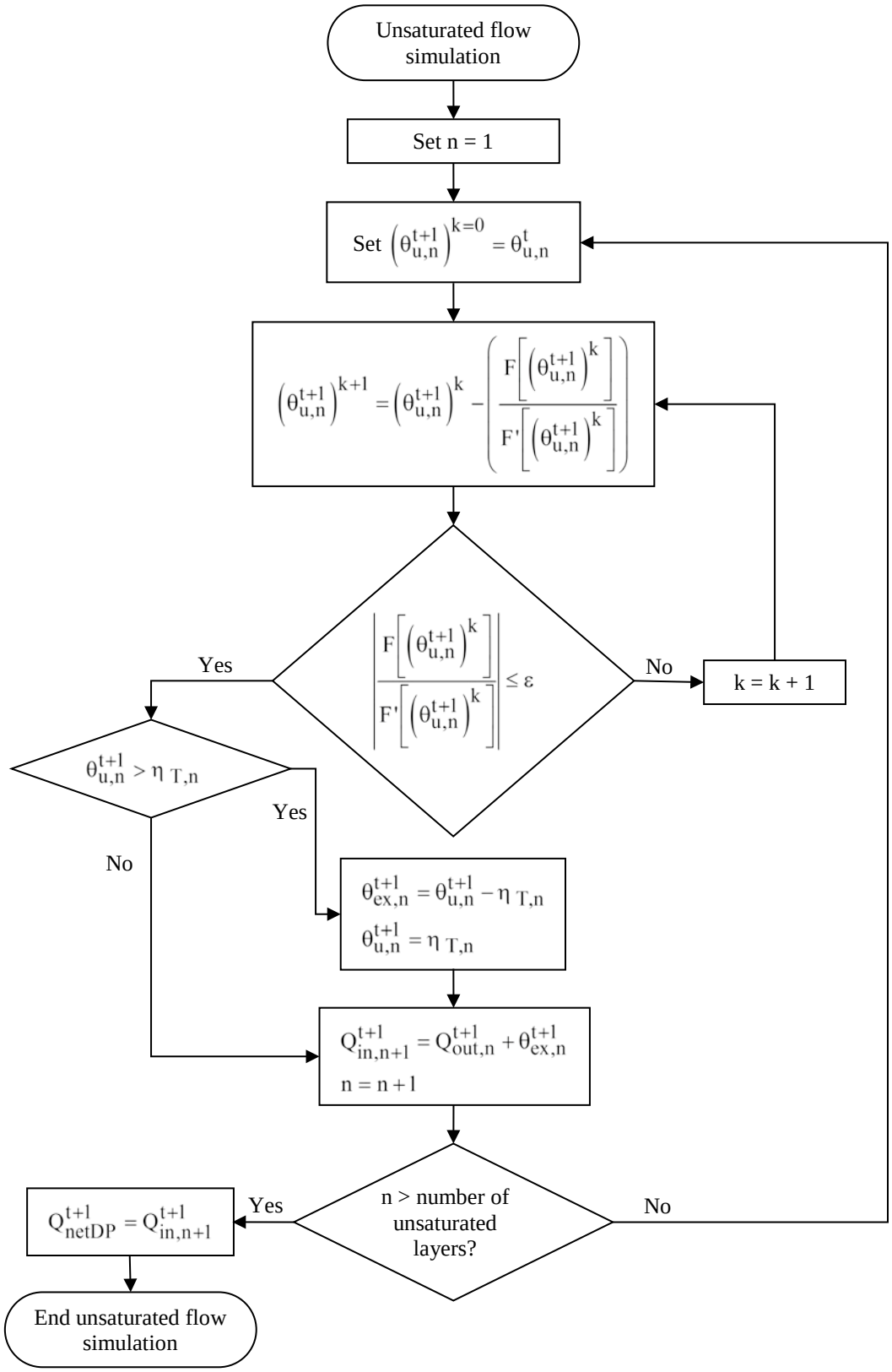

Figure 3.6 Flowchart for the unsaturated zone flow simulation

root zone is the inflow to the first unsaturated layer. First, the moisture content at the first unsaturated layer $\left(\theta_{u,1}^{t+1}\right)$ is computed, iteratively. The outflow, $Q_{out,1}^{t+1}$, can then be redefined as a function of $\left(\theta_{u,1}^{t+1}\right)^{k+1}$. Based on the conservation of mass, $Q_{out,2}^{t+1} = Q_{out,1}^{t+1}$. Therefore, the soil moisture in layer 2 and the flow out of layer 2 are simulated in the same manner as layer 1. This procedure is performed for each layer until the net deep percolation into groundwater is calculated.

When simulating the soil moisture at each layer, IWFM checks that the soil moisture is less than or equal to the total porosity. If the soil moisture exceeds the total porosity of unsaturated layer n, the excess soil moisture, $\theta_{ex,n}^{t+1}$ is assumed to drain due to gravitational force and is routed to unsaturated layer n+1, unless the layer is the last unsaturated layer within the system. The last layer's excess soil moisture is routed to the saturated groundwater below it.

3.6. Small Watersheds

The conservation equation for the groundwater storage at a small watershed is discretized in IWFM using the implicit discretization method:

$$S_{wg}^{t+1} = S_{wg}^{t} + \left(D_{wp}^{t+1} - Q_{wg}^{t+1} - Q_{wgs}^{t+1}\right)\Delta t \qquad (3.100)$$

where

S_{wg} = groundwater storage within the small watershed boundary, (L^3);

D_{wp} = net deep percolation, i.e. recharge, to the groundwater storage within the small watershed domain, (L^3/T);

Q_{wg} = subsurface outflow from the small watershed that contributes to the groundwater storage at the modeled area, (L^3/T);

Q_{wgs} = contribution of groundwater storage to the surface flow at the small watershed, (L^3/T);

Δt = length of time step, (T);

t = index for time step, (dimensionless).

The net deep percolation, D_{wp}^{t+1}, is computed numerically using the same methodology described in the preceding section. Subsurface outflow from the small watershed, Q_{wg}^{t+1}, and the contribution of groundwater storage to the surface flow at the small watershed, Q_{wgs}^{t+1}, are computed as functions of the groundwater storage at the previous time step and the net deep percolation:

$$Q_{wg}^{t+1} = C_{wg}\left(S_{wg}^{t} + D_{wp}^{t+1}\right)\Delta t \tag{3.101}$$

$$Q_{wgs}^{t+1} = C_{ws}\left[\left(S_{wg}^{t} + D_{wp}^{t+1}\right)\Delta t - S_{wgt}\right] \tag{3.102}$$

where

C_{wg} = subsurface flow recession coefficient, (1/T);

C_{ws} = surface runoff recession coefficient, (1/T);

S_{wgt} = threshold value for groundwater storage within the small watershed above which groundwater at the small watershed contributes to surface flow, (L^3).

3.7. Solution of the System of Equations

Simulation of the hydrological processes that are included in IWFM requires the simultaneous solution of three equations; namely groundwater flow equation, stream flow equation and the lake storage equation. Spatial and temporal discretization of the groundwater, stream and lake equations result in a system of non-linear algebraic equations where the unknowns are the groundwater head $\left(h^{t+1}\right)$, stream surface elevation $\left(h_s^{t+1}\right)$ and the lake elevation $\left(h_{lk}^{t+1}\right)$ at the present time step. This system of equations can be represented in a matrix form as

$$[X]\left\{\mathbb{H}^{t+1}\right\}+\{F\}=0 \tag{3.103}$$

In (3.103), $\left\{\mathbb{H}^{t+1}\right\}$ is the vector of unknowns that is generated by augmenting the unknown groundwater heads, stream surface elevations and the lake surface elevations at the present time step:

$$\left\{\mathbb{H}^{t+1}\right\}=\begin{Bmatrix} h_{s_1}^{t+1} \\ \vdots \\ h_{s_{NR}}^{t+1} \\ h_{lk_1}^{t+1} \\ \vdots \\ h_{lk_{NLK}}^{t+1} \\ h_1^{t+1} \\ \vdots \\ h_{N_L \cdot N}^{t+1} \end{Bmatrix} \tag{3.104}$$

where

NR = total number of stream nodes, (dimensionless);

NLK = total number of lakes, (dimensionless);

N_L = number of aquifer layers, (dimensionless);

N = number of finite element nodes in an aquifer layer, (dimensionless).

Therefore, equation (3.103) represents a system of $NR + NLK + N_L \cdot N$ equations. The first NR equations are expressed as in (3.81), the $(NR+1)^{th}$ to $(NR+NLK)^{th}$ equations are expressed as in (3.85), and the rest of the equations are given in (3.10).

IWFM uses Newton-Raphson method in order to linearize the equation set (3.103). This method utilizes the Taylor series expansion of (3.103) around starting values of unknowns and truncates the second and higher order terms. Using the Newton-Raphson method, the rth equation of (3.103), $\mathbb{F}_r$, can be expressed as (Huyakorn and Pinder, 1983)

$$\sum_{i=1}^{NR+NLK+N_L \cdot N} \left(\frac{\partial \mathbb{F}_r}{\partial \mathbb{H}_i^{t+1}} \right)^k \left(\Delta \mathbb{H}_i^{t+1} \right)^{k+1} = \mathbb{F}_r^k \tag{3.105}$$

where

$$\mathbb{F}_r = \mathbb{F}_r \left\{ \mathbb{H}_1, \mathbb{H}_2, \cdots, \mathbb{H}_{NR+NLK+N_L \cdot N-1}, \mathbb{H}_{NR+NLK+N_L \cdot N} \right\} \tag{3.106}$$

and

$$\left(\Delta \mathbb{H}_i^{t+1} \right)^{k+1} = \left(\mathbb{H}_i^{t+1} \right)^{k+1} - \left(\mathbb{H}_i^{t+1} \right)^k \tag{3.107}$$

In (3.105)-(3.107), k is the iteration level. For $r = 1, \cdots, NR + NLK + N_L \cdot N$

equation (3.105) represents a system of linear equations that needs to be solved for $\left(\Delta\mathbb{H}_i^{t+1}\right)^{k+1}$. This system of equation can be expressed in matrix notation as

$$\left[\mathbb{X}^k\right]\left\{\left(\Delta\mathbb{H}^{t+1}\right)^{k+1}\right\}=\left\{\mathbb{F}^k\right\} \tag{3.108}$$

The aim is to estimate the unknown values of $\mathbb{H}_i^{t+1}$, compute the components of the matrix $\left[\mathbb{X}^k\right]$ and the vector $\left\{\mathbb{F}^k\right\}$ and solve the equation system (3.108) for $\left(\Delta\mathbb{H}_i^{t+1}\right)^{k+1}$. The L_2-norm of the difference vector is used to check the convergence:

$$\left\|\left(\Delta\mathbb{H}^{t+1}\right)^{k+1}\right\|_2=\sqrt{\sum_{i=1}^{NR+NLK+N_L\cdot N}\left[\left(\Delta H_i^{t+1}\right)^{k+1}\right]^2} \tag{3.109}$$

If the L_2-norm given in (3.109) is not smaller than a pre-specified tolerance, the unknown values of $\mathbb{H}_i^{t+1}$ are re-estimated using (3.107), and the procedure is continued until convergence is achieved. The components of $\left[\mathbb{X}^k\right]$ and $\left\{\mathbb{F}^k\right\}$ are listed in Appendix A.

The coefficient matrix $\left[\mathbb{X}^k\right]$ in (3.108) is a sparse matrix. The level of its sparseness depends on the numbering of groundwater, stream and lake nodes. IWFM uses either the over-relaxation method combined with the Jacobi method (Gerald and Wheatley, 1994), or a modified pre-conditioned conjugate gradient method (Dixon et. al, 2010 and 2011) to solve the equation system in (3.108), iteratively. The over-relaxation method will be explained in this document. The details of the modified pre-conditioned

conjugate gradient method are explained by Dixon et. al (2010, 2011).

The over-relaxation method starts with an initial estimate to the solution vector, $\left\{\left[\left(\Delta\mathbb{H}^{t+1}\right)^{k+1}\right]^{r}\right\}$, where *r* is the iteration counter for the iterative solution of (3.108). It should be noted that the iteration counter *r* is different than the iteration counter *k*. Index *k* is the iteration counter for Newton-Raphson method which is used to solve a system of non-linear equations. On the other hand, index *r* is the iteration counter for the matrix inversion method that is used to solve the matrix equation that is generated by a single iteration of the Newton-Raphson method.

With initial estimates, the ith equation of (3.108) can be solved for the new estimate of the unknown value:

$$\left[\left(\Delta\mathbb{H}_{i}^{t+1}\right)^{k+1}\right]^{r+1} = \frac{\mathbb{F}_{i}^{k} - \sum\limits_{\substack{j=1\\ j\neq i}}^{NR+NLK+N_L\cdot N} \mathbb{X}_{i,j}^{k}\left[\left(\Delta\mathbb{H}_{j}^{t+1}\right)^{k+1}\right]^{r}}{\mathbb{X}_{i,i}^{k}} \tag{3.110}$$

Equation (3.110) is used to compute all the components of the solution vector, and the convergence between the initial estimates and the newly computed values is checked:

$$\sqrt{\sum_{i}\left(\left[\left(\Delta\mathbb{H}_{i}^{t+1}\right)^{k+1}\right]^{r+1} - \left[\left(\Delta\mathbb{H}_{i}^{t+1}\right)^{k+1}\right]^{r}\right)^{2}} \leq \varepsilon \tag{3.111}$$

where $i = 1, \cdots, NR + NLK + N_L \cdot N$. If the convergence criteria given in (3.111) is not satisfied for all unknowns, the over-relaxation method is used to update their values:

$$\left[\left(\Delta\mathbb{H}_i^{t+1}\right)^{k+1}\right]^{r+1^*}$$

$$=\left[\left(\Delta\mathbb{H}_i^{t+1}\right)^{k+1}\right]^{r}+\beta\left\{\left[\left(\Delta\mathbb{H}_i^{t+1}\right)^{k+1}\right]^{r+1}-\left[\left(\Delta\mathbb{H}_i^{t+1}\right)^{k+1}\right]^{r}\right\} \qquad (3.112)$$

where $i=1,\cdots,NR+NLK+N_L\cdot N$. In (3.112), $\left[\left(\Delta\mathbb{H}_i^{t+1}\right)^{k+1}\right]^{r+1^*}$ is the new estimate that will be used in the next iteration instead of $\left[\left(\Delta\mathbb{H}_i^{t+1}\right)^{k+1}\right]^{r+1}$, and β is the relaxation parameter.

3.7.1. Compressed Storage of Matrices

In order to decrease the computer storage requirements, IWFM only stores the non-zero components of the coefficient matrix $\left[\mathbb{X}^k\right]$ (see Appendix A for expressions of non-zero components). These values are stored in a one-dimensional array in order to decrease the array access times and, hence, computer run times.

Storing only some of the components of a two-dimensional matrix in a one-dimensional array requires the storage of locations of these components to be able to re-construct the matrix. The location of a non-zero component in the matrix $\left[\mathbb{X}^k\right]$ depends on the node numbering in the model and the stream, lake and groundwater nodes that interact with each other. As an example, consider Figure 3.7 where a hypothetical model domain with 2 aquifer layers is represented by 6 finite elements, 12 groundwater nodes, 5

stream nodes and 1 lake. Therefore, there are a total of 18 unknown parameters whose values are computed by solving the stream, lake and groundwater conservation equations simultaneously.

A stream node is connected to a groundwater node and other stream nodes that are located directly upstream of it; a lake is connected to multiple groundwater nodes; a groundwater node is connected to an upper groundwater node, a lower groundwater node, surrounding groundwater nodes and a stream node or a lake. The node connection scheme for the system shown in Figure 3.7 is tabulated in Table 3.1. The global unknown numbers are printed in bold and the corresponding stream node, groundwater node or lake numbers are printed in parentheses.

Table 3.1 lists the locations of the non-zero components of the coefficient matrix $\left[\mathbb{X}^k\right]$. An "unknown number-connecting node" pair represents the row and column numbers of a non-zero component. An "unknown number-unknown number" pair represents a component located on the diagonal of the matrix. For instance, an unknown number of 10 and connecting node number 4 represents the component in the 10th row and the 4th column of the coefficient matrix (see Table 3.1). This component is the derivative of the conservation equation written at groundwater node 4 with respect to the stream surface elevation at stream node 4.

Table 3.1 lists the global unknown numbers and the connecting nodes as they are stored in IWFM. For some groundwater nodes, a value of zero appears for upper or lower connecting groundwater nodes. When IWFM encounters a value of zero, this means that there is no upper or lower aquifer layer for the groundwater node being considered.

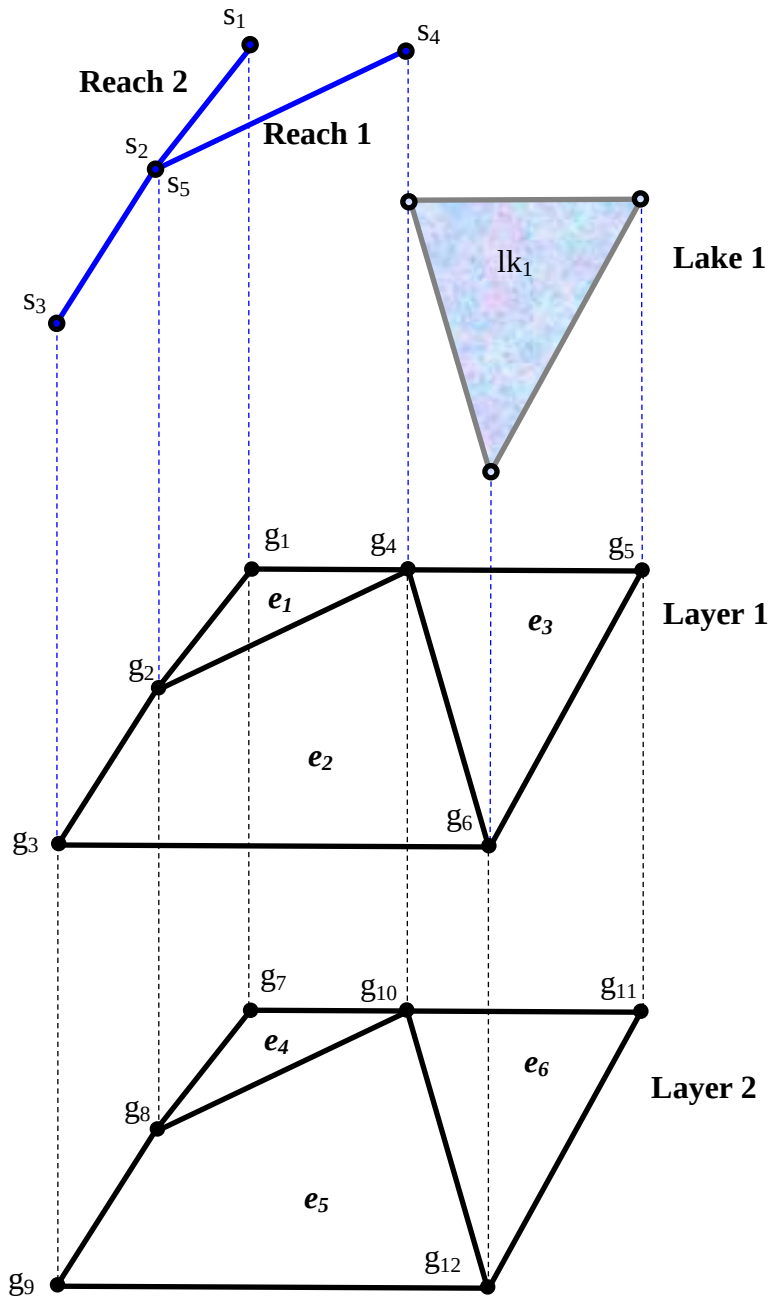

Figure 3.7 Hypothetical model domain

Unknown Number	Connecting Nodes: GW Node	Upstream Node 1	Upstream Node 2
1 (s_1)	**7** (g_1)		
2 (s_2)	**8** (g_2)	**1** (s_1)	**5** (s_5)
3 (s_3)	**9** (g_3)	**2** (s_2)	
4 (s_4)	**10** (g_4)		
5 (s_5)	**8** (g_2)	**4** (s_4)	

(a) Connecting nodes for stream nodes

Unknown Number	Connecting Nodes: GW Node 1	GW Node 2	GW Node 3
6 (lk_1)	**10** (g_4)	**12** (g_6)	**11** (g_5)

(b) Connecting nodes for lakes

Unknown Number	Connecting Nodes: Upper GW Node	Lower GW Node	Stream/Lake Node 1	Stream/Lake Node 2	Surrounding GW Node 1	Surrounding GW Node 2	Surrounding GW Node 3	Surrounding GW Node 4	Surrounding GW Node 5
7 (g_1)	**0**	**13** (g_7)	**1** (s_1)		**8** (g_2)	**10** (g_4)			
8 (g_2)	**0**	**14** (g_8)	**2** (s_2)	**5** (s_5)	**10** (g_4)	**7** (g_1)	**9** (g_3)	**12** (g_6)	
9 (g_3)	**0**	**15** (g_9)	**3** (s_3)		**12** (g_6)	**10** (g_4)	**8** (g_2)		
10 (g_4)	**0**	**16** (g_{10})	**4** (s_4)	**6** (lk_1)	**7** (g_1)	**8** (g_2)	**9** (g_3)	**12** (g_6)	**11** (g_5)
11 (g_5)	**0**	**17** (g_{11})		**6** (lk_1)	**10** (g_4)	**12** (g_6)			
12 (g_6)	**0**	**18** (g_{12})		**6** (lk_1)	**10** (g_4)	**8** (g_2)	**9** (g_3)	**11** (g_5)	
13 (g_7)	**7** (g_1)	**0**			**14** (g_8)	**16** (g_{10})			
14 (g_8)	**8** (g_2)	**0**			**16** (g_{10})	**13** (g_7)	**15** (g_9)	**18** (g_{12})	
15 (g_9)	**9** (g_3)	**0**			**18** (g_{12})	**16** (g_{10})	**14** (g_8)		
16 (g_{10})	**10** (g_4)	**0**			**13** (g_7)	**14** (g_8)	**15** (g_9)	**18** (g_{12})	**17** (g_{11})
17 (g_{11})	**11** (g_5)	**0**			**16** (g_{10})	**18** (g_{12})			
18 (g_{12})	**12** (g_6)	**0**			**16** (g_{10})	**14** (g_8)	**15** (g_9)	**17** (g_{11})	

(c) Connecting nodes for groundwater nodes

Table 3.1 Node connection scheme for the example shown in Figure 3.7

IWFM uses a one-dimensional array, $\{\mathrm{JND}\}$, to store the information given in Table 3.1. Another one-dimensional array, $\{\mathrm{NJD}\}$, is used to store the index numbers in $\{\mathrm{JND}\}$, where information for a node, i.e. for a row of $\left[\mathbb{X}^k\right]$, starts:

$$\{\mathrm{JND}\} = \left\{ \overbrace{1,7}^{\substack{\text{Unknown 1} \\ \left(\text{row 1 of } \left[\mathbb{X}^k\right]\right)}} , \overbrace{2,8,1,5}^{\substack{\text{Unknown 2} \\ \left(\text{row 2 of } \left[\mathbb{X}^k\right]\right)}} ,\cdots, \overbrace{6,10,12,11}^{\substack{\text{Unknown 6} \\ \left(\text{row 6 of } \left[\mathbb{X}^k\right]\right)}} ,\cdots, \overbrace{18,12,0,16,14,15,17}^{\substack{\text{Unknown 18} \\ \left(\text{row 18 of } \left[\mathbb{X}^k\right]\right)}} \right\} \quad (3.113)$$

$$\{\mathrm{NJD}\} = \{ 1 , 3 ,\cdots, 15 ,\cdots, 96\} \quad (3.114)$$

With the information stored in the arrays $\{\mathrm{JND}\}$ and $\{\mathrm{NJD}\}$, the coefficient matrix can be reconstructed. For the example shown in Figure 3.7, the coefficient matrix $\left[\mathbb{X}^k\right]$ has a total of 324 (= 18 $\times$ 18) components. The above methodology for storing information has a total of 222 components (102 components for $\{\mathrm{JND}\}$, 18 components for $\{\mathrm{NJD}\}$ and 102 components for the array that stores the actual values of non-zero components of $\left[\mathbb{X}^k\right]$). This amounts to around 30% of savings in computer storage requirements even for a small problem as shown in Figure 3.7. For larger problems, savings in storage requirements will be larger.

Another two-dimensional matrix that arises due to the numerical methods used in IWFM is the conductance matrix (see equation (3.10)):

$$AT_{i,j}^{t+1} = \sum_{e=N_e\cdot(m-1)+1}^{N_e\cdot m} \left(T^e\right)^{t+1} \iint_{\Omega^e} \bar{\nabla}\omega_i^e \bar{\nabla}\omega_j^e d\Omega^e \quad (3.115)$$

where $1 \le m \le N_L$ and . $N \cdot (m-1)+1 \le i, j \le N \cdot m$.

The components of $\left[AT^{t+1}\right]$ are stored for each groundwater node. As an example, consider the finite element mesh depicted in Figure 3.7. For elements 1, 2, and 3 of Figure 3.7, the element conductance matrices for the first aquifer layer will have the following structure:

$$\left[AT^{e1}\right] = \begin{array}{cc} & \begin{array}{ccc} \boldsymbol{g_1} & \boldsymbol{g_2} & \boldsymbol{g_4} \end{array} \\ & \begin{bmatrix} AT^{e1}_{g1,g1} & AT^{e1}_{g1,g2} & AT^{e1}_{g1,g4} \\ AT^{e1}_{g2,g1} & AT^{e1}_{g2,g2} & AT^{e1}_{g2,g4} \\ AT^{e1}_{g4,g1} & AT^{e1}_{g4,g2} & AT^{e1}_{g4,g4} \end{bmatrix} \end{array} \begin{array}{c} \\ \boldsymbol{g_1} \\ \boldsymbol{g_2} \\ \boldsymbol{g_4} \end{array} \tag{3.116}$$

$$\left[AT^{e2}\right] = \begin{array}{cc} & \begin{array}{cccc} \boldsymbol{g_2} & \boldsymbol{g_3} & \boldsymbol{g_6} & \boldsymbol{g_4} \end{array} \\ & \begin{bmatrix} AT^{e2}_{g2,g2} & AT^{e2}_{g2,g3} & AT^{e2}_{g2,g6} & AT^{e2}_{g2,g4} \\ AT^{e2}_{g3,g2} & AT^{e2}_{g3,g3} & AT^{e2}_{g3,g6} & AT^{e2}_{g3,g4} \\ AT^{e2}_{g6,g2} & AT^{e2}_{g6,g3} & AT^{e2}_{g6,g6} & AT^{e2}_{g6,g4} \\ AT^{e2}_{g4,g2} & AT^{e2}_{g4,g3} & AT^{e2}_{g4,g6} & AT^{e2}_{g4,g4} \end{bmatrix} \end{array} \begin{array}{c} \\ \boldsymbol{g_2} \\ \boldsymbol{g_3} \\ \boldsymbol{g_6} \\ \boldsymbol{g_4} \end{array} \tag{3.117}$$

$$\left[AT^{e3}\right] = \begin{array}{cc} & \begin{array}{ccc} \boldsymbol{g_4} & \boldsymbol{g_6} & \boldsymbol{g_5} \end{array} \\ & \begin{bmatrix} AT^{e3}_{g4,g4} & AT^{e3}_{g4,g6} & AT^{e3}_{g4,g5} \\ AT^{e3}_{g6,g4} & AT^{e3}_{g6,g6} & AT^{e3}_{g6,g5} \\ AT^{e3}_{g5,g4} & AT^{e3}_{g5,g6} & AT^{e3}_{g5,g5} \end{bmatrix} \end{array} \begin{array}{c} \\ \boldsymbol{g_4} \\ \boldsymbol{g_6} \\ \boldsymbol{g_5} \end{array} \tag{3.118}$$

In equations (3.116)-(3.118), the time step index t+1 is dropped for simplicity. Element conductance matrices will have the similar structure for other layers of the aquifer system except that the indexing will change with the changing node numbers. The component values are also likely to be different for each layer since the transmissivities at a vertical cross-section may differ. IWFM stores the following

components of matrices (3.116)-(3.118) in an augmented one-dimensional array:

$$
\begin{array}{ll}
\{AT\} = \Big\{ AT^{e_1}_{g_1,g_2}, AT^{e_1}_{g_1,g_4}, & \textbf{\textit{node } g_1} \\
\quad AT^{e_1}_{g_2,g_4} + AT^{e_2}_{g_2,g_4}, AT^{e_1}_{g_2,g_1}, AT^{e_2}_{g_2,g_3}, AT^{e_2}_{g_2,g_6}, & \textbf{\textit{node } g_2} \\
\quad AT^{e_2}_{g_3,g_6}, AT^{e_2}_{g_3,g_4}, AT^{e_2}_{g_3,g_2}, & \textbf{\textit{node } g_3} \\
\quad AT^{e_1}_{g_4,g_1}, AT^{e_1}_{g_4,g_2} + AT^{e_2}_{g_4,g_2}, AT^{e_2}_{g_4,g_3}, AT^{e_2}_{g_4,g_6} + AT^{e_3}_{g_4,g_6}, AT^{e_3}_{g_4,g_5}, & \textbf{\textit{node } g_4} \\
\quad AT^{e_3}_{g_5,g_4}, AT^{e_3}_{g_5,g_6}, & \textbf{\textit{node } g_5} \\
\quad AT^{e_2}_{g_6,g_4} + AT^{e_3}_{g_6,g_4}, AT^{e_2}_{g_6,g_2}, AT^{e_2}_{g_6,g_3}, AT^{e_3}_{g_6,g_5}, & \textbf{\textit{node } g_6} \\
\quad AT^{e_4}_{g_7,g_8}, AT^{e_4}_{g_7,g_{10}}, & \textbf{\textit{node } g_7} \\
\quad \vdots & \vdots \\
\quad AT^{e_5}_{g_{12},g_{10}} + AT^{e_6}_{g_{12},g_{10}}, AT^{e_5}_{g_{12},g_8}, AT^{e_5}_{g_{12},g_9}, AT^{e_6}_{g_{12},g_{11}} \Big\} & \textbf{\textit{node } g_{12}}
\end{array}
\quad \begin{array}{l} \left.\begin{array}{l} \\ \\ \\ \\ \\ \\ \end{array}\right\} \textbf{\textit{Layer 1}} \\ \left.\begin{array}{l} \\ \\ \\ \end{array}\right\} \textbf{\textit{Layer 2}} \end{array}
\tag{3.119}
$$

where $\{AT\}$ is the one-dimensional storage array for the non-zero elements of the conductance matrix $[AT]$. As can be seen from (3.120), $\{AT\}$ stores the non-zero components of the global conductance matrix $[AT]$, excluding the diagonal components. As discussed earlier, the diagonal components of $[AT]$ are not stored due to the simplification performed in the derivation of the system of equations (refer to equations (3.31)-(3.35)). IWFM uses the information stored in $\{JND\}$ and $\{NJD\}$ to reconstruct the two dimensional matrix $[AT]$ from the one-dimensional array $\{AT\}$.

3.8. Usage of Parametric Grid

To compute the matrix and the vector components appearing in equation (3.108) for groundwater nodes, it is necessary to define aquifer parameter values (namely horizontal and vertical hydraulic conductivities, specific storage coefficient, specific

yield, interbed thickness, elastic and inelastic storage coefficients, and pre-compaction head value) at each finite element node. IWFM allows the user to define these values through input files.

However, in most practical applications it is not possible to compile the required parameter values for each node of the finite element mesh. Instead, sets of values measured at a small number of observation sites will be available. Furthermore, the locations of these sites will generally not coincide with any of the nodes of the finite element mesh. To overcome this problem, IWFM allows the user to interpolate the parameter values measured at a small number of locations in order to specify values at the nodes of the finite element mesh. The interpolation is based purely on the geographic locations of the observation sites and the finite element nodes. IWFM uses the term *parametric node* for an observation site in order to differentiate it from a finite element node. A collection of parametric nodes forms the *parametric mesh* as opposed to finite element mesh. A parametric mesh may consist of triangular and/or quadrilateral elements (Figure 3.8). An individual parametric mesh can be used for specification of parameter values at finite element nodes of the entire model domain, or several parametric meshes covering smaller portions of the model domain can be utilized.

The mathematical theory underlying the interpolation technique used in IWFM is similar to that of the finite element method discussed earlier in this chapter. The continuous function of a particular parameter over a parametric element can be approximated by the discrete parameter values defined at the parametric nodes as

$$\phi_{ep}(x,y) \cong \hat{\phi}_{ep}(x,y) = \sum_{i=1}^{N_{ep}} \phi_i^{ep} \omega_i^{ep}(x,y) \tag{3.121}$$

where

$\phi_{ep}(x, y)$ = continuous function of a particular aquifer parameter over the parametric element *ep*;

$\hat{\phi}_{ep}(x,y)$ = approximation for $\phi_{ep}(x, y)$;

ϕ_i^{ep} = parameter value at parametric node *i*;

$\omega_i^{ep}(x,y)$ = element shape function defined for the parametric node *i*;

N_{ep} = number of parametric nodes that define a parametric element; 3 for a triangular element and 4 for a quadrilateral element.

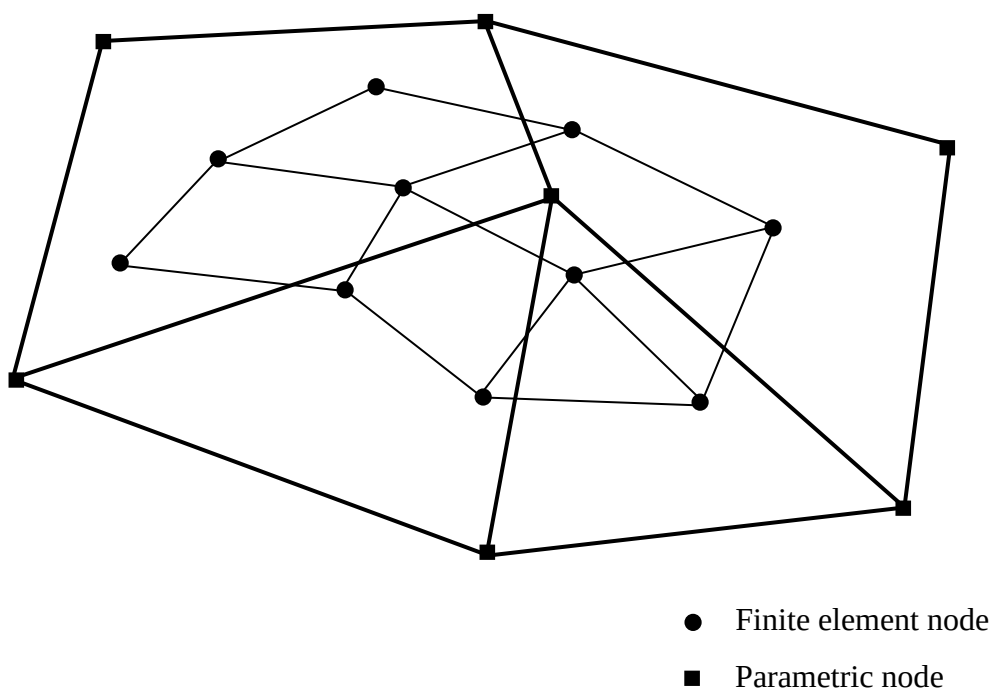

Figure 3.8 An example of parametric and finite element mesh system

The expressions for element shape functions, $\omega_i^{ep}(x, y)$, are given in section 3.1.1 for both linear triangular and linear quadrilateral elements. These expressions are also valid for parametric linear elements. Equation (3.121) reveals that, for a finite element node that is located in a parametric element, the parameter value at the finite element node can be expressed as a linear algebraic function of the parameter values at the surrounding parametric nodes. If the coordinates of the finite element node is given as (x_o, y_o), the parameter value at this node can be expressed by equation (3.121) as

$$\hat{\phi}(x_o, y_o) = \phi_j^{ef} = \sum_{i=1}^{N_{ep}} \phi_i^{ep} \omega_i^{ep}(x_o, y_o) \tag{3.122}$$

where ϕ_j^{fe} is the value of the parameter at the finite element node j. Therefore, $\omega_i^{ep}(x_o, y_o)$ are the interpolating coefficients corresponding to each of the surrounding parametric nodes.

The shape functions for a linear quadrilateral element are defined in (ξ, η) space instead of (x, y) space as given in equations (3.20)-(3.23). Therefore, it is necessary to convert the coordinates of the finite element node (x_o, y_o) into (ξ_o, η_o) in order to define the interpolating coefficients for a quadrilateral parametric element. This can be achieved by first solving equations (3.17) and (3.18) for $\xi(x, y)$ and $\eta(x, y)$, simultaneously and substituting x_o and y_o into the resulting solutions to obtain ξ_o and η_o.

4. Demand and Supply

An important objective of IWFM is to simulate the water supply to meet a specified agricultural and urban demand. This chapter explains the computation of urban and agricultural demand, simulation of water supply, and the water allocation process with respect to different land use types.

4.1. Land Use

IWFM has the capability to model flow processes over agricultural, urban, native and riparian lands. The land use areas must be specified for every grid cell within the model domain for the purpose of simulating root zone flows. The area of each crop, as well as urban, native and riparian lands are to be specified for each cell in order to compute runoff, infiltration, soil moisture, and deep percolation based on land use information.

In a hydrologic basin, the extent of the agricultural and urban areas defines a specific water demand that needs to be met by stream flow diversions and groundwater pumping. Diverting stream flows and extracting water from the groundwater storage, and distributing it over the modeled area to meet the water demand, changes the natural runoff characteristics of the basin. The approach taken in IWFM to model hydrologic processes based on each land use type plays a key role in the effectiveness of IWFM as a planning model. With this approach, demand is computed or specified for agricultural and urban areas separately. The allocation of surface water diversions and pumping to agricultural and urban lands is determined by defining the fraction of the specified

diversion and pumping that is intended for irrigation purposes, and designating the remaining portion for urban use. Once stream flows are simulated, actual surface water diversions are computed based on the available stream flows, and applied to agricultural and urban areas according to user-specified fractions to meet the appropriate demands. Groundwater pumping and recharge can be specified in several ways, but IWFM has the functionality to pump or recharge by element, based on the relative agricultural and urban areas within a cell. Similar to surface water diversions, groundwater pumping can also be distributed among agricultural and urban lands with respect to predefined fractions.

4.2. Agricultural and Urban Water Demands

Agricultural and urban water demands can either be computed dynamically or specified by the user as input data. Both agricultural and urban water demands are computed at each finite element based on the respective land-use area, soil and climatic conditions, and crop management practices. A detailed explanation of how these demands are computed is given in DWR (2015) and will not be repeated in this document.

4.3. Supply

Figure 4.1 illustrates the sources of water supply in IWFM, as well as the allocation of water for different uses. Surface water diversions and groundwater pumping are the two processes that define prime water supply. Re-use of return flow can also be considered as a source of water. The surface water and groundwater supply as

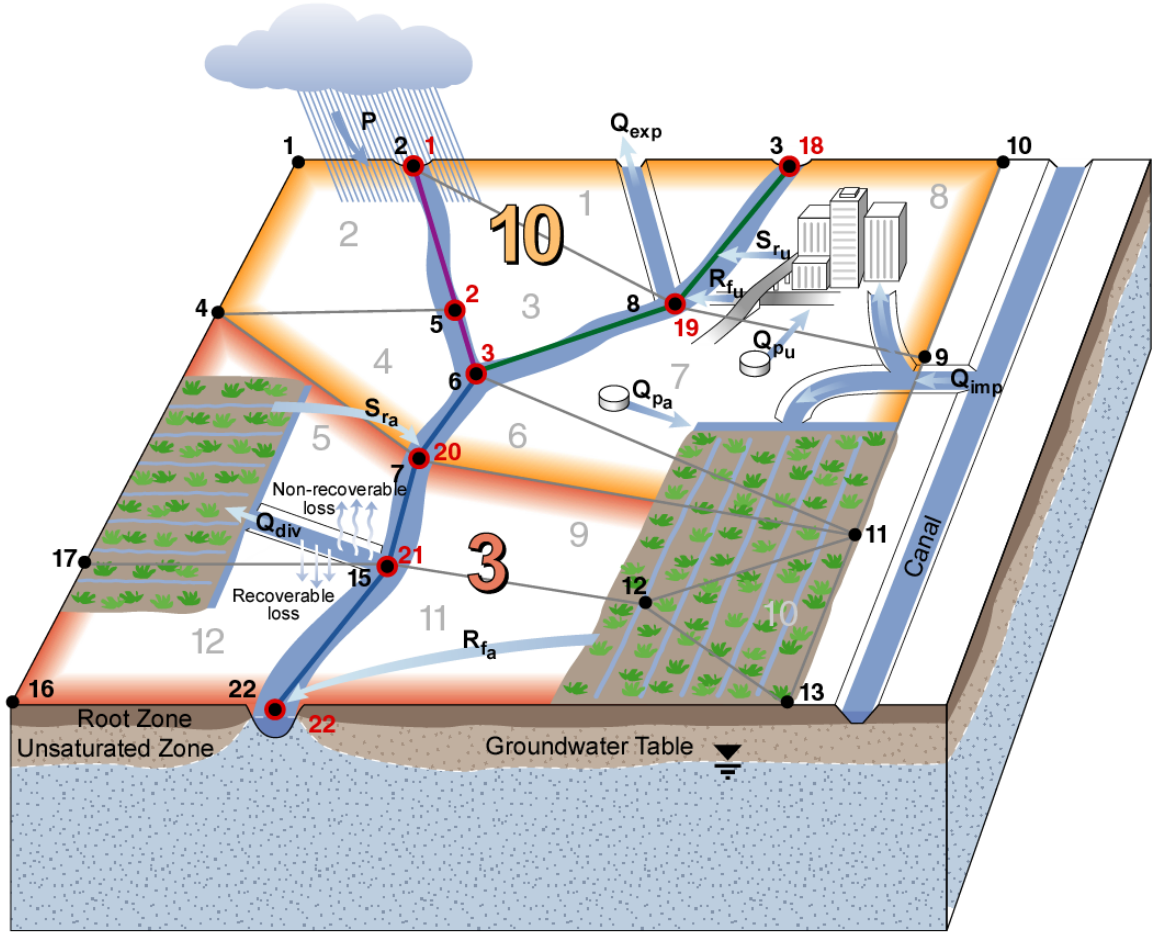

LEGEND

3,10 *Subregions*	P.....*Precipitation*	Q_{exp} .... *Export*
Subregion boundaries	S_{ra}.....*Agricultural runoff*	Q_{div}..... *Surface water diversion*
8 *Element numbers*	S_{ru}.....*Urban runoff*	Q_{pu}.....*Pumping for urban use*
17● *Groundwater nodes*	R_{fa}.....*Agricultural return flow*	Q_{pa}.....*Pumping for agriculture*
2● *Stream nodes*	R_{fu}.....*Urban return flow*	
Stream Reach 1	Q_{imp} .... *Import*	
Stream Reach 2		
Stream Reach 3		

Figure 4.1 Water use and supply

well as re-used return flow are determined by the simulation of stream flows, groundwater flow and return flow of applied water.

4.3.1. Surface Water Diversions and Deliveries

Each surface water diversion modeled in IWFM is associated with a stream node and may be limited with a user-specified maximum diversion amount that represents the capacity of the conveyance system. A surface water diversion can be delivered to an element, to a group of elements, to a subregion or it can be exported outside the model domain. Specified for every diversion is the amount of water used for irrigation purposes and to meet the urban water demand. IWFM computes the actual diversion and delivery amounts, and reports any diversion shortages or surplus. The actual amount of water available for delivery is based on the simulated stream flows.

The conveyance losses for each diversion are specified as a fraction of the total diversion. Recoverable losses are one type of conveyance loss modeled in IWFM. This type of loss is termed “recoverable”, since the water is assumed to eventually percolate to the groundwater, and become part of groundwater storage which can later be pumped and used as water supply. A non-recoverable loss is the other type of conveyance loss modeled in IWFM. This water leaves the system through evaporation. Under circumstances where shortages occur, recoverable and non-recoverable losses are adjusted to reflect the actual amount of water that is diverted. Based on the above discussion, applied water to agricultural and urban lands at the destination of the delivery (i.e. a single element, a group of elements or a subregion) are computed in IWFM as

$$AW_{ag,i}^{div} = Q_{div,i}\left(1 - R_{L_i} - NR_{L_i}\right)f_{ag_i} \tag{4.1}$$

$$AW_{u,i}^{div} = Q_{div,i}\left(1 - R_{L_i} - NR_{L_i}\right)\left(1 - f_{ag_i}\right) \tag{4.2}$$

where

i = index for diversion number, (dimensionless);

$AW_{ag,i}^{div}$ = actual amount of water delivered to agricultural lands from diversion number *i*, (L^3/T);

$AW_{u,i}^{div}$ = actual amount of water delivered to urban lands from diversion number *i*, (L^3/T);

$Q_{div,i}$ = stream diversion at diversion number *i* before conveyance losses, (L^3/T);

R_{L_i} = fraction of the stream diversion that becomes recoverable loss at diversion number *i*, (dimensionless);

NR_{L_i} = fraction of the stream diversion that becomes non-recoverable loss at diversion number *i*, (dimensionless);

f_{ag_i} = fraction of the diversion at diversion number *i* that is delivered to the agricultural lands, (dimensionless).

AW_{ag}^{div} and AW_{u}^{div} are the total agricultural and urban water deliveries, respectively, at the destination of the delivery. IWFM computes water demands for each individual crop and urban land at the cell level. To further distribute the deliveries to urban lands and individual crops at cell level, IWFM uses the computed water demands. Each land-use type receives water in proportion to their water demands to the total water

demand in the delivery destination. For instance, if the delivery goes to a single element, then IWFM distributes the agricultural water among the crops in the destination element with respect to their water demands. Urban water goes to the urban lands in that element without modification. If the delivery goes to a group of elements or a subregion, then IWFM distributes agricultural and urban water deliveries to individual elements first according to the fraction of the water demand in each element to the total water demand in the group of elements or the subregion. Once the element-level delivery is computed, it is distributed among individual crops in that element according to the water demands of each crop. If, for any reason, the agricultural or urban water demand at the delivery destination is zero (i.e. if there is water surplus), then IWFM distributes the water delivery with respect to the area of individual crops or urban lands.

IWFM has the functionality to model bypass flows, which serves as a method of re-routing flow to avoid flooding. The model simulates flow through a bypass canal by diverting water from a stream node and adding the diverted water to another downstream node. When simulating bypass flows, conveyance losses are accounted for by assigning percentages of the bypass flow to recoverable and non-recoverable losses occurring in the bypass canal.

4.3.2. Groundwater Pumping and Recharge

IWFM has the functionality to simulate groundwater pumping and recharge by well location or on an element-by-element basis. Pumping is a source of water supply, whereas recharge is the replenishment of the aquifer system during a model simulation.

The only difference computationally between pumping and recharge in IWFM is the sign convention. A negative value represents pumping and a positive value represents recharge.

4.3.2.a. Pumping and Recharge at Well Locations

IWFM has the capability to simulate pumping and recharge at user-specified well locations. Pumping and recharge at specific well locations require the user to input all simulated well locations in (x,y) coordinates. Based on the well location, IWFM identifies the finite element that contains the location of the well and computes the interpolating coefficients (refer to section 3.8 for the interpolation method) to distribute the pumping/recharge amount to the groundwater nodes that correspond to that element.

Since IWFM has the capability to model multiple layers, the vertical distribution of pumping from each layer must be computed. The vertical distribution of pumping to each aquifer layer is proportional to the length of the well screen and the transmissivity of the aquifer layer:

$$Q_{P_m} = Q_{P_T} \frac{f_m T_m}{\sum_{i=1}^{N_L} f_i T_i} \tag{4.3}$$

where

Q_{P_m} = pumping from aquifer layer m, (L^3/T);

Q_{P_T} = total pumping at the well, (L^3/T);

f = fraction of vertical distribution for each layer, (dimensionless);

T = transmissivity, (L^2/T);

N_L = total number of aquifer layers, (dimensionless).

The Kozeny equation is used to define the fraction of vertical distribution, f, which accounts for the effect of partial penetration of a well in an aquifer layer (Driscoll, 1986):

$$f_m = \ell_s \left[1 + 7\sqrt{\frac{r}{2b\ell_s}} \cos\left(\frac{\pi \ell_s}{2} \right) \right] \tag{4.4}$$

where

f_m = fraction of pumping from aquifer layer m, (dimensionless);

ℓ_s = well screen length as a fraction of the aquifer thickness, (dimensionless);

r = well radius, (L);

b = aquifer thickness, (L).

4.3.2.b. Elemental Distribution of Pumping and Recharge

It is sometimes impossible to locate every well in the modeled area and access the pumping records. Instead, average values for the pumping or recharge amounts may be available for a section of the modeled area. For this reason, IWFM has the functionality to distribute regional pumping/recharge values to elements when they are specified for areas containing well locations that are not defined in terms of specific coordinates. The distribution of pumping to elements can be done in one of the following five ways in IWFM:

(i) Pumping can be distributed based on a factor specified for each element associated with the total pumping, P_T:

$$Q_{P_e} = f_e Q_{P_T} \tag{4.5}$$

where

Q_{P_e} = pumping at element *e*, (L^3/T);

Q_{P_T} = total pumping from an area, (L^3/T);

f_e = factor that defines the amount of pumping allocated to element *e*, (dimensionless).

(ii) The second option when distributing pumping to an element is to define the pumping with respect to the area of each element relative to the area that corresponds to the total pumping value and a user defined fraction:

$$Q_{P_e} = \frac{Q_{P_T} f_{i=e} A_{i=e}}{\sum_{i=1}^{n} \left(f_i \times A_i \right)} \tag{4.6}$$

where

f_i = fraction that defines the amount of pumping from element *i*, (dimensionless);

A_i = area of element *i*, which is also associated with the total pumping Q_{P_T}, (L^2);

n = number of elements that the total pumping, Q_{P_T} is distributed to, (dimensionless).

(iii) The third option is based on the relative amount of agricultural and urban

area in an element with respect to the agricultural and urban areas in all other elements that the total pumping, Q_{P_T} is distributed to:

$$Q_{P_e} = \frac{Q_{P_T} f_{i=e}\left(A_{i=e,ag} + A_{i=e,ur}\right)}{\sum_{i=1}^{n}\left[f_i \times \left(A_{i,ag} + A_{i,ur}\right)\right]} \tag{4.7}$$

where

$A_{i,ag}$ = agricultural area within element i, (L^2);

$A_{i,ur}$ = urban area within element i, (L^2).

(iv) The elemental pumping distribution can be computed based on the relative amount of agricultural area in an element with respect to the agricultural areas in all other elements that are assigned pumping from Q_{P_T} .

$$Q_{P_e} = \frac{Q_{P_T} f_{i=e} A_{i=e,ag}}{\sum_{i=1}^{n}\left(f_i \times A_{i,ag}\right)} \tag{4.8}$$

(v) The final option to be discussed is the elemental distribution of pumping with respect to the relative amount of urban area in an element to the urban areas of all other elements that are assigned a portion of the total pumping (Q_{P_T}):

$$Q_{P_e} = \frac{Q_{P_T} f_{i=e} A_{i=e,ur}}{\sum_{i=1}^{n}\left(f_i \times A_{i,ur}\right)} \tag{4.9}$$

For simplicity, the computations described in equations (4.5) - (4.9) are defined in terms of pumping. However, recharge is computed in the same manner as pumping, with the exception of the sign convention.

Similar to applied water from diversions, pumping is also used to meet agricultural and urban water demands at a single element, at a group of elements or at a subregion. It can also be exported outside the model area. Pumping can be limited with user-specified maximum amounts representing the pump capacities. Similar to diversions, well and elemental pumping are proportioned between the agricultural and urban lands based on user-specified fractions:

$$AW^{p}_{ag,i} = Q_{P,i} f_{ag_i} \tag{4.10}$$

$$AW^{p}_{u,i} = Q_{P,i}\left(1 - f_{ag_i}\right) \tag{4.11}$$

where

i = index for pumping, (dimensionless);

$AW^{p}_{ag,i}$ = actual amount of water supplied to agricultural lands from pump number *i*, (L^3/T);

$AW^{p}_{u,i}$ = actual amount of water supplied to urban lands from pump number *i*, (L^3/T);

$Q_{P,i}$ = actual pumping at pump number *i*, (L^3/T);

f_{ag_i} = fraction of the pumping that is supplied to the agricultural lands from pump number *i*, (dimensionless).

IWFM uses the same methods as for the diversions to distribute pumping to individual crops and urban lands at each element at the delivery destination once $AW^{p}_{ag,i}$ and $AW^{p}_{u,i}$ are computed.

4.3.2.c. Computation of Pumping at Drying Wells

IWFM strives not only to compute groundwater heads and stream flows accurately but also to define the actual amount of water supply that is distributed over the model area to meet the water demand. During pumping, if a well dries during a time step the groundwater head will be computed as being less than the elevation of the bottom of the deepest aquifer that the well is drilled to. However, this is not possible since IWFM only models the saturated groundwater flow. Furthermore, it is important to identify the exact time that the well dries in order to compute the total amount of water that is actually pumped from the well. In general, this is an inverse problem and it requires the solution of the inverse of the groundwater conservation equation. In order to address these two problems, IWFM uses an iterative method.

If the groundwater head at a node falls below the bottom of the aquifer due to pumping during a time step, IWFM enters the mode of iterative inverse-problem solution. The estimated pumping is calculated as

$$\left(Q_{p_i}^{t+1}\right)^{k+1} = \frac{\left(Q_{p_i}^{t+1}\right)^{k} + \left(Q_{p_i}^{t+1}\right)^{k'}}{2} \tag{4.12}$$

where

$$\left(Q_{p_i}^{t+1}\right)^{k'} = \begin{cases} \left(Q_{p_i}^{t+1}\right)^{k} - \dfrac{\left(z_{k_i} - h_i^{t+1}\right) S_{y_i} A_i}{\Delta t} & \text{if } h_i^{t+1} \le z_{k_i} \\ \min\left[\dfrac{\left(h_i^{t+1} - z_{k_i}\right) S_{y_i} A_i}{\Delta t}, \left(Q_{p_i}^{t+1}\right)^{req}\right] & \text{if } h_i^{t+1} > z_{k_i} \text{ ; } \left(Q_{p_i}^{t+1}\right)^{k} < \left(Q_{p_i}^{t+1}\right)^{req} \end{cases} \tag{4.13}$$

i = finite element node at which pumping occurs, (dimensionless);

$\left(Q_{p_i}^{t+1}\right)^{k}$ = pumping rate at node *i*, at the kth iteration level, (L^3/T);

$\left(Q_{p_i}^{t+1}\right)^{k+1}$ = pumping rate at node *i*, at the $(k+1)^{th}$ iteration level, (L^3/T);

$\left(Q_{p_i}^{t+1}\right)^{req}$ = required pumping rate at node *i* specified by the user, (L^3/T);

h_i = groundwater head at node *i*, (L);

z_{k_i} = elevation of the bottom of the aquifer at node *i*, (L);

S_{y_i} = specific yield at node *i*, (dimensionless);

A_i = area associated with node *i*, (L^2);

Δt = length of time step, (T);

t = index for time step, (dimensionless);

k = iteration level, (dimensionless).

The iteration is stopped when the ratio of the difference between the two pumping rates from consecutive iteration levels to the pumping rate at the previous iteration level is smaller than a tolerance value:

$$\left|\frac{\left(Q_{p_i}^{t+1}\right)^{k+1}-\left(Q_{p_i}^{t+1}\right)^{k}}{\left(Q_{p_i}^{t+1}\right)^{k}}\right| \le \varepsilon \qquad (4.14)$$

Estimating $Q_{p_i}^{t+1}$ iteratively results in a pumping rate that will drawdown the groundwater head at a well to the elevation of the bottom of the aquifer. Once the pumping rate is computed, it is multiplied by the time step length, Δt, to compute the actual volume of pumping that is supplied to urban and agricultural lands.

4.3.3. Re-use of Irrigation Water

Re-used irrigation water is another water supply in addition to the prime water (i.e. irrigation water before the application of re-used water) that is delivered to the fields in terms of groundwater pumping or surface water diversions. IWFM simulates only the re-use of return flow. The agricultural return flow computed by IWFM is assumed to be the net return flow after the user-specified portion of the initial return flow is re-used. IWFM allows the user to direct the net return flow from one element to another element, to another subregion or to a stream node. All these options represent different types of re-use that may take place in the modeled boundary.

When the net-return flow from an element is directed to a downstream element, IWFM treats this flow as a separate water supply to meet the agricultural and urban water demands in the destination element. When the net return flow from an element is directed to a subregion, IWFM distributes this flow among the elements of the destination subregion with respect to the water demand at each element and again treats it as a separate water supply. Finally, in the case that the net return flow is directed to a stream node, it contributes to the stream flow and can be diverted by downstream diverters.

4.3.4. Agricultural Water Use

Agricultural water use is the amount of the agricultural water demand that can be met by the simulated water supply. The total amount of water delivered to agricultural lands from surface water diversions and pumping is

$$AW_{ag} = AW_{ag}^{div} + AW_{ag}^{p} \tag{4.15}$$

where AW_{ag}^{div} and AW_{ag}^{p} are given in equations (4.1) and (4.10), respectively. If the simulated supply equals demand, the agricultural water use is simply the demand that is specified or computed (refer to section 4.2). If simulated water supply is less than the demand, then water use is equal to the water supply. On the other hand, if water supply is larger than the demand, then water use is equal to the demand and the amount of supply in excess of demand contributes to surface runoff, increases the soil moisture in the root zone without being used by the plants, or percolates into the unsaturated zone and groundwater. The water supply is delivered to the appropriate locations based on input that specifies the fraction of each surface water diversion that is to be used for irrigation purposes and the fraction of groundwater pumping to be applied to agricultural lands.

4.3.5. Urban Water Use

The total amount of water delivered to the urban lands is

$$AW_u = AW_u^{div} + AW_u^{p} \tag{4.16}$$

where AW_u^{div} and AW_u^{p} are given in equations (4.2) and (4.11), respectively. Furthermore, based on the simulated water supply, the amount of water available for indoor and outdoor urban use can be expressed as

$$AW_{u_i} = \left(AW_u\right)\left(\%AW_{u_i}\right) \tag{4.17}$$

$$AW_{u_o} = AW_u - AW_{u_i} \tag{4.18}$$

where

AW_{u_i} = indoor urban water use, (L^3/T);

$\%AW_{u_i}$ = fraction of urban water use specified for indoors, (dimensionless);

AW_{u_o} = water applied to outdoor urban areas, (L^3/T).

If supply equals demand, or the model simulates that the supply meets or exceeds the demand, the total urban water use is the urban water demand itself. However, if the simulated water supply is short of meeting the demand, the urban indoor and outdoor water use values are computed by equations (4.17) and (4.18) based on the available water supply.

4.4. Automated Supply Adjustment

An important task in water resources planning studies is to find answers to questions such as if there is enough water supply in the modeled area to meet the agricultural and urban water demand, and how to operate the pumping and diversion facilities in order to minimize the discrepancy between the supply and demand. In order to achieve this task, the functionally to adjust the surface water diversions and/or pumping automatically has been included in IWFM.

The user can choose some or all of the diversions, pumping or both to be adjusted by IWFM in order to meet the agricultural and urban water demand, or to minimize the surplus supply amounts. It should be noted at this point that IWFM does not incorporate optimization techniques in adjusting the water supply. Instead, it tries to distribute the discrepancy between the supply and demand among adjusted diversions or pumping as equally as possible without considering any operation rules. Thus, the resulting diversion

and pumping amounts after the adjustment may not be the optimum management of the water resources in terms of financial, environmental and legal constraints. However, these results may help the user to identify hot spots of the modeled region such as streams and pumping locations that may be utilized when there is a shortage of supply, or diversion and pumping locations that constantly fail to produce required amounts of water supply.

In IWFM, the term "adjustment of supply" stands for the procedure of modifying the *required* amount of diversions and pumping to minimize the discrepancy between the water demand and water supply to meet this demand. An adjusted amount of required diversion or pumping does not necessarily mean that that much water can actually be diverted or pumped. For instance, in dry years it may not be possible to divert as much water as the adjusted amount of required diversions. Therefore, it is important to understand that automated adjustment of diversions and pumping will not always generate a perfect match between the water demand and the actual amount of water supplied to meet this demand.

In the following sections, the methods used in adjusting the surface water diversions and pumping are detailed. If the adjustment of both surface water diversions and pumping is desired, then surface water diversions are adjusted first and pumping rates are adjusted second.

4.4.1. Adjustment of Surface Water Diversions

Surface water diversions are adjusted according to their ranks based on the

number of upstream diversion locations. Figure 4.2 shows a hypothetical stream system with four diversion points. These diversion points are ranked as follows:

- *Rank 0:* Diversions 1 and 2 (0 upstream diversion points);
- *Rank 1:* Diversion 3 (1 upstream diversion point, namely diversion 1);
- *Rank 3:* Diversion 4 (3 upstream diversion points, namely diversions 1, 2 and 3).

In the list above, rank 2 is omitted since there are no diversions with two upstream diversion locations. Adjustment of diversions is performed with a multi-step procedure. In the first step, all adjustable diversions (the criteria used to specify a diversion as adjustable is listed below) of all ranks are adjusted and the required amounts of diversions to meet the water demand are computed. If the newly computed diversion requirements can be met, then the adjustment was successful and no further steps are performed. However, if there is still a discrepancy between the actual diversion amounts and the water demand, then the second step of adjustment is performed. In the second step, all adjustable diversions except those with rank 0 are adjusted. At the end of this

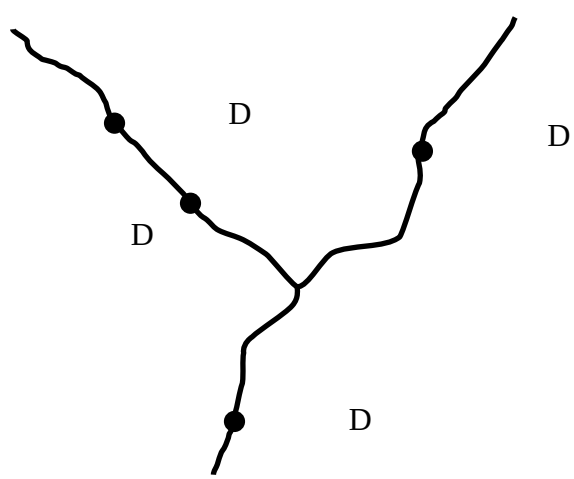

Figure 4.2 A stream system with 4 diversion locations

step if there are still discrepancies between actual diversions and water demands, then IWFM goes to the third step. In the third step, all adjustable diversions except those with ranks 0 and 1 are adjusted. This procedure is performed until the discrepancies are minimized or all ranks of diversions have been adjusted. As an example, IWFM will perform a maximum of three adjustment steps for the hypothetical case shown in Figure 4.2. In the first step all diversions will be adjusted. In the second step diversions 3 and 4, and in the third step only diversion 4 will be adjusted.

As mentioned earlier, agricultural and urban water demands are specified or computed for urban lands and for each crop at every finite element. Each diversion is assigned a delivery destination, either a single element, a group of elements or a subregion, and the amount delivered to the destination is proportioned between urban and agricultural water use based on a fraction specified by the user. Since the final destination of diversions is a finite element regardless of the destination type, the adjustment of diversions is performed to meet the element level water demand. Each diversion can be adjusted to meet only the agricultural demand, only the urban demand or both at an element.

For the simplicity of explanation, only the procedure that is used to adjust diversions to meet agricultural water demand will be discussed in the following paragraphs. Adjustment of diversions to meet the urban water demand is exactly the same.

First, the discrepancies between the agricultural water demand and the amount of delivery to agricultural lands at an element is computed. If there is a supply shortage, i.e. water demand is larger than the actual delivery to the agricultural lands, the total number

of diversions that can be adjusted is computed. When computing the total number of adjustable diversions, the following criteria are used: (i) diverted water is delivered to the element in concern, (ii) diversion originates from a stream node that is not dry (i.e. diversion amount can be increased), (iii) diversion is specified by the user to be adjusted to meet the agricultural water requirement at the element, (iv) the rank of the diversion is greater than or equal to the adjustment step, and (v) the diversion amount before adjustment is less than the maximum amount specified by the user (i.e. diversion amount can be increased). Once the total number of adjustable diversions is computed, the new diversion requirements are calculated by distributing the supply shortage equally among adjustable diversions that deliver water to the specified element. If the adjusted diversion for a specific diversion location is greater than the maximum amount specified by the user, the amount that is above the maximum is further distributed equally among other diversion locations that have not yet reached their own maximum amounts.

With the adjusted diversion requirements, the stream flows are simulated by solving the coupled groundwater-surface water equation set. If the diversion requirements are met, i.e. simulated stream flows are large enough to support the required diversion rates, the adjustment procedure is aborted. Otherwise, above procedure is repeated for the next adjustment step to adjust the diversions with appropriate ranks.

Generally, it is not possible to match the water demand with the actual water supply perfectly when there is a supply shortage. For this reason, IWFM allows the user to define a tolerance value. If the ratio of the actual supply to the water demand falls below this tolerance value, it is assumed that the supply is satisfactorily close to the water demand and the adjustment procedure is aborted.

If there is a supply surplus, i.e. water demand is less than the actual delivery to the agricultural lands, then it is necessary to decrease the diversion amounts. In this case, the total amount of actual deliveries to the agricultural lands that originate from adjustable diversion locations is computed. The same criteria listed above with the exception of the second (dry stream node) and last (diversion at its maximum) items are used in specifying a diversion as adjustable. The second criterion in this case is redundant since the diversions will be decreased and a dry stream node does not pose a constraint. Similarly, the last item, i.e. the unadjusted diversion being at its maximum, is also no longer a constraint. Once the total amount of actual deliveries from adjustable diversion locations is computed, the required diversion rates are calculated by decreasing each of the adjustable diversion rates with respect to the magnitude of the original diversion rate:

Similar methods are used to adjust deliveries to meet urban water demands. It should be noted that once the deliveries to agricultural and urban lands are adjusted, the fraction f_{ag} (see equations (4.1) and (4.2)) that is used to partition the total delivery between agricultural and urban lands also changes.

4.4.2. Adjustment of Pumping

The adjustment of pumping in order to minimize the discrepancy between the water supply and demand is similar to the adjustment of surface water diversions, except that pumping wells or elements are not ranked the same as diversion points. Instead, pumping requirements are adjusted until the ratio between the actual supply and demand is smaller than the tolerance specified by the user, until further adjustment does not

change the required pumping values or until pumping rates reach the maximum amounts specified by the user. The case where required pumping rates no longer change can occur when the required pumping rates are so high that the wells eventually go dry and actual pumping cannot be increased any more. The adjustment can be performed for well pumping as well as elemental pumping.

Appendix A

A.1. Components of $\left\{\mathbb{F}^{\mathbf{k}}\right\}$ and $\left[\mathbb{X}^{\mathbf{k}}\right]$ for Stream Nodes

Stream Routing Component Version 4.0:

For $i = 1, \cdots, NR$:

♦ $$\mathbb{F}_i^k = Q_{s_i}\left[\left(\mathbb{H}_i^{t+1}\right)^k\right] - \sum_j Q_{s_j}\left[\left(\mathbb{H}_j^{t+1}\right)^k\right]$$

$$-R_{f_i}^{t+1} - S_{r_i}^{t+1} - Q_{ws_i}^{t+1} - Q_{brs_i}^{t+1} - Q_{td_i}^{t+1} - Q_{lko_i}^{t+1} - Q_{h_i}^{t+1}$$

$$+Q_{rip}^{t+1} + Q_{b_i}^{t+1} + Q_{div_i}^{t+1}$$

$$+C_{s_i}\left\{\max\left[\left(\mathbb{H}_i^{t+1}\right)^k, h_{b_i}\right] - \max\left[\left(\mathbb{H}_n^{t+1}\right)^k, h_{b_i}\right]\right\} \qquad \text{(A.1)}$$

♦ $$\mathbb{X}_{i,i}^k = \left(\frac{\partial \mathbb{F}_i}{\partial \mathbb{H}_i^{t+1}}\right)^k = \left(\frac{\partial Q_{s_i}\left(\mathbb{H}_i^{t+1}\right)}{\partial \mathbb{H}_i^{t+1}}\right)^k + \left(\frac{\partial Q_{sint_i}^{t+1}}{\partial \mathbb{H}_i^{t+1}}\right)^k \qquad \text{(A.2)}$$

$$\left(\frac{\partial Q_{sint_i}^{t+1}}{\partial \mathbb{H}_i^{t+1}}\right)^k = \begin{cases} C_{s_i} & \text{if} \quad \left(\mathbb{H}_i^{t+1}\right)^k > h_{b_i} \\ 0 & \text{if} \quad \left(\mathbb{H}_i^{t+1}\right)^k \le h_{b_i} \end{cases} \qquad \text{(A.3)}$$

♦ $$\mathbb{X}_{i,j}^{k} = \left(\frac{\partial \mathbb{F}_i}{\partial \mathbb{H}_j^{t+1}}\right)^k = -\left(\frac{\partial Q_{s_i}^{t+1}\left[\mathbb{H}_j^{t+1}\right]}{\partial \mathbb{H}_j^{t+1}}\right)^k + \left(\frac{\partial Q_{b_i}^{t+1}}{\partial \mathbb{H}_j^{t+1}}\right)^k + \left(\frac{\partial Q_{div_i}^{t+1}}{\partial \mathbb{H}_j^{t+1}}\right)^k \qquad \text{(A.4)}$$

If the bypass rate, Q_{b_i}, is specified as constant, then (A.4) can be expressed as

$$\mathbb{X}_{i,j}^{k} = \begin{cases} -\left(\dfrac{\partial Q_{s_i}^{t+1}\left[\mathbb{H}_j^{t+1}\right]}{\partial \mathbb{H}_j^{t+1}}\right)^k & Q_{in_i} \geq Q_{divreq_i}^{t+1} \;\; ; \;\; Q_i^{**} \geq Q_{breq_i}^{t+1} \\ 0 & \text{otherwise} \end{cases} \qquad \text{(A.5)}$$

On the other hand, if the bypass rate is specified as a function of stream flow through a rating table $\left(\text{i.e. } Q_{b_i} = Q_{b_i}\left(Q_i^{**}\right)\right)$ then (A.4) is expressed as

$$\mathbb{X}_{i,j}^{k} = \begin{cases} \left(\dfrac{\partial Q_{s_i}^{t+1}\left[\mathbb{H}_j^{t+1}\right]}{\partial \mathbb{H}_j^{t+1}}\right)^k \left(\dfrac{\partial Q_{b_i}^{t+1}}{\partial Q_i^{**}} - 1\right) & Q_{in_i} \geq Q_{divreq_i}^{t+1} \\ 0 & \text{otherwise} \end{cases} \qquad \text{(A.6)}$$

where

$$Q_{in_i} = \sum_j Q_{s_j}\left[\left(\mathbb{H}_j^{t+1}\right)^k\right]$$

$$+ R_{f_i}^{t+1} + S_{r_i}^{t+1} + Q_{ws_i}^{t+1} + Q_{brs_i}^{t+1} + Q_{td_i}^{t+1} + Q_{lko_i}^{t+1} + Q_{h_i}^{t+1} \qquad \text{(A.7)}$$

$$Q_i^{**} = Q_{in_i} - Q_{div_i}^{t+1} \tag{A.8}$$

- $$\mathbb{X}_{i,n}^k = \left(\frac{\partial \mathbb{F}_i}{\partial \mathbb{H}_n^{t+1}} \right)^k = \left(\frac{\partial Q_{sint_i}^{t+1}}{\partial \mathbb{H}_n^{t+1}} \right)^k \tag{A.9}$$

$$\left(\frac{\partial Q_{sint_i}^{t+1}}{\partial \mathbb{H}_i^{t+1}} \right)^k = \begin{cases} -C_{s_i} & \text{if} \quad \left(\mathbb{H}_n^{t+1} \right)^k > h_{b_i} \\ 0 & \text{if} \quad \left(\mathbb{H}_n^{t+1} \right)^k \le h_{b_i} \end{cases} \tag{A.10}$$

Stream Routing Component Version 4.1:

For $i = 1, \cdots, NR$:

- $$\begin{aligned} \mathbb{F}_i^k = {} & Q_{s_i} \left[\left(\mathbb{H}_i^{t+1} \right)^k \right] - \sum_j Q_{s_j} \left[\left(\mathbb{H}_j^{t+1} \right)^k \right] \\ & - R_{f_i}^{t+1} - S_{r_i}^{t+1} - Q_{ws_i}^{t+1} - Q_{brs_i}^{t+1} - Q_{td_i}^{t+1} - Q_{lko_i}^{t+1} - Q_{h_i}^{t+1} \\ & + Q_{rip}^{t+1} + Q_{b_i}^{t+1} + Q_{div_i}^{t+1} \\ & + C_{s_i} \left\{ \max\left[\left(\mathbb{H}_i^{t+1} \right)^k, h_{b_i} \right] - \max\left[\left(\mathbb{H}_n^{t+1} \right)^k, h_{b_i} \right] \right\} \end{aligned} \tag{A.11}$$

♦ $$\mathbb{X}_{i,i}^{k} = \left(\frac{\partial \mathbb{F}_i}{\partial \mathbb{H}_i^{t+1}}\right)^k = \left(\frac{\partial Q_{s_i}\left(\mathbb{H}_i^{t+1}\right)}{\partial \mathbb{H}_i^{t+1}}\right)^k + \left(\frac{\partial Q_{sint_i}^{t+1}}{\partial \mathbb{H}_i^{t+1}}\right)^k \tag{A.12}$$

$$\left(\frac{\partial Q_{sint_i}^{t+1}}{\partial \mathbb{H}_i^{t+1}}\right)^k = \begin{cases} \frac{\partial C_{s_i}}{\partial \mathbb{H}_i^{t+1}}\left(G^{t+1}\right)^k + C_{s_i} & \left(\mathbb{H}_i^{t+1}\right)^k > \left(\mathbb{H}_n^{t+1}\right)^k \;;\; \left(\mathbb{H}_i^{t+1}\right)^k > h_{b_i} \\ C_{s_i} & \left(\mathbb{H}_i^{t+1}\right)^k \le \left(\mathbb{H}_n^{t+1}\right)^k \;;\; \left(\mathbb{H}_i^{t+1}\right)^k > h_{b_i} \\ 0 & \left(\mathbb{H}_i^{t+1}\right)^k \le h_{b_i} \end{cases} \tag{A.13}$$

where

$$C_{s_i} = \begin{cases} \frac{K_{s_i}}{d_{s_i}} L_i W_i\left(\left(\mathbb{H}_i^{t+1}\right)^k\right) & \left(\mathbb{H}_i^{t+1}\right)^k > \left(\mathbb{H}_n^{t+1}\right)^k \;;\; \left(\mathbb{H}_i^{t+1}\right)^k > h_{b_i} \\ \frac{K_{s_i}}{d_{s_i}} L_i W_i\left(\left(\mathbb{H}_n^{t+1}\right)^k\right) & \left(\mathbb{H}_i^{t+1}\right)^k \le \left(\mathbb{H}_n^{t+1}\right)^k \;;\; \left(\mathbb{H}_n^{t+1}\right)^k > h_{b_i} \\ 0 & \left(\mathbb{H}_i^{t+1}\right)^k \le h_{b_i} \;;\; \left(\mathbb{H}_n^{t+1}\right)^k \le h_{b_i} \end{cases} \tag{A.14}$$

$$\frac{\partial C_{s_i}}{\partial \mathbb{H}_i^{t+1}} = \begin{cases} \frac{K_{s_i}}{d_{s_i}} L_i \frac{\partial W_i}{\partial \mathbb{H}_i^{t+1}} & \left(\mathbb{H}_i^{t+1}\right)^k > \left(\mathbb{H}_n^{t+1}\right)^k \;;\; \left(\mathbb{H}_i^{t+1}\right)^k > h_{b_i} \\ 0 & \text{otherwise} \end{cases} \tag{A.15}$$

$$\left(G^{t+1}\right)^k = \left(\mathbb{H}_i^{t+1}\right)^k - \max\left[\left(\mathbb{H}_n^{t+1}\right)^k, h_{b_i}\right] \tag{A.16}$$

In (A.13) - (A.16), K_{s_i} is the stream bed hydraulic conductivity, L_i is the length of stream at stream node *i*, W_i is the wetted perimeter, d_{s_i} is the thickness of the stream bed material, h_{b_i} is the elevation of the stream bed, $\mathbb{H}_n$ is the groundwater head at the finite element node *n* that corresponds to the stream node *i*, and $NR + NLK + 1 \le n \le NR + NLK + N_L \cdot N$

- $$\mathbb{X}_{i,j}^{k} = \left(\frac{\partial \mathbb{F}_i}{\partial \mathbb{H}_j^{t+1}} \right)^k = -\left(\frac{\partial Q_{s_i}^{t+1}\left[\mathbb{H}_j^{t+1}\right]}{\partial \mathbb{H}_j^{t+1}} \right)^k + \left(\frac{\partial Q_{b_i}^{t+1}}{\partial \mathbb{H}_j^{t+1}} \right)^k + \left(\frac{\partial Q_{div_i}^{t+1}}{\partial \mathbb{H}_j^{t+1}} \right)^k \qquad \text{(A.17)}$$

If the bypass rate, Q_{b_i}, is specified as constant, then (A.4) can be expressed as

$$\mathbb{X}_{i,j}^{k} = \begin{cases} -\left(\dfrac{\partial Q_{s_i}^{t+1}\left[\mathbb{H}_j^{t+1}\right]}{\partial \mathbb{H}_j^{t+1}} \right)^k & Q_{in_i} \ge Q_{divreq_i}^{t+1} \;\; ; \;\; Q_i^{**} \ge Q_{breq_i}^{t+1} \\ 0 & \text{otherwise} \end{cases} \qquad \text{(A.18)}$$

On the other hand, if the bypass rate is specified as a function of stream flow through a rating table $\left(\text{i.e. } Q_{b_i} = Q_{b_i}\left(Q_i^{**}\right)\right)$ then (A.4) is expressed as

$$\mathbb{X}_{i,j}^{k} = \begin{cases} \left(\dfrac{\partial Q_{s_i}^{t+1}\left[\mathbb{H}_j^{t+1}\right]}{\partial \mathbb{H}_j^{t+1}} \right)^k \left(\dfrac{\partial Q_{b_i}^{t+1}}{\partial Q_i^{**}} - 1 \right) & Q_{in_i} \geq Q_{divreq_i}^{t+1} \\ 0 & \text{otherwise} \end{cases} \tag{A.19}$$

where

$$Q_{in_i} = \sum_j Q_{s_j}\left[\left(\mathbb{H}_j^{t+1}\right)^k\right]$$

$$+R_{f_i}^{t+1} + S_{r_i}^{t+1} + Q_{ws_i}^{t+1} + Q_{brs_i}^{t+1} + Q_{td_i}^{t+1} + Q_{lko_i}^{t+1} + Q_{h_i}^{t+1} \tag{A.20}$$

$$Q_i^{**} = Q_{in_i} - Q_{div_i}^{t+1} \tag{A.21}$$

♦ $$\mathbb{X}_{i,n}^{k} = \left(\frac{\partial \mathbb{F}_i}{\partial \mathbb{H}_n^{t+1}} \right)^k = \left(\frac{\partial Q_{sint_i}^{t+1}}{\partial \mathbb{H}_n^{t+1}} \right)^k \tag{A.22}$$

$$\left(\frac{\partial Q_{sint_i}^{t+1}}{\partial \mathbb{H}_n^{t+1}} \right)^k = \begin{cases} \dfrac{\partial C_{s_i}}{\partial \mathbb{H}_n^{t+1}}\left(E^{t+1}\right)^k - C_{s_i} & \left(\mathbb{H}_n^{t+1}\right)^k > \left(\mathbb{H}_i^{t+1}\right)^k \;\; ; \;\; \left(\mathbb{H}_n^{t+1}\right)^k > h_{b_i} \\ -C_{s_i} & \left(\mathbb{H}_n^{t+1}\right)^k \leq \left(\mathbb{H}_i^{t+1}\right)^k \;\; ; \;\; \left(\mathbb{H}_n^{t+1}\right)^k > h_{b_i} \\ 0 & \left(\mathbb{H}_n^{t+1}\right)^k \leq h_{b_i} \end{cases} \tag{A.23}$$

where

$$\frac{\partial C_{s_i}}{\partial \mathbb{H}_n^{t+1}} = \begin{cases} \frac{K_{s_i}}{d_{s_i}} L_i \frac{\partial W_i}{\partial \mathbb{H}_n^{t+1}} & \left(\mathbb{H}_i^{t+1}\right)^k \le \left(\mathbb{H}_n^{t+1}\right)^k \;\; ; \;\; \left(\mathbb{H}_n^{t+1}\right)^k > h_{b_i} \\ 0 & \text{otherwise} \end{cases} \tag{A.24}$$

$$\left(E^{t+1}\right)^k = \max\left[\left(\mathbb{H}_i^{t+1}\right)^k, h_{b_i}\right] - \left(\mathbb{H}_n^{t+1}\right)^k \tag{A.25}$$

The expression for the stream bed conductance, C_s, that appears in (A.23) is already given in (A.14).

Stream Routing Component Version 5.0:

For $i = 1, \cdots, NR$:

♦

$$\begin{aligned} \mathbb{F}_i^k = & \frac{\left(A_i^{t+1}\right)^k + \left(A_{i-1}^{t+1}\right)^k - \left(A_i^t + A_{i-1}^t\right)}{2\Delta t} \\ & + \frac{\left(Q_{s_i}^{t+1}\right)^k - \left(Q_{s_{i-1}}^{t+1}\right)^k}{\Delta x_i} \\ & - \frac{1}{2}\left(\frac{Q_{in_i}^{t+1} - Q_{out_i}^{t+1}}{L_i} + \frac{Q_{in_{i-1}}^{t+1} - Q_{out_{i-1}}^{t+1}}{L_{i-1}}\right) \\ & + C_{s_i}\left\{\max\left[\left(\mathbb{H}_i^{t+1}\right)^k, h_{b_i}\right] - \max\left[\left(\mathbb{H}_n^{t+1}\right)^k, h_{b_i}\right]\right\} \end{aligned} \tag{A.26}$$

where

$$\left(A_i^{t+1}\right)^k = A\left[\left(\mathbb{H}_i^{t+1}\right)^k\right] = \left[\left(\mathbb{H}_i^{t+1}\right)^k - h_{b_i}\right] \times \left[B + s\left(\mathbb{H}_i^{t+1}\right)^k\right] \tag{A.27}$$

$$\left(Q_{s_i}^{t+1}\right)^k = Q_s\left[\left(\mathbb{H}_i^{t+1}\right)^k\right] = \frac{\gamma\sqrt{S_o}}{n}\left(A_i^{t+1}\right)^k\left[\left(R_i^{t+1}\right)^k\right]^{2/3} \tag{A.28}$$

$$\left(R_i^{t+1}\right)^k = R\left[\left(\mathbb{H}_i^{t+1}\right)^k\right] = \frac{\left[\left(\mathbb{H}_i^{t+1}\right)^k - h_{b_i}\right]\left\{B + s\left[\left(\mathbb{H}_i^{t+1}\right)^k - h_{b_i}\right]\right\}}{B + 2\left[\left(\mathbb{H}_i^{t+1}\right)^k - h_{b_i}\right]\sqrt{1+s^2}} \tag{A.29}$$

$$Q_{in_i}^{t+1} = R_{f_i}^{t+1} + S_{r_i}^{t+1} + Q_{ws_i}^{t+1} + Q_{brs_i}^{t+1} + Q_{td_i}^{t+1} + Q_{lko_i}^{t+1} + Q_{h_i}^{t+1} \tag{A.30}$$

$$Q_{out_i}^{t+1} = Q_{rip}^{t+1} + Q_{b_i}^{t+1} + Q_{div_i}^{t+1} \tag{A.31}$$

♦ $$\mathbb{X}_{i,i}^k = \left(\frac{\partial \mathbb{F}_i}{\partial \mathbb{H}_i^{t+1}}\right)^k = \frac{1}{\Delta t}\left(\frac{\partial A_i^{t+1}}{\partial \mathbb{H}_i^{t+1}}\right)^k + \frac{1}{\Delta x_i}\left(\frac{\partial Q_{s_i}^{t+1}}{\partial \mathbb{H}_i^{t+1}}\right)^k + \left(\frac{\partial Q_{sint_i}^{t+1}}{\partial \mathbb{H}_i^{t+1}}\right)^k \tag{A.32}$$

where

$$\left(\frac{\partial A_i^{t+1}}{\partial \mathbb{H}_i^{t+1}}\right)^k = B + 2s\left[\left(\mathbb{H}_i^{t+1}\right)^k - h_{b_i}\right] \tag{A.33}$$

$$\left(\frac{\partial Q_{s_i}^{t+1}}{\partial \mathbb{H}_i^{t+1}}\right)^k = \frac{\gamma\sqrt{S_o}\left(R_i^{t+1}\right)^k}{n}\left[\left(\frac{\partial A_i^{t+1}}{\partial \mathbb{H}_i^{t+1}}\right)^k + \frac{2}{3}\left(W_i^{t+1}\right)^k\left(\frac{\partial R_i^{t+1}}{\partial \mathbb{H}_i^{t+1}}\right)^k\right] \tag{A.34}$$

$$\left(W_i^{t+1}\right)^k = W\left[\left(\mathbb{H}_i^{t+1}\right)^k\right] = B + 2\left[\left(\mathbb{H}_i^{t+1}\right)^k - h_{b_i}\right]\sqrt{1+s^2} \tag{A.35}$$

$$\left(\frac{\partial R_i^{t+1}}{\partial \mathbb{H}_i^{t+1}}\right)^k = \left[\frac{\left(\frac{\partial A_i^{t+1}}{\partial \mathbb{H}_i^{t+1}}\right)^k\left(W_i^{t+1}\right)^k - 2\left(A_i^{t+1}\right)^k\sqrt{1+s^2}}{\left[\left(W_i^{t+1}\right)^k\right]^2}\right] \tag{A.36}$$

$$\left(\frac{\partial Q_{sint_i}^{t+1}}{\partial \mathbb{H}_i^{t+1}}\right)^k = \begin{cases} \frac{\partial C_{s_i}}{\partial \mathbb{H}_i^{t+1}}\left(G^{t+1}\right)^k + C_{s_i} & \left(\mathbb{H}_i^{t+1}\right)^k > \left(\mathbb{H}_n^{t+1}\right)^k \;\; ; \;\; \left(\mathbb{H}_i^{t+1}\right)^k > h_{b_i} \\ C_{s_i} & \left(\mathbb{H}_i^{t+1}\right)^k \le \left(\mathbb{H}_n^{t+1}\right)^k \;\; ; \;\; \left(\mathbb{H}_i^{t+1}\right)^k > h_{b_i} \\ 0 & \left(\mathbb{H}_i^{t+1}\right)^k \le h_{b_i} \end{cases} \tag{A.37}$$

$$C_{s_i} = \begin{cases} \frac{K_{s_i}}{d_{s_i}} L_i W_i\left(\left(\mathbb{H}_i^{t+1}\right)^k\right) & \left(\mathbb{H}_i^{t+1}\right)^k > \left(\mathbb{H}_n^{t+1}\right)^k \;\; ; \;\; \left(\mathbb{H}_i^{t+1}\right)^k > h_{b_i} \\ \frac{K_{s_i}}{d_{s_i}} L_i W_i\left(\left(\mathbb{H}_n^{t+1}\right)^k\right) & \left(\mathbb{H}_i^{t+1}\right)^k \le \left(\mathbb{H}_n^{t+1}\right)^k \;\; ; \;\; \left(\mathbb{H}_n^{t+1}\right)^k > h_{b_i} \\ 0 & \left(\mathbb{H}_i^{t+1}\right)^k \le h_{b_i} \;\; ; \;\; \left(\mathbb{H}_n^{t+1}\right)^k \le h_{b_i} \end{cases} \tag{A.38}$$

$$\frac{\partial C_{s_i}}{\partial \mathbb{H}_i^{t+1}} = \begin{cases} \frac{K_{s_i}}{d_{s_i}} L_i \frac{\partial W_i}{\partial \mathbb{H}_i^{t+1}} & \left(\mathbb{H}_i^{t+1}\right)^k > \left(\mathbb{H}_n^{t+1}\right)^k \quad ; \quad \left(\mathbb{H}_i^{t+1}\right)^k > h_{b_i} \\ 0 & \text{otherwise} \end{cases} \tag{A.39}$$

$$\left(G^{t+1}\right)^k = \left(\mathbb{H}_i^{t+1}\right)^k - \max\left[\left(\mathbb{H}_n^{t+1}\right)^k, h_{b_i}\right] \tag{A.40}$$

In (A.38) - (A.40), K_{s_i} is the stream bed hydraulic conductivity, L_i is the length of stream at stream node *i*, W_i is the wetted perimeter, d_{s_i} is the thickness of the stream bed material, h_{b_i} is the elevation of the stream bed, $\mathbb{H}_n$ is the groundwater head at the finite element node *n* that corresponds to the stream node *i*, and $NR + NLK + 1 \le n \le NR + NLK + N_L \cdot N$

- $$\mathbb{X}_{i,i-1}^k = \left(\frac{\partial \mathbb{F}_i}{\partial \mathbb{H}_{i-1}^{t+1}}\right)^k = \frac{1}{2\Delta t}\left(\frac{\partial A_{i-1}^{t+1}}{\partial \mathbb{H}_{i-1}^{t+1}}\right)^k - \frac{1}{\Delta x_i}\left(\frac{\partial Q_{s_{i-1}}^{t+1}}{\partial \mathbb{H}_{i-1}^{t+1}}\right)^k \tag{A.41}$$

- $$\mathbb{X}_{i,n}^k = \left(\frac{\partial \mathbb{F}_i}{\partial \mathbb{H}_n^{t+1}}\right)^k = \left(\frac{\partial Q_{sint_i}^{t+1}}{\partial \mathbb{H}_n^{t+1}}\right)^k \tag{A.42}$$

$$\left(\frac{\partial Q_{sint_i}^{t+1}}{\partial \mathbb{H}_n^{t+1}}\right)^k = \begin{cases} \frac{\partial C_{s_i}}{\partial \mathbb{H}_n^{t+1}}\left(E^{t+1}\right)^k - C_{s_i} & \left(\mathbb{H}_n^{t+1}\right)^k > \left(\mathbb{H}_i^{t+1}\right)^k \;\; ; \;\; \left(\mathbb{H}_n^{t+1}\right)^k > h_{b_i} \\ -C_{s_i} & \left(\mathbb{H}_n^{t+1}\right)^k \le \left(\mathbb{H}_i^{t+1}\right)^k \;\; ; \;\; \left(\mathbb{H}_n^{t+1}\right)^k > h_{b_i} \\ 0 & \left(\mathbb{H}_n^{t+1}\right)^k \le h_{b_i} \end{cases} \quad \text{(A.43)}$$

where

$$\frac{\partial C_{s_i}}{\partial \mathbb{H}_n^{t+1}} = \begin{cases} \frac{K_{s_i}}{d_{s_i}} L_i \frac{\partial W_i}{\partial \mathbb{H}_n^{t+1}} & \left(\mathbb{H}_i^{t+1}\right)^k \le \left(\mathbb{H}_n^{t+1}\right)^k \;\; ; \;\; \left(\mathbb{H}_n^{t+1}\right)^k > h_{b_i} \\ 0 & \text{otherwise} \end{cases} \quad \text{(A.44)}$$

$$\left(E^{t+1}\right)^k = \max\left[\left(\mathbb{H}_i^{t+1}\right)^k, h_{b_i}\right] - \left(\mathbb{H}_n^{t+1}\right)^k \quad \text{(A.45)}$$

The expression for the stream bed conductance, C_s, that appears in (A.23) is already given in (A.14)

A.2. Components of $\left\{\mathbb{F}^{\mathbf{k}}\right\}$ and $\left[\mathbb{X}^{\mathbf{k}}\right]$ for Lakes

For $i = NR+1, \cdots, NR+NLK$:

♦ $$\mathbb{F}_i^k = \frac{S_{lk}\left[\left(\mathbb{H}_i^{t+1}\right)^k\right] - S_{lk}\left[\mathbb{H}_i^t\right]}{\Delta t}$$

$$-Q_{divlk}^{t+1} - Q_{bplk}^{t+1} - Q_{rflk}^{t+1} - Q_{rtlk}^{t+1} - Q_{inlk}^{t+1} + Q_{lko}^{t+1}$$

$$-\sum_{j=1}^{N_{lk}}\left(P_{lk_j}^{t+1}A_{lk_j} - EV_{lk_j}^{t+1}A_{lk_j} - Q_{lkint_j}^{t+1}\right) \tag{A.46}$$

where

$$Q_{lkint_j}^{t+1} = C_{lk_j}\left\{\max\left[\left(\mathbb{H}_j^{t+1}\right)^k, h_{blk_j}\right] - \max\left[\left(\mathbb{H}_n^{t+1}\right)^k, h_{blk_j}\right]\right\} \tag{A.47}$$

$$EV_{lk_j}^{t+1}A_{lk_j} \le \frac{A_{lk_j}}{\Delta t}\max\left[\mathbb{H}_i^t - h_{blk_i}, 0\right] + P_{lk_j}^{t+1}A_{lk_j} + \frac{A_{lk_j}}{A_{lk}}\left(Q_{brlk}^{t+1} + Q_{inlk}^{t+1}\right) \tag{A.48}$$

In (A.46)-(A.48), N_{lk} is the number of lake nodes that make up a single lake and A_{lk} is the total surface area of a lake.

♦ $$\mathbb{X}_{i,i}^k = \left(\frac{\partial \mathbb{F}_i}{\partial \mathbb{H}_i^{t+1}}\right)^k = \frac{1}{\Delta t}\left(\frac{\partial S_{lk}\left[\mathbb{H}_i^{t+1}\right]}{\partial \mathbb{H}_i^{t+1}}\right)^k + \sum_{j=1}^{N_{lk}}\left(\frac{\partial Q_{lkint_j}^{t+1}}{\partial \mathbb{H}_i^{t+1}}\right)^k \tag{A.49}$$

where

$$\left(\frac{\partial S_{lk}\left[\mathbb{H}_i^{t+1}\right]}{\partial \mathbb{H}_i^{t+1}}\right)^k = \sum_{j=1}^{N_{lk}} H\left[\left(\mathbb{H}_i^{t+1}\right)^k - h_{blk_j}\right] A_{lk_j} \tag{A.50}$$

$$\left(\frac{\partial Q_{lkint_j}^{t+1}}{\partial \mathbb{H}_i^{t+1}}\right)^k = \begin{cases} C_{lk_j} & \text{if} \quad \left(\mathbb{H}_i^{t+1}\right)^k \geq h_{blk_j} \\ 0 & \text{if} \quad \left(\mathbb{H}_i^{t+1}\right)^k < h_{blk_j} \end{cases} \tag{A.51}$$

and $H[\bullet]$ is the Heaviside function.

- $$\mathbb{X}_{i,n}^k = \left(\frac{\partial \mathbb{F}_i}{\partial \mathbb{H}_n^{t+1}}\right)^k = \left(\frac{\partial Q_{lkint_j}^{t+1}}{\partial \mathbb{H}_n^{t+1}}\right)^k = \begin{cases} -C_{lk_j} & \text{if} \quad \left(H_n^{t+1}\right)^k \geq h_{blk_j} \\ 0 & \text{if} \quad \left(H_n^{t+1}\right)^k < h_{blk_j} \end{cases} \tag{A.52}$$

where $\mathbb{H}_n$ is the groundwater head at finite element node *n* that corresponds to lake node *j*.

A.3. Components of $\left\{\mathbb{F}^{\mathbf{k}}\right\}$ and $\left[\mathbb{X}^{\mathbf{k}}\right]$ for Groundwater Nodes

For $i = NR + NLK + 1, \cdots, NR + NLK + N_L \cdot N$:

♦
$$\mathbb{F}_i^k = \frac{S_{s_i}^{t+1} A_i \left(\left(\mathbb{H}_i^{t+1} \right)^k - TOP_i \right) + S_{s_i}^t A_i \left(TOP_i - \mathbb{H}_i^t \right)}{\Delta t}$$

$$- \sum_{e=N_e \cdot (m-1)+1}^{N_e \cdot m} \iint_{\Gamma^e} q_{\Gamma^e}^{t+1} \omega_i^e d\Gamma^e$$

$$- \sum_{\substack{j=N\cdot(m-1)+1 \\ j \neq i}}^{N \cdot m} \left(AT_{i,j}^{t+1} \right)^k \left(\left(\mathbb{H}_i^{t+1} \right)^k - \left(\mathbb{H}_j^{t+1} \right)^k \right)$$

$$+ H(m-2) L_{i-N} \left(\left(\Delta \mathbb{H}_i^u \right)^{t+1} \right)^k A_i$$

$$+ \left[1 - H(m - N_L) \right] L_{i+N} \left(\left(\Delta \mathbb{H}_i^d \right)^{t+1} \right)^k A_i$$

$$- q_{o_i}^{t+1} A_i + \left\{ \left(S_{s_i}^{'} \right)^t \frac{\left(h_i^{t+1} - h_{c_i}^t \right)}{\Delta t} + S_{se_i} b_{o_i}^t \frac{\left(h_{c_i}^t - h_i^t \right)}{\Delta t} \right\} A_i + q_{et_i}^{t+1} A_i$$

$$- Q_{sint_i}^{t+1} - Q_{lkint_i}^{t+1} - Q_{td_i}^{t+1} \qquad \text{(A.53)}$$

where

$$\left(AT_{i,j}^{t+1} \right)^k = \sum_{e=N_e \cdot (m-1)+1}^{N_e \cdot m} \left(\left(T^e \right)^{t+1} \right)^k \iint_{\Omega^e} \vec{\nabla} \omega_i^e \vec{\nabla} \omega_j^e d\Omega^e \qquad \text{(A.54)}$$

$$Q_{sint_i}^{t+1} = C_{s_{ns}} \left\{ \max\left[\left(\mathbb{H}_{ns}^{t+1} \right)^k, h_{b_{ns}} \right] - \max\left[\left(\mathbb{H}_i^{t+1} \right)^k, h_{b_{ns}} \right] \right\} \tag{A.55}$$

$$Q_{lkint_i}^{t+1} = C_{lk_{nlk}} \left\{ \max\left[\mathbb{H}_{lk}^{t+1}, h_{blk_{nlk}} \right] - \max\left[\mathbb{H}_i^{t+1}, h_{blk_{nlk}} \right] \right\} \tag{A.56}$$

$$Q_{td_i}^{t+1} = C_{td_i} \left(z_{td_i} - \mathbb{H}_i^{t+1} \right) \tag{A.57}$$

In (A.53)-(A.57) *ns* is the stream node number that corresponds to groundwater node number *i* $\left(1 \le ns \le \mathrm{NR}\right)$, *lk* is the lake number plus the total stream nodes $\left(\mathrm{NR}+1 \le lk \le \mathrm{NR}+\mathrm{NLK}\right)$, and *nlk* is the lake node number that corresponds to groundwater node number *i*.

♦

$$\begin{aligned}
\mathbb{X}_{i,i}^k &= \left(\frac{\partial \mathbb{F}_i}{\partial \mathbb{H}_i^{t+1}} \right)^k \\
&= \frac{S_{s_i}^{t+1} A_i}{\Delta t} - \sum_{\substack{j=N\cdot(m-1)+1 \\ j \ne i}}^{N\cdot m} \left(AT_{i,j}^{t+1} \right)^k \\
&\quad + H(m-2) L_{i-N} A_i \left(\frac{\partial \left(\Delta \mathbb{H}_i^u \right)^{t+1}}{\partial \mathbb{H}_i^{t+1}} \right)^k \\
&\quad + \left[1 - H(m - N_L) \right] L_{i+N} A_i \left(\frac{\partial \left(\Delta \mathbb{H}_i^d \right)^{t+1}}{\partial \mathbb{H}_i^{t+1}} \right)^k \\
&\quad + \frac{\left(S_{s_i}^{'} \right)^t A_i}{\Delta t} - \left(\frac{\partial Q_{sint_i}^{t+1}}{\partial \mathbb{H}_i^{t+1}} \right)^k - \left(\frac{\partial Q_{lkint_i}^{t+1}}{\partial \mathbb{H}_i^{t+1}} \right)^k - \left(\frac{\partial Q_{td_i}^{t+1}}{\partial \mathbb{H}_i^{t+1}} \right)^k
\end{aligned} \tag{A.58}$$

where

$$\left(\frac{\partial\left(\Delta\mathbb{H}_i^u\right)^{t+1}}{\partial\mathbb{H}_i^{t+1}}\right)^k = \begin{cases} 1 & \text{if} \quad \mathbb{H}_i^t \geq z_{b_i} \left(\text{or } z_{k_i} \text{ if no aquitard is present}\right) \\ 0 & \text{if} \quad \mathbb{H}_i^t < z_{b_i} \left(\text{or } z_{k_i} \text{ if no aquitard is present}\right) \end{cases} \tag{A.59}$$

$$\left(\frac{\partial\left(\Delta\mathbb{H}_i^d\right)^{t+1}}{\partial\mathbb{H}_i^{t+1}}\right)^k = \begin{cases} 1 & \text{if} \quad \mathbb{H}_i^t \geq z_{t_i} \left(\text{or } z_{k_i} \text{ if no aquitard is present}\right) \\ 0 & \text{if} \quad \mathbb{H}_i^t < z_{t_i} \left(\text{or } z_{k_i} \text{ if no aquitard is present}\right) \end{cases} \tag{A.60}$$

$$\left(\frac{\partial Q_{sint_i}^{t+1}}{\partial\mathbb{H}_i^{t+1}}\right)^k = \begin{cases} -C_{s_{ns}} & \text{if} \quad \left(\mathbb{H}_i^{t+1}\right)^k > h_{b_{ns}} \\ 0 & \text{if} \quad \left(\mathbb{H}_i^{t+1}\right)^k \leq h_{b_{ns}} \end{cases} \tag{A.61}$$

$$\left(\frac{\partial Q_{lkint_i}^{t+1}}{\partial\mathbb{H}_i^{t+1}}\right)^k = \begin{cases} -C_{lk_{nlk}} & \text{if} \quad \left(\mathbb{H}_i^{t+1}\right)^k > h_{blk_{nlk}} \\ 0 & \text{if} \quad \left(\mathbb{H}_i^{t+1}\right)^k \leq h_{blk_{nlk}} \end{cases} \tag{A.62}$$

$$\left(\frac{\partial Q_{td_i}^{t+1}}{\partial\mathbb{H}_i^{t+1}}\right)^k = -C_{td_i} \tag{A.63}$$

♦ $$\mathbb{X}_{i,i-N}^k = \left(\frac{\partial\mathbb{F}_i}{\partial\mathbb{H}_{i-N}^{t+1}}\right)^k = H\left(m-2\right)L_{i-N}A_i\left(\frac{\partial\left(\Delta\mathbb{H}_i^u\right)^{t+1}}{\partial\mathbb{H}_{i-N}^{t+1}}\right)^k \tag{A.64}$$

where

$$\left(\frac{\partial\left(\Delta\mathbb{H}_i^u\right)^{t+1}}{\partial\mathbb{H}_{i-N}^{t+1}}\right)^k = \begin{cases} -1 \text{ if } \quad \mathbb{H}_{i-N}^t > z_{t_i} \left(\text{or } \ z_{k_i} \ \text{ if no aquitard is present}\right) \\ \\ 0 \quad \text{if } \quad \mathbb{H}_{i-N}^t \le z_{t_i} \left(\text{or } \ z_{k_i} \ \text{ if no aquitard is present}\right) \end{cases} \tag{A.65}$$

♦ $$\mathbb{X}_{i,i+N}^k = \left(\frac{\partial\mathbb{F}_i}{\partial\mathbb{H}_{i+N}^{t+1}}\right)^k = \left[1 - H\left(m - N_L\right)\right] L_{i+N} A_i \left(\frac{\partial\left(\Delta\mathbb{H}_i^d\right)^{t+1}}{\partial\mathbb{H}_{i+N}^{t+1}}\right)^k \tag{A.66}$$

where

$$\left(\frac{\partial\left(\Delta\mathbb{H}_i^d\right)^{t+1}}{\partial\mathbb{H}_{i+N}^{t+1}}\right)^k = \begin{cases} -1 \text{ if } \quad \mathbb{H}_{i+N}^t > z_{b_i} \left(\text{or } \ z_{k_i} \ \text{ if no aquitard is present}\right) \\ \\ 0 \quad \text{if } \quad \mathbb{H}_{i+N}^t \le z_{b_i} \left(\text{or } \ z_{k_i} \ \text{ if no aquitard is present}\right) \end{cases} \tag{A.67}$$

♦ $$\mathbb{X}_{i,j}^k = \left(\frac{\partial\mathbb{F}_i}{\partial\mathbb{H}_j^{t+1}}\right)^k = \left(AT_{i,j}^{t+1}\right)^k \tag{A.68}$$

♦ $$\mathbb{X}_{i,ns}^k = \left(\frac{\partial\mathbb{F}_i}{\partial\mathbb{H}_{ns}^{t+1}}\right)^k \tag{A.69}$$

If stream routing component version 4.0 is used, then

$$\left(\frac{\partial \mathbb{F}_i}{\partial \mathbb{H}_{ns}^{t+1}}\right)^k = \begin{cases} -C_{s_{ns}} & \text{if} \quad \left(\mathbb{H}_{ns}^{t+1}\right)^k \geq h_{b_{ns}} \\ 0 & \text{if} \quad \left(\mathbb{H}_{ns}^{t+1}\right)^k < h_{b_{ns}} \end{cases} \tag{A.70}$$

If stream routing component version 4.1 or 5.0 is used, then

$$\left(\frac{\partial \mathbb{F}_i}{\partial \mathbb{H}_{ns}^{t+1}}\right)^k = \begin{cases} -\frac{\partial C_{s_{ns}}}{\partial \mathbb{H}_{ns}^{t+1}}\left(G^{t+1}\right)^k - C_{s_{ns}} & \left(\mathbb{H}_{ns}^{t+1}\right)^k > \left(\mathbb{H}_i^{t+1}\right)^k \;;\; \left(\mathbb{H}_{ns}^{t+1}\right)^k > h_{b_{ns}} \\ -C_{s_{ns}} & \left(\mathbb{H}_{ns}^{t+1}\right)^k \leq \left(\mathbb{H}_i^{t+1}\right)^k \;;\; \left(\mathbb{H}_{ns}^{t+1}\right)^k > h_{b_{ns}} \\ 0 & \left(\mathbb{H}_{ns}^{t+1}\right)^k \leq h_{b_{ns}} \end{cases} \tag{A.71}$$

where

$$\left(G^{t+1}\right)^k = \left(\mathbb{H}_{ns}^{t+1}\right)^k - \max\left[\left(\mathbb{H}_i^{t+1}\right)^k, h_{b_{ns}}\right] \tag{A.72}$$

♦ $$\mathbb{X}_{i,lk}^k = \left(\frac{\partial \mathbb{F}_i}{\partial \mathbb{H}_{lk}^{t+1}}\right)^k = \begin{cases} C_{lk_{nlk}} & \text{if} \quad \left(\mathbb{H}_{lk}^{t+1}\right)^k \geq h_{blk_{nlk}} \\ 0 & \text{if} \quad \left(\mathbb{H}_{lk}^{t+1}\right)^k < h_{blk_{nlk}} \end{cases} \tag{A.73}$$

Appendix B - Chronology of the Development of IGSM, IGSM2, and IWFM

The roots of the IGSM code date back to an earlier code called FEGW2, developed by Dr. Young Yoon at UCLA in 1976. The first version of IGSM was also developed by Dr. Yoon (and his consulting staff) in 1990 as part of a contract funded by the Bureau of Reclamation Mid Pacific Region (MP), California Department of Water Resources (DWR), State Water Resources Control Board (SWRCB), and Contra Costa Water District (CCWD) (James M. Montgomery Consul. Eng. Inc., 1990).

Over the years, IGSM has undergone various upgrades by different groups based on specific applications to numerous basins in the United States (Table B.1); the model has been applied to groundwater basins in California, Colorado, and Florida. Applications of IGSM in California include the Central Valley, Sacramento County, Pajaro Valley, Friant Service Area, Alameda County, City of Sacramento, Pomona Valley, Salinas Valley, and the Chino Basin (Montgomery Watson, 1993).

No formalized version numbering system for IGSM was created until IGSM Version 3.0 in 1996. As a result, IGSM codes were not referenced in terms of a version number prior to 1996 (WRIME, 2000).

Thereafter, two separate groups developed IGSM versions 3.1 and 4.0 for application in the CVPIA-PEIS and Salinas Valley projects, respectively. However, not all the features developed for version 3.1 were included in version 4.0. The development of IGSM 5.0 in 2000 was an effort to consolidate all the features from both version 3.1 and 4.18 into a one comprehensive and upgraded IGSM version (Technical Memorandum

IGSM 5.0, 2000). Around that time, an IGSM User's Group was developed to discuss and share input, recommendations, and experiences of the IGSM users in the water community. Following the Peer Review process of IGSM conducted by the California Water and Environmental Modeling Forum, CWEMF (previously known as the Bay-Delta Modeling Forum, BDMF), the members of the IGSM Users Group strongly urged DWR to take the lead in overseeing the future development and technical support of IGSM. DWR has a strong interest in IGSM because of the use of the application of IGSM to the Central Valley in California CVGSM (Central Valley Groundwater and Surface water Model) in supporting the hydrology development and groundwater simulation in the CVP/SWP simulation model CalSim (previously known as DWRSIM).

DWR initiated a comprehensive review of the IGSM version 5.0 theories and code in January 2001. Following extensive revisions and enhancements to the theoretical basis of many of the processes simulated in IGSM and to the FORTRAN codes, it was decided to call the newly developed model IGSM2. The basic acronym was retained since to the end user many of the features between IGSM and IGSM2 were very similar. IGSM2 Version 1.0 was made available to the public in December 2002. Effective September 2005, IWFM was the new name for IGSM2. IWFM Version 2.4 was released in May 2006, Version 3.0 was released in February 2007, Version 3.02 in April 2010 and Version 4.0 in May 2012.

Version	Date	Model Features	Application Area	Model Author(s)
IGSM--	1976	New groundwater model	--	Young Yoon (UCLA)
IGSM--	1979	Major revisions to 1976 version	Basin Wide	Young Yoon Tetra Tech, Inc.
IGSM--	1979-1983	Enhancements	--	Young Yoon Boyle Engineering
IGSM--	1987	Stream routing	Central Valley	Young Yoon Boyle Engineering
IGSM 1.0	1990	Surface water and land surface processes, groundwater simulation	Central Valley and Other Applications	Young Yoon, Saquib Najmus, Ali Taghavi
IGSM 2.0	1994	Water quality simulation	Pajaro Valley Chino Basin	Young Yoon, Saquib Najmus
IGSM 2.1	1995	Reservoir operations	Salinas Valley	Young Yoon, Saquib Najmus, Ali Taghavi
IGSM 2.2	1995	Vadose zone, water quality improvements, land use	Chino Basin	Saquib Najmus
IGSM 2.3	1996	Regional scale tile drain simulation	Imperial County	Ali Taghavi
IGSM 3.0	1996	Multi-model integration	ARWRI	Young Yoon
IGSM 3.1	1997	Land subsidence	CVPIA-PEIS	Ali Taghavi
IGSM 4.0	1997	English and SI units	--	Ali Taghavi
IGSM 4.10-4.18	1998-1999	Reservoir operations improvements, crop water use	Salinas Valley	Ali Taghavi
IGSM 5.0	2000	Consolidation of all previous versions of IGSM	DWR-ISI	Ali Taghavi Saquib Najmus

Table B.1 Chronological development of IGSM (up to version 5.0), IGSM2 and IWFM

Version	Date	Model Features	Application Area	Model Author(s)
IGSM2 1.0	2002	Major revisions to IGSM 5.0 theories and code	--	Emin Can Dogrul
IGSM2 1.01	2003	Bug fixes	--	Emin Can Dogrul
IGSM2 2.0	2003	More robust solution techniques, improved simulation of aquifer-surface water interactions and output files	--	Emin Can Dogrul
IGSM2 2.01	2004	Bug fixes	--	Emin Can Dogrul
IGSM2 2.2	2005	Zone budgeting post-processor	--	Emin Can Dogrul
IWFM 2.3	2005	Re-use of irrigation return flow	--	Emin Can Dogrul
IWFM 2.4	2006	Modified routing procedure for root zone moisture	Butte County	Emin Can Dogrul
IWFM 3.0	2007	Enhancements in root zone moisture simulation, improved print-out features	Central Valley, Walla Walla Basin (OR)	Emin Can Dogrul
IWFM 3.02	2010	Efficient generalized preconditioned conjugate gradient solver, modifications for faster run-times, bug fixes	Central Valley, Walla Walla Basin (OR and WA)	Emin Can Dogrul
IWFM 4.0	2012	Enhanced component modularity, land-use and root zone flow processes simulated at cell level, explicit simulation of rice fields and managed refuges	Yolo, Butte, Merced and Kings counties; stand-alone root zone component, IDC, applied in many parts of CA and in Treasure Valley, ID	Emin Can Dogrul

Table B.1 Chronological development of IGSM (up to version 5.0), IGSM2 and IWFM *(continued)*

Version	Date	Model Features	Application Area	Model Author(s)
IWFM-2015	2014	Full component modularity, kinematic wave routing of stream flows, simulation of root water uptake from groundwater, riparian vegetation access to stream flows	Central Valley Natural Flow Model; Butte, Merced and Kings counties	Emin Can Dogrul

Table B.1 Chronological development of IGSM (up to version 5.0), IGSM2 and IWFM *(continued)*

Appendix C - References

Allen, M. B., Herrera, I. and Pinder, G. F. 1988. *Numerical modeling in science and engineering*. Wiley-Interscience Pub., New York.

Bear, J. 1972. *Dynamics of fluids in porous media.* Dover Publications, Inc. New York.

Bear, J. and Verruijt, A. 1987. *Modeling groundwater flow and pollution*. D. Reidel Publishing Co., Holland.

Campbell, G. S. 1974. A simple method for determining unsaturated hydraulic conductivity from moisture retention data. *Soil Sci.*, 117(6), 311-314.

Chaundry, M. H. 1993. Open-channel flow. Prentice Hall, New Jersey.

Dixon, M. F., Bai, Z., Brush, C. F., Chung, F. I., Dogrul, E. C. and Kadir, T. N. 2010. "Accuracy control and performance enhancement of linear solvers for the Integrated Water Flow Model." <http://baydeltaoffice.water.ca.gov/modeling/hydrology/IWFM/Publications/downloadables/Reports/UCDCS_IWFM_TR.pdf> (October 14, 2011).

Dixon, M. F., Bai, Z., Brush, C. F., Chung, F. I., Dogrul, E. C. and Kadir, T. N. 2011. Error control of iterative linear solvers for integrated groundwater models. *Ground Water*, 49 (6), 859-865.

Driscoll, F. G. 1986. *Groundwater and wells.* Johnson Division, 2nd ed., St. Paul, Minnesota.

Dunne, T. 1978. Field studies of hillslope flow processes. M. J. Kirkby, ed., *Hillslope Hydrology*, Wiley-Interscience, New York, 227-293.

DWR, 2015. *IWFM Demand Calculator: IDC-2015 – Theoretical Documentation and User's Manual*. Integrated Hydrologic Models Development Unit, Modeling Support Branch, Bay-Delta Office, CADWR, Sacramento, CA <http://baydeltaoffice.water.ca.gov/modeling/hydrology/IWFM/IDC/index_IDC.cfm> (October 6, 2015)

Gerald, C. F., and Wheatley, P. O. 1994. *Applied numerical analysis.* Addison-Wesley Pub. Co. Inc., Reading.

Helm, D. C. 1975. One-dimensional simulation of aquifer-system compaction near Pixley, California. 1, constant parameters. *Water Resour. Res.*, 11(3), 465-478.

Holden, A. P. and Stephenson, D. 1995. Finite difference formulations of kinematic equations. *J. Hydraul. Eng.*, 121(5), 423–426.

Huyakorn, P. S., and Pinder, G. F. 1983. *Computational methods in subsurface flow.* Academic Press Inc., San Diego.

Leake, S. A. and Prudic, D. E. 1988. *Documentation of a computer program to simulate aquifer-system compaction using the modular finite-difference ground-water flow model*, Department of the Interior, U.S. Geological Survey Open-File Report 88-482.

Luthin, J. N. 1973. *Drainage engineering.* John Wiley & Sons, Inc., New York, 174-176.

McDonald, M. G., and Harbaugh, A. W. 1988. *A modular three-dimensional finite-difference ground-water flow model*. USGS Tech. Water Resources Investigation, Book 6, Chap. A1.

Mualem, Y. 1976. A new model for predicting the hydraulic conductivity of unsaturated porous media. *Water Resour. Res.*, 12, 513-522.

Poland, J. F., and Davis, G. H. 1969. Land subsidence due to withdrawal of fluids. *Rev. Eng. Geol.*, Vol. 2, 187-269.

Riley, F. S. 1969. *Analysis of borehole extensometer data from central California in land subsidence*. Publ. 89(2), L. J. Tison, ed., International Association of Hydrologic Sciences, Wallingford, England, 423-431.

Smedema, L. K. and Rycroft, D. W. 1983. *Land drainage.* Cornell University Press, Ithaca, NY.

van Genuchten, M. T. 1985. A closed-form solution for predicting the conductivity of unsaturated soils. *Soil Sci. Soc. Am. J.*, 44, 892-898.

Wang, H. F. and Anderson, M. P. 1982. *Introduction to groundwater modeling: finite difference and finite element methods.* Academic Press, Inc., San Diego.